Characterization of novel protein players in pain

Dissertation

for the award of the degree

Doctor rerum naturalium

(Dr. rer. nat.)

of the Georg-August-Universität Göttingen

within the doctoral program *Sensory and Motor Neuroscience* of the Göttingen Graduate School for Neurosciences, Biophysics, and Molecular Biosciences (GGNB)

of the Georg-August University School of Science (GAUSS)

submitted by

Hanna Kristina Fischer

from Marburg, Germany

Göttingen, 2022

Characterization of novel protein players in pain

Dissertation

for the award of the degree

Doctor rerum naturalium

(Dr. rer. nat.)

of the Georg-August-Universität Göttingen

within the doctoral program *Sensory and Motor Neuroscience* of the Göttingen Graduate School for Neurosciences, Biophysics, and Molecular Biosciences (GGNB)

of the Georg-August University School of Science (GAUSS)

submitted by

Hanna Kristina Fischer

from Marburg, Germany

Göttingen, 2022

Thesis Advisory Committee

Prof. Manuela Schmidt, PhD

Somatosensory Signaling & Systems Biology Group, Max Planck Institute for Multidisciplinary Sciences, Göttingen, Germany
Systems Biology of Pain Group, University of Vienna, Austria

Prof. Dr. Thomas Dresbach

Synaptogenesis Group, Department of Anatomy and Embryology, Georg August University of Göttingen, Germany

Prof. Dr. Nils Brose

Department of Molecular Neurobiology, Max Planck Institute for Multidisciplinary Sciences, Göttingen, Germany

Members of the Examination Board

Referee:

Prof. Manuela Schmidt, PhD

2nd Referee:

Prof. Dr. Thomas Dresbach

Further members of the Examination Board

Prof. Dr. Nils Brose

Prof. Dr. Martin Göpfert

Department of Cellular Neurobiology, Georg August University of Göttingen, Germany

Prof. Dr. Ralf Heinrich

Department of Cellular Neurobiology, Georg August University of Göttingen, Germany

Prof. Dr. Tobias Moser

Molecular Anatomy, Physiology, and Pathology of Sound Coding and Prosthetics, Department of Otolaryngology, University Medical Center Göttingen, Germany

Date of oral examination: 23rd February 2023

Contents

List of Figures

List of Tables

List of Abbreviations

Abbreviation	Name
AITC	Allyl isothiocyanate
ANOVA	Analysis of variance
ACC	Anterior cingulate cortex
ATP	Adenosine triphosphate
Bin2	Bridging integrator-2
BSA	Bovine serum albumin
Caps	Capsaicin
CAT	Catalase
Ca^{2+}- imaging	Calcium-imaging
CD48	Cluster of differentiation 48
CFA	Complete Freund's adjuvant
CNS	Central nervous system
con	Contralateral
CRISPR/Cas9	Clustered regularly interspaced short palindromic repeats/CRISPR associated enzyme 9
d	Day
DEPs	Differentially expressed proteins
DIA	Data-independent acquisition
Disp3	Dispatched 3 gene
DMEM	Dulbecco's modified eagle medium
cDNA	Complementary DNA
DRG	Dorsal root ganglion
lDRG	Lumbar DRG
ETC	Electron transport chain
FBS	Fetal bovine serum
FC	Fold change
FCCP	Carbonyl cyanide p-trifluoromethoxyphenylhydrazone
fl/fl	Both alleles floxed (flanked by LoxP sites, a marker for recombination when cre-recombinase is used) (in this case floxed for *Tmem160*)
GAPDH	Glyceraldehyde 3-phosphate dehydrogenase
GM-CSF	Granulocyte-monocytes-colony stimulating factor
GSTA	Glutathione S-transferase alpha
HEK	Human embryonic kidney cells
HeLa	Cervix cancer cell line derived from Henrietta Lacks
HepG2	Hepatoblastoma cell line
HRP	Horseradish peroxidase
HyPer-mito-YFP	Mitochondrial yellow fluorescent protein-based sensor for hydrogen peroxide
Iba1	Ionized calcium binding adaptor molecule 1
IgG	Immunoglobulin G
IL	Interleukin
ipsi	Ipsilateral
KO	Knockout
cKO	Conditional KO (in this case in sensory neurons)
m	Minutes
MITRAC12	A cytochrome c oxidase assembly intermediate
MMP9	Matrix metallopeptidase 9
MP	Mitoplast
MS	Mass spectrometry
mt/ mito	mitochondrial
n	Number of cohorts/mice in a specific experiment
N	Number of cells/mice in a specific experiment
Ndufv2	NADH dehydrogenase [ubiquinone] flavoprotein 2, mitochondrial

NEP	Non-evoked pain
NF	Neurofilament
NGF	Nerve growth factor
NSAID	Non-steroidal anti-inflammatory drugs
NT	Neurotrophin
PASEF	Parallel accumulation – serial fragmentation
PBS	Phosphate buffered saline
PCA	Principal component analysis
PCR	Polymerase chain reaction
qPCR/qRT-PCR	Quantitative real-time polymerase chain reaction
PFA	Paraformaldehyde
PK	Proteinase K
POD	Post-operative day
Protein ID	Protein identification
PSN	Primary sensory neurons
ROS	Reactive oxygen species
s	Seconds
SCN	Sciatic nerve
SEM	Standard error of the mean
Serpina	Serpin family A member
SNI	Spared nerve injury
S1	primary sensory cortex
Sparc	Secreted protein acidic and cysteine rich
TACO1	Translational activator of cytochrome c oxidase I
Tmem	Transmembrane
TMRM	Tetramethylrhodamin methyl ester
TO(M)M	Translocase of outer (mitochondrial) membrane
TNFα	Tumor necrosis factor α
TRP	Transient receptor potential (channel)
TRPA1	Transient receptor potential ankyrin 1
TRPM	Transient receptor potential melastatin
TRPV1	Transient receptor potential vanilloid 1
U	Unit of enzyme 's catalytic activity
UPR^{mt}	Mitochondrial unfolded protein response
VGCC	Voltage gated Ca^{2+} channels
w	Weeks
WT	Wildtype

Abstract

Despite its high prevalence in the human society, the mechanisms underlying chronic pain and pain chronification are still poorly understood. The shortage of potential targets that are specific to pathological chronic pain, as opposed to the physiologically necessary acute pain, lead to limited treatment options. With the few treatment options that are available, it often comes to a lack of efficacy and a high rate of side effects, including addiction, especially in the case of opioids. Additionally, it is well described that pain perception and the underlying mechanisms differ immensely depending on age and sex of the subject, which is usually not considered for treatment.

A possible method to improve treatment options in the future is targeting molecules relevant to chronic pain and specific to the different phenotypes and characteristics of the subjects. Therefore, it is of high importance to understand mechanistical differences between acute pain and different types of chronic pain in more detail, but also between sexes and juvenile and adult individuals.

Different experimental concepts were applied throughout this thesis to enhance the understanding of the processes underlying pain. In a first section, one specific protein, Tmem160, was targeted by generating a knockout (KO) mouse line to investigate its role in chronic pain. This study also focused on the influence of sex within this context. Tmem160 was chosen as a promising target, as this hitherto undescribed protein was recently shown to be downregulated in murine chronic pain models. The *Tmem160* KO mice were subjected to multiple pain models and compared to their wildtype (WT) littermates. Under neuropathic pain condition, as caused by the spared nerve injury (SNI) model, deletion of *Tmem160* elicited a concise phenotype in male mice in the initiation phase, namely a delay in the development of tactile hypersensitivity and an absence of increased self-grooming behavior in contrast to WT littermates. Also, the function of Tmem160 displayed a sexual dimorphism: female *Tmem160* KO mice presented WT-like behavior within the SNI model. Furthermore, mouse models for acute, incisional and inflammatory pain showed that Tmem160 is dispensable under these conditions, indicating an important specificity to neuropathic pain.

Possible action mechanisms of Tmem160 were investigated using *in vitro* experiments. Male *Tmem160* KO mice revealed an overall reduction of cytokine levels in naïve DRG that potentially influenced neuronal excitability by reducing the percentage of cells responding to activation of the Transient receptor potential ankyrin 1 (TRPA1) channel. This reduction compared to WT could be restored by previous incubation with Tumor necrosis factor-α (TNFα), one of the cytokines found to be downregulated. Investigation of a marker for microglia/macrophages in spinal cord, indicates a reduction in spinal activation of these cells

upon nerve injury. Additionally, a conditional knockout (cKO) of *Tmem160* in primary sensory neurons suggests non-neuronal cells as the primary site of action for Tmem160 in the chronic pain context, since the cKO showed WT-like behavior and characteristics, implying that the neuronal Tmem160 is dispensable for the observed processes. Taking together, a hypothetic working model for its action mechanism was developed, with non-neuronal Tmem160 influencing neuroimmune crosstalk in the DRG in the early phase of neuropathic pain: It interacts with TRPA1 expression levels, conceivably via TNFα and affects neuronal excitability of the primary sensory neurons. The non-neuronal Tmem160 is most likely relevant in microglia/macrophages, also explaining the sex-differences related to the higher relevance of these cells for pain pathways in males compared to females.

The investigation of specific individual characteristics was even more important in the second study where the influence of age and sex on somatosensation and on the proteomic composition of the dorsal root ganglia (DRG), a tissue crucial for somatosensation, was investigated. Under naïve conditions, male juvenile mice showed a decrease in thermal sensitivity throughout maturation, while the nocifensive response within a model for acute pain increased with age. To investigate underlying mechanisms *in vitro* experiments were performed on DRG. Transient receptor potential vanilloid 1 (TRPV1) channel expression levels, as well as the neuronal excitability in response to TRPV1 stimulation, revealed differences depending on age. The proteome of the DRG under naïve conditions was studied and compared between juvenile and adult, male and female mice using quantitative proteomics. Many proteins showed an age-dependent differential expression, including multiple candidates involved in pain and neuroimmune interactions. The number of age-dependent differentially expressed proteins (DEPs) was significantly higher in female than in male mice. When comparing the sexes directly within the age groups very few differences in the proteome were detected. This shows that maturation and age have a stronger influence on the composition of the DRG proteome than sex. Even though the composition of the DRG does not differ a lot between sexes within age groups, it must be acknowledged that the changes occurring during maturation showed a difference between sexes.

In addition to the identification of Tmem160 as a promising candidate to specifically target chronic pain, while leaving acute pain functions intact, this study underlines the need of an adequate selection of animals in pain research, both regarding their sex and age. It shows the importance to match the characteristics of the research animals with the impacted group of society. A better matching of characteristics has the power to improve translation between animals and humans to enhance and enable targeted treatment options at the level of individuals and their specific disease.

1 Introduction

1.1 Prevalence of Chronic Pain and Current Treatment Options

The international association for the study of pain (IASP) defines pain as: “An unpleasant sensory and emotional experience associated with, or resembling that associated with, actual or potential tissue damage” (Raja et al., 2020). Pain is highly subjective, depends on personal experiences and conscious awareness and is not objectively measurable (Raja et al., 2020). It has to be clearly distinguished from nociception, the measurable nerve response to an adequate stimulus (Treede, 2018). Pain can be subdivided into chronic and acute pain. Acute pain perception is of utmost importance for the body to avoid (further) dangerous situations or to take care of the damaged tissue. It elicits an – usually immediate - defensive response. Patients that are insensitive to pain due to genetic mutations show a highly increased number of injuries, because they are missing the important feedback mechanism of acute pain perception (D. L. H. Bennett & Woods, 2014). While acute pain fulfils a physiological function, chronic pain that persists after removal of the danger is a pathological state of the body (Basbaum et al., 2009). Per definition, chronic pain is pain that is perceived persistently or recurrently over a duration of minimally 3 months (Treede et al., 2019). In the most recent International Classification of Diseases (ICD-11), chronic pain is systematically grouped under the code MG30: Chronic pain. It is specifically separated from acute pain (Code MG31). Furthermore, MG30 is subdivided into different categories including, but not limited to, Chronic primary pain (MG30.0), which is defined as a disease state per se without influences by other diseases (Korwisi et al., 2022). It is commonly accepted that acute and chronic pain as well as multiple subtypes of chronic pain differ in the underlying (patho)physiological mechanisms (Basbaum et al., 2009; Bourinet et al., 2014; Price & Gold, 2018).

Chronic pain is a major health issue contributing to an economic burden for the public health sector and society while having crucial impact on affected patients, their quality of life and social participation. It is highly prevalent all over the world (Dahlhamer et al., 2018; Doth et al., 2010; Glare et al., 2019; Price & Gold, 2018). A survey in 2019 revealed that around 20% of the adult US American population suffers from chronic pain and for around 7.4% of the population this pain showed a high impact on their lives (Zelaya et al., 2020). In a survey all over Europe performed in 2003, the prevalence of chronic pain of a duration of 6 months or more was 19% (Breivik et al., 2006). This high prevalence produces high costs for the society, both directly for the treatment and indirectly for example due to absenteeism at work. Considering only absenteeism at work, it is resulting in a cost of € 240 billion in Europe (Eccleston et al., 2018). Furthermore chronic pain is a major cause of disability retirement (Saastamoinen et al., 2012) and pain is one of the most frequent reasons to search for medical help (Dueñas et al., 2016). The total direct and indirect cost of back pain of adults under 75 years in Germany alone was estimated to nearly €49 billion, being approximately 2.2% of the German gross domestic product (Wenig et al., 2009), emphasizing the immense economic burden of pain.

Despite its prevalence, the treatment options for chronic pain are still very limited (Hylands-White et al., 2017), due to a lack of specificity and a high rate of adverse effects. Currently, treatment of chronic pain is usually performed following the so-called analgesic ladder of the world health organisation (WHO), developed initially specifically for cancer pain. The first step of the ladder includes non-opioid analgesics, the next step consists of opioid analgesics side by side with co-analgesics including anticonvulsants and antidepressants. Commonly, chronic pain is treated as ongoing acute pain. This is problematic due to the lack of efficacy. Additionally, adverse effects occur in other organs of the body besides the involvement in pain. Non-opioid analgesics such as non-steroidal anti-inflammatory drugs (NSAIDs) – e.g., Ibuprofen, Metamizol and Paracetamol can cause side-effects such as renal insufficiency, gastric ulcer resulting in gastrointestinal bleeding, cardiovascular side effects, agranulocytosis and liver failure. Furthermore, it has been recently discovered in lower back pain patients as well as in multiple mouse models, that an initial treatment with corticosteroids or NSAIDs was able to relief the acute pain but contributed to pain chronification in the long run (Parisien et al., 2022). This means, that the treatment of inflammation-associated pains with anti-inflammatory drugs has to be considered carefully. Opioid analgesics do not only cause somatic side-effects (e.g., risk for respiratory depression or constipation) but also drug addiction. The complex treatment of chronic pain, the good efficacy of opioids in acute pain and the few existing alternatives to opioid analgesics in chronic pain resulted in a vast problem of opioid addiction (Glare et al., 2019), especially - but not only - in the United States. In the United States a metaanalysis showed an opioid analgesics addiction rate of 8-12% in patients with chronic non-cancer pain (Vowles et al., 2015).

The insufficient current treatment options in chronic pain urge for pharmaceutical research in finding targeted treatment options, improving efficacy and reducing side effects. To enable targeted treatment a specific understanding of the underlying pathological mechanisms is of utmost importance, requiring further research (Borsook et al., 2014; Davis et al., 2020; Gereau, 2014; Price & Gold, 2018).

1.2 Physiology of Somatosensation

The mammalian body provides different systems and organs to perceive – both internal and external - stimuli. The most common systems are temperature sensing (thermosensation), touch (mechanosensation), sensation of the body itself, and orientation and movement of the body parts (proprioception) and pain (nociception) (*Somatosensory System - Latest Research* *and News* | *Nature*, 2022). The stimulus in the periphery is detected by either specific receptors for the sensation type (e.g., Meissner's corpuscles, Pacinian corpuscles, Merkel's disks, and Ruffini's corpuscles for mechanosensation (Purves et al., 2001)) or directly by free nerve endings. If the stimulation surpasses a threshold level, the cells get activated and trigger action potentials. The primary sensory neurons (PSN), also known as “thermoreceptors”, “mechanoreceptors” and “nociceptors” respectively, propagate the signal from the periphery to the spinal cord. The PSN are pseudounipolar neurons, i.e., they consist of a soma and only one axon that is split into two directions. While the soma is located in ganglia (e.g., dorsal root ganglia (DRG)), the axon spreads to both the periphery and the spinal cord (Moraes et al., 2017) (Figure 1). PSN can be activated by chemical, mechanical and thermal stimuli (Basbaum et al., 2009; Belmonte & Viana, 2008; Dubin & Patapoutian, 2010). Due to the composition including the somata of the PSN, the DRG are of high interest for us to study PSN and (pain) perception. The first synapse occurs in the spinal cord, from where the second order neuron takes over and transmits the information to supraspinal centers for integration and further processing via a second synapse in the brain (Purves, 2008).

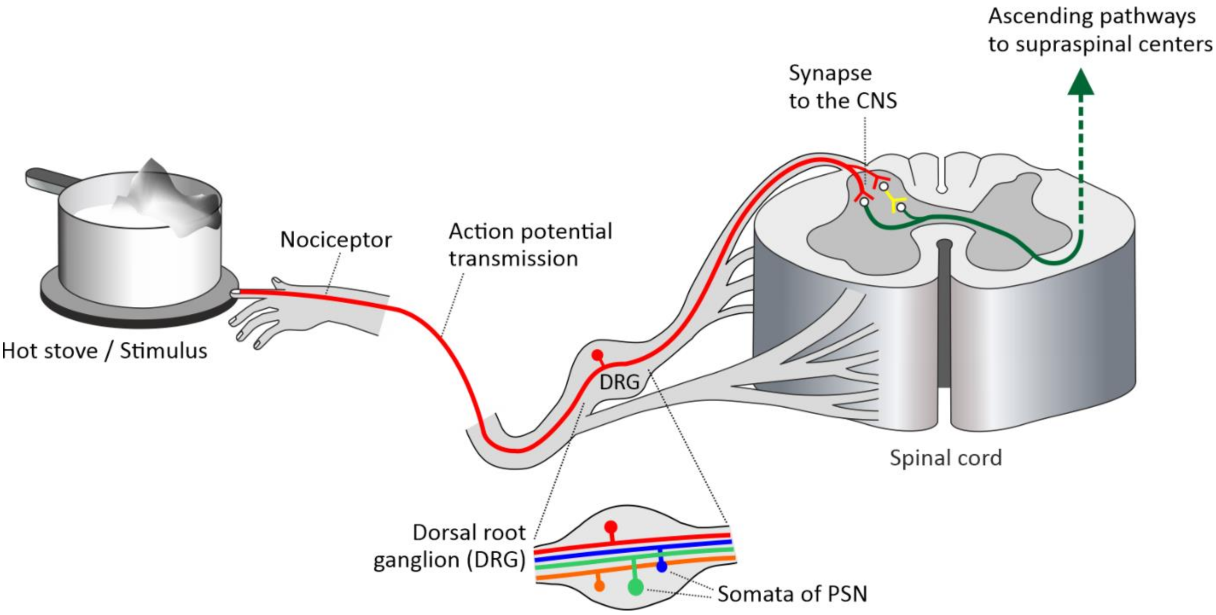

Figure 1: Schematic of the afferent nociceptive pathways.

Pseudounipolar nociceptors (red) are responsible for detecting noxious stimuli in the periphery. Their somata are located in the DRG, together with other types of peripheral sensory neurons (PSNs), of different cells sizes and myelination statuses. The noxious signal is transmitted through the nociceptor and propagated to the second-order neuron within the dorsal horn of the spinal cord. In the CNS the signal is then propagated to supraspinal centers for further processing and to elicit the conscious feeling of pain.

1.2.1 Pain and Its Subtypes

Based on axon diameter, myelination and conduction velocity, in the context of pain, PSN are further subdivided. Aδ- fibers conduct mechanical and thermal stimuli responsible for acute pain. They show slight myelination, a medium diameter and transmit the signal fast. C-fibers possess a small diameter, are non-myelinated and slower conducting. The pain transmitted by them is known as “second pain”. While in acute pain this ascending pain neuraxis is highly functional, chronic pain can be caused both in peripheral and central loci (Basbaum et al., 2009), with possible changes in pain signaling pathways (Bourinet et al., 2014) such as hypersensitivity of the PSN. Two common supraspinal centers involved in pain processing are the primary sensory cortex (S1) for the “discriminative” aspect of pain (Vierck et al., 2013) and the anterior cingulate cortex (ACC) for the ”motivational” aspect of pain (Bushnell et al., 2013; Fuchs et al., 2014; Sewards & Sewards, 2002; Vogt, 2005).

Three subtypes of pain are of specific relevance for this thesis. First of all, acute pain. It is the type of pain that fulfils a physiological function as a warning system and is highly damaging when missing (D. L. H. Bennett & Woods, 2014). It is usually of short duration and warns about internal and external dangers. In mice, it is mimicked for example by a localized injection of a receptor-agonist into the hind paw followed by observations (Avenali et al., 2014; Sondermann et al., 2019). Second, inflammatory pain. This subtype is longer lasting and caused by inflammatory processes usually at a site of injury. Indicative of this is that pain counts as one of five hallmarks of inflammation (Ji et al., 2014). The inflammation causes among other processes the release of cytokines (see below), important mediators of sensitization. A rodent model for inflammatory pain is elicited by unilateral injection of Complete Freund’s Adjuvant (CFA) into the hind paw. CFA consists of an emulsion of mineral oil and heat-inactivated Mycobacterium (*Mycobacterium tuberculosis*) and causes a localized inflammation (Patapoutian et al., 2009; Stein et al., 1988). Within this model paw withdrawal tests were performed to measure hypersensitivity and a localized response in only the injected paw was confirmed (Stein et al., 1988). Third, neuropathic pain. This subtype is initiated by nerve damage or trauma. An example in human patients is the pain that is developed after a treatment with chemotherapeutics. In rodents, several prominent models for neuropathic pain exist, that are usually linked to a nerve compression or transection. During this study, the spared nerve injury (SNI) model was used (Bourinet et al., 2014). Within this model, neuropathic pain is elicited by the transection of two branches of the sciatic nerve, sparing the third branch, the sural nerve (Decosterd & Woolf, 2000). Tactile hypersensitivity is caused in the dermatome of the spared nerve. It has been presented that the immune system specifically influences tactile hypersensitivity within the SNI model (Cobos et al., 2018).

1.3 Membrane Proteins are Important for Somatosensation

Around 30% of the proteome are membrane-associated proteins. They can be subdivided into integral membrane proteins, integrated into the membrane, and peripheral membrane proteins that are only loosely attached. They fulfill important functions as receptors and ion channels, for signal transduction, as well as to maintain the structure of the cellular membrane (Marx et al., 2020). These activities are very important to maintain a normal cellular functionality. Therefore, it is no surprise that defects in membrane proteins cause serious deficits. Around 60% of the drugs on the market affect membrane proteins (Marx et al., 2020). While many membrane proteins are well characterized, like for example the TRP channels, about others very little is known so far. Among those are multiple integral membrane proteins that span the membranes completely. Due to this fact, they are named as transmembrane proteins (Tmem). While little is known about most of them, some have been described in the context of oncology as potential biomarkers (Tmem48, Tmem97), or to play a role in tumor progression (Tmem45A, Tmem205) and therefore provide a valuable potential target for future therapeutic options (Schmit & Michiels, 2018). Tmem160, the protein we are specifically focusing on in this study, is a hitherto undescribed transmembrane protein, that we revealed to be involved in chronic neuropathic pain. It is located in the inner mitochondrial membrane and previous studies discovered its downregulation in murine models for inflammatory and neuropathic pain (Rouwette et al., 2016).

1.3.1 Ion Channels in Somatosensation and Pain

Ion channels are membrane proteins and play an essential role in neurons during somatosensory processes. They allow an influx or efflux of charged ions and therefore cause depolarization of the neurons followed by neurotransmitter release and/or the generation of an action potential (Purves et al., 2001). This action potential is then propagated to other neurons and eventually to supraspinal centers where the sensation is perceived. Multiple ion channels including transient receptor potential (TRP) channels and voltage gated calcium channels (VGCC) are penetrable for Ca^{2+}-ions. This ion is specifically important as an intracellular messenger. It activates enzymes, influences gene expression levels and initiates the release of neurotransmitters (Bourinet et al., 2014). Changes in ion channel activatability and expression level can therefore influence perception and, in a long-term situation, benefit pain chronification. Mutations of several ion channels have been described to show an effect on pain and pain perception in human patients ranging from a complete insensitivity to pain to increased pain in a neuropathic condition (D. L. H. Bennett & Woods, 2014).

1.3.1.1 Transient Receptor Potential Channels

Transient Receptor Potential (TRP) channels are relevant for the perception of temperature, pressure, touch, and pain and are often expressed in the primary sensory neurons. They consist of six transmembrane helices and are divided into seven subfamilies (Bourinet et al., 2014). TRP channels are non-specific cation channels and are most often activated in a polymodal manner, among others by different thermal and painful stimuli. Sensing of the surrounding temperature is important to regulate the internal temperature of the body. Homoiothermic mammals rely on a constant body temperature since many metabolic processes are highly temperature dependent. If the temperature is too high, proteins and enzymes will degrade, if it is too low, the processes will be performed too slow. TRP channels help conveying temperature information to supraspinal centers for temperature regulation purposes. As described above, an influx of Ca^{2+}-ions through this channel superfamily elicits several intracellular responses (Bourinet et al., 2014). TRP channels often show a specific temperature range at which they are activated. TRP vanilloid 1 (TRPV1) is activated above 43°C, TRPV2 above 52°C, TRPV3 above 34-38°C, TRPV4 above 27-35°C, TRP melastatin 8 (TRPM8) below 25-28°C and TRP ankyrin 1 (TRPA1) below 17°C (Tominaga & Caterina, 2004). If the temperature is lower than 15°C or higher than 43°C the same channels can not only transmit information about temperature but are also able to elicit a sensation of pain. Many TRP channels are sensitized or activated additionally by pro-inflammatory agents. The TRP channels most relevant for pain signaling in mouse models of pain are TRPV1-4, TRPM3, TRPM8 and TRPA1 (Bourinet et al., 2014). Mutations of the TRP channels influence the normal body functions in different organs including but not limited to the nervous system, the lungs, the heart and the gastrointestinal tract. Hence, TRP channels are promising targets for therapeutics (Kaneko & Szallasi, 2014) including new analgesics (Tsagareli, 2020).

1.3.1.1.1 TRPA1

TRPA1 is a non-selective cation channel. It is permeable for Ca^{2+}-ions and is the only member of the subfamily of TRP ankyrin channels. Like many TRP channels, it is a polymodal receptor. It is responsible for thermosensation, mechanosensation and responds to chemical stimuli. The most prominent chemical activating TRPA1 is allyl isothiocyanate (AITC) the pungent structure in mustard oil (MO). Furthermore, TRPA1 is activated at critically low temperatures and perceives noxious cold (Patapoutian et al., 2009). Reactive oxygen species (ROS) are upregulated or sensitized under inflammatory and oxidative stress conditions and lead to an elevated expression of TRPA1 (Andersson et al., 2008). Consequently, the higher number of channels in the membrane leads to a low activation threshold of the nociceptors. The TRPA1 channel therefore also propagates acute and inflammatory pain. Apart from its role in neurons, TRPA1 expression and activatability was found to be elevated in odontoblast-like cells after the addition of tumor necrosis factor alpha (TNFα) (El Karim et al., 2015). A deletion of TRPA1 in mice caused a reduction in mechanical and cold hyperalgesia, an increased pain response to a stimulus that is normally already painful. Upon inhibition of TRPA1, wildtype mice did not develop mechanical hyperalgesia as normally expected in the CFA model (see above for detail) for inflammatory pain (Patapoutian et al., 2009).

1.3.1.1.2 TRPV1

TRPV1 is expressed in a subpopulation of sensory neurons, specifically in C- and Aδ-fibres and is highly relevant in thermosensation as well as pain perception. The channel is activated in a polymodal manner, i.e., it is not limited to one specific stimulus. The threshold for activation by temperature lies at 43°C (Purves, 2008). Additionally, low pH, metabolic products of arachidonic acids (Mathie, 2010) and multiple chemicals can cause an activation of the TRPV1 channel. The most prominent chemical activating the channel is capsaicin (Caps) (Bourinet et al., 2014), the pungent molecule in chili (Purves, 2008). TRPV1 is a non-specific cation channel. Upon activation, it opens and is highly permeable to Ca^{2+}-ions (Jeffry et al., 2009). The influx of positive charges causes a depolarization and consequently an action potential. This signal elicits a painful, burn-like sensation. TRPV1 is located in peripheral sensory neurons, not only at their distal but also in their proximal terminals where it can contribute to synaptic transmission (Jeffry et al., 2009). Additionally, it is expressed in other organs such as lung and bladder, where it is considered to detect visceral pain. In the sensory neurons TRPV1 often shows colocalization with TRPA1 to detect and convey information on dangerous stimuli. Under neuropathic pain conditions, TRPV1 expression levels are increased promoting hyperalgesia and allodynia, the painful perception of a normally innocuous stimulus. Knockout (KO) mice for TRPV1 respond normally to pressure and touch, while heat hypersensitivity is reduced in different pain models (Patapoutian et al., 2009). The importance of TRPV1 in pain perception, specifically under neuropathic conditions makes its antagonists favorable targets in drug discovery (Bourinet et al., 2014).

1.3.1.1.2.1 Sensitization and Desensitization of TRPV1

Tissue damage and localized inflammatory processes lead to the release of multiple mediators including bradykinin and prostaglandins. These mediators can increase the sensitivity of TRPV1 channels and therefore of the nociceptors. Mechanistically, this occurs by phosphorylation of the channel by protein kinase C. This reduces the activation threshold temperature of TRPV1. For example, on sunburnt skin taking showers at a normal temperature causes burn-like pain. This phenomenon is known as allodynia. On the other hand, (heat-induced) activation of TRPV1 leads to conformational changes including a closed channel pore (L. Luo et al., 2019; Sanz-Salvador et al., 2012; Touska et al., 2011; Vyklický et al., 2008). This initiates a quick response preventing immediate repeated activation of the same channels. A more long-term desensitization can be caused by a degradation of Caps-responsive neurons. Opposing to murine and human TRPV1, the platypus TRPV1 channel lacks the ability to conformationally change to a desensitized state. Additionally, the platypus is unable to bear higher surrounding temperatures (L. Luo et al., 2019), possibly due to the inability to desensitize.

1.3.1.2 Voltage Gated Calcium Channels

Voltage gated calcium channels (VGCC) are localized in the membrane of excitable cells, i.e., neurons and muscle cells (Shilpi & Uddin, 2020). Upon membrane depolarization, the channels open and enable an influx of Ca^{2+}-ions (Heck et al., 2021). This influx causes different processes as described above (Bourinet et al., 2014) and also initiates a desensitization and downregulation of VGCC (Wu et al., 2006). VGCC are known to play an important role in pain signaling, not only in the primary sensory neurons but also in the neurons of the spinal dorsal horn and supraspinal centers (Harding & Zamponi, 2022; Zamponi et al., 2009). In the periphery they contribute to hypersensitivity during inflammation, namely by causing thermal hyperalgesia. This is achieved by a change in firing rate as well as an outgrowth of additional neurites (Pitake et al., 2019).

1.4 Mechanisms of Pain

1.4.1 Mitochondria and Their (Dys)Function in Pain

Mitochondria are organelles present in almost all cells of the body. Their main function lies in the generation of energy in form of adenosine triphosphate (ATP). During this process of oxidative phosphorylation, the mitochondrial electron transport chain (ETC) also produces ROS (E. Murphy et al., 2016) and consumes oxygen (Flatters, 2015). Furthermore, mitochondrial post-translational modifications are used to transfer information within the cell. An involvement of mitochondria with cell death has also been described (E. Murphy et al., 2016). Multiple metabolic processes are influenced by mitochondria (DiMauro & Schon, 2003; Zeviani & Di Donato, 2004). Additionally, mitochondria serve as an intracellular storage for calcium buffering (Flatters, 2015; Rouwette et al., 2016). Moreover, mitochondrial dysfunction correlates with many diseases including pain. For example, in humans, the majority of patients with mitochondrial diseases reported pain as a symptom (van den Ameele et al., 2020). Mitochondrial dysfunction contributes to chronic pain in patients and animal models (Flatters, 2015). Furthermore, each major mitochondrial function as listed above can affect neuropathic and inflammatory pain if it is not acting normally (Sui et al., 2013) including oxidative stress and compilation of misfolded proteins (Yousuf et al., 2020). In multiple pain models in mice, mitochondria showed irregular distribution and morphology in neurons (Guo et al., 2013). Models for inflammatory (CFA, see above) and neuropathic (SNI, see above) pain revealed an increase in mitochondria in the dorsal horn of the spinal cord. Upon inhibition of mitochondria, pain behavior was averted in both models (Guo et al., 2013). Moreover, antioxidants showed an effect as pain-treating substances (Guo et al., 2013).

1.4.2 Neuroimmune Interactions in Pain

Neuroimmune crosstalk gains more and more importance in pain research (Cook et al., 2018; Ren & Dubner, 2010). In humans, it has been described that the pain pathways differ immensely between men and women, both strongly depending on neurons as well as immune cells. More specifically, pain signaling in men was reported to rely on microglia and macrophages while women would need T-Cells in their pain pathway instead (Dance, 2019; Rosen et al., 2017). The existence of sex-differences regarding neuroimmune interactions were confirmed in rodent pain models (Lopes, Malek, et al., 2017). Microglia also play an important role in the context of pain by influencing the neuroimmune crosstalk in the central nervous system (CNS) (G. Chen et al., 2018). Furthermore, an influence of the immune response on mechanical hypersensitivity has been confirmed specifically while cold-elicited hypersensitivity remained unchanged (Cobos et al., 2018). Neuroimmune crosstalk is often facilitated by cytokines and chemokines (Cook et al., 2018). They are small proteins released to the extracellular space where they perform their action either in an autocrine (acting on the releasing cell), paracrine (acting on surrounding cells) or endocrine (acting on distant cells) manner. Chemokines are a specific subgroup of cytokines that are specialized on attracting other cells, most often lymphocytes, hence the name "chemoattractant cytokines" (chemokines) (Zhang & An, 2007). Other cytokines activate other immune cells (interleukins (IL)) or stimulate cell growth (colony-stimulating factors (CSF)) (K. Murphy & Weaver, 2018). Cytokines can act both pro- and anti-inflammatory. Proinflammatory cytokines have been described to activate neurons directly under chronic pain conditions (Zhang & An, 2007). Both pro- and anti-inflammatory cytokines are highly relevant in neuropathic pain conditions (Sommer et al., 2018). This indicates a high importance of balanced levels of pro- and anti-inflammatory cytokines.

Examples for cytokines investigated in this study, that showed a high relevance in the pain context, are IL10 and IL13, both anti-inflammatory cytokines. IL10 decreases the activation of macrophages while IL13 reduces production of cytokines in macrophages (K. Murphy & Weaver, 2018). Two pro-inflammatory cytokines are CCL17 that collaborates with TNFα in pain generation (Cook et al., 2018) and CXCL12 that is involved in neuropathic pain (Y. Yu et al., 2017) and shows a regulation in the DRG of rats in the SNI model for neuropathic pain (Bai et al., 2016). sICAM-1 is another pro-inflammatory cytokine (Witkowska & Borawska, 2004) discussed in the context of inflammatory and neuropathic pain (Luchting et al., 2017). On the other hand, IL1ra is commonly known as anti-inflammatory and even causes analgesia when injected centrally (Webster et al., 2017). The pro-inflammatory cytokine MIP1β has been described to be upregulated upon peripheral nerve injury and to play a role in inducing tactile allodynia (Saika et al., 2012). IL2 is described to act in both a pro (Koch et al., 2007) - and an anti (Banchereau et al., 2012) - inflammatory manner. It has been found to reduce inflammation and avoid an uncontrolled immune response (Banchereau et al., 2012) but it was also discovered to be elevated in the serum of severe pain patients among other pro-inflammatory cytokines (Koch et al., 2007).

1.4.3 Peripheral and Central Sensitization

Neuronal excitability in the context of pain is not constant, meaning that the same stimulus not always elicits the same response. This is heavily influenced by sensitization processes. Two important concepts in this context are allodynia and hyperalgesia. Allodynia describes the painful response to a normally innocuous stimulus, while hyperalgesia is an increased pain response to a stimulus that is normally already painful. This hypersensitivity can either occur at the site of injury in the periphery, where it is usually caused by peripheral sensitization or the causes lie in spinal or supraspinal regions and are termed central sensitization (Vardeh & Naranjo, 2017). Both peripheral and central sensitization have been described in the generation of musculoskeletal pain (Graven-Nielsen & Arendt-Nielsen, 2002), as well as pain hypersensitivity in general (Latremoliere & Woolf, 2009). In healthy humans and pain patients, processes of central sensitization were studied. This revealed mechanisms such as increased excitability, disinhibition and an overall engagement of signals that would not usually trigger an action potential on their own. This uncoupling can cause hyperalgesia and allodynia (Latremoliere & Woolf, 2009). Peripheral sensitization is normally connected to inflammatory surroundings after a local tissue injury. In detail, specific neurotransmitters from neighboring neurons act locally in this context (Wei et al., 2020). Additionally, diverse other mechanism can cause peripheral sensitization (Dubin & Patapoutian, 2010; Patapoutian et al., 2009).

1.5 Proteomics to Reveal New Potential Targets

The term proteomics falls under the umbrella of all -omics describing high-throughput methods in biology. Proteomics is the study of all proteins within a specific cell or organism (Husi & Albalat, 2014). The advantage of proteomics compared to transcriptomics, the study of RNA, is that the proteins are the main actors in the body and an increase or decrease in RNA level does not necessarily cause an immediate change in protein expression level. This is mainly due to posttranscriptional and posttranslational modifications. Proteomic studies are performed using mass spectrometry and have increased in output and quality recently. To study the membrane-based proteome, earlier, it was necessary to perform membrane-enrichment steps (Rouwette et al., 2016), which is not required anymore, as proven by this study. Due to its high output, proteomics is a convenient resource to generate hypotheses. In this case, proteomics was performed on DRG of mouse models for inflammatory (CFA, injection of PBS as vehicle control) and neuropathic (SNI, sham surgery in controls) pain (Rouwette et al., 2016). 12 proteins were found to be differentially regulated in both pain models. One protein among those that was downregulated in both pain models was Tmem160. Since this candidate was undescribed so far, it was chosen as a candidate protein for further characterization.

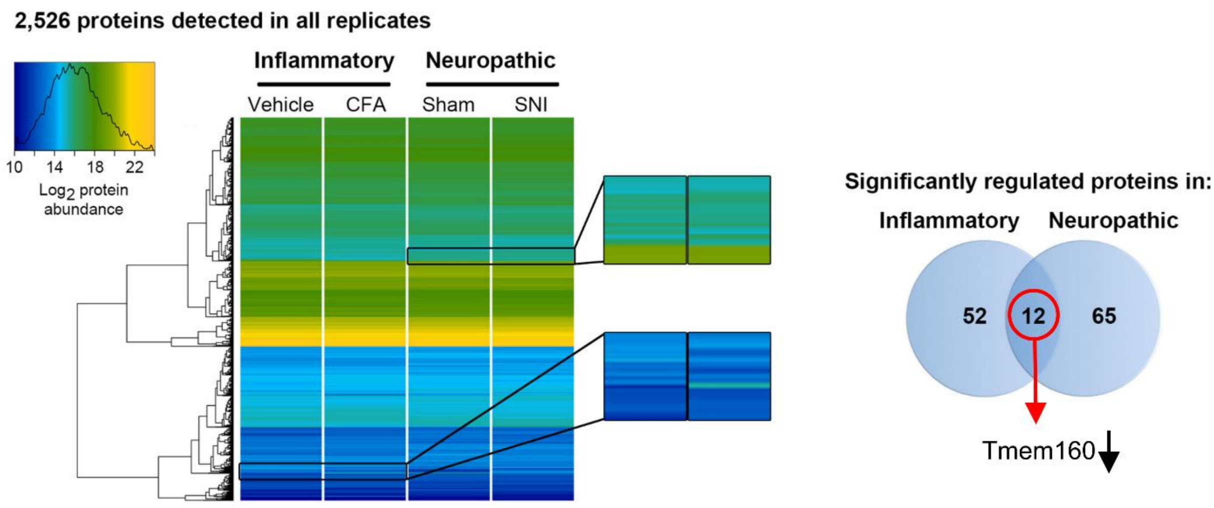

Figure 2: Proteomic analysis of different murine pain models, adapted from (Rouwette et al., 2016).

Membrane-enriched quantitative proteomics was performed on DRG of two different pain models (CFA, inflammatory pain and SNI, neuropathic pain) and appropriate controls. Multiple proteins were found to be significantly regulated, including 12 overlapping between the models. Tmem160 expression was found to be downregulated in both pain models. Therefore, it was picked as a protein of interest in this study.

1.5.1 Tmem160

This work is the first to gain a functional insight into Tmem160. But the protein itself has occurred in proteomic and transcriptomic data sets of murine DRG before. It is known to be expressed across cell types in primary sensory neurons. In addition, it was found to be expressed in other tissues and cell types in transcriptome-based data sets (Thakur et al., 2014; Usoskin et al., 2015) (database:mousebrain.org (Zeisel et al., 2018)). Recently, Tmem160 expression was confirmed in immune cells, more specifically a subset of microglia in male mice (Tansley et al., 2022). Tmem160 showed a downregulation in two different murine pain models (Rouwette et al., 2016) (Figure 2) but has not been described further in the context of pain and its chronification.

1.6 Age and Sex as Biological Variables in Animal Studies

As described above, sex has been recognized as an important factor in preclinical research (Mapplebeck et al., 2016; Mapplebeck et al., 2018; Millecamps et al., 2022; Mogil, 2012; Price et al., 2018; Price & Gold, 2018; Segelcke, Fischer, et al., 2021; Sorge et al., 2011; Sorge et al., 2015). Multiple mechanisms in physiology and pathology differ immensely between male and female. This includes differential pain pathways, mainly via microglia in male and T-cells and macrophages in females (Dance, 2019; Grace et al., 2021; X. Luo et al., 2021; Mapplebeck et al., 2016; Sorge et al., 2015).

Another factor, that was so far not focused on is age. In 2017, a survey revealed that the age of rodents used in preclinical experiments highly varied between laboratories. Often the reasons why specific ages were chosen lied in practical reasons (housing costs, availability) rather than scientific decisions. An additional problem is that the age is often reported in an imprecise way, using terms such as “adult” instead of a specific age in days, weeks or months. Researchers reported that they deemed mice adult from 6 to 20 weeks (w) upwards (Jackson et al., 2017). The Jackson Laboratory, a common provider for laboratory mice, more specifically of the strain C57BL/6J, considers this strain as mature adults once they reached the age of 12w in both sexes (Flurkey et al., 2007). Sexual maturation is already achieved at 5w of age (Flurkey et al., 2007) but many developmental processes continue subsequently. These processes include the immune system (Kincade, 1981), the nervous system (Fu et al., 2013) and the sense of touch (Michel et al., 2020).

Due to these results, it is highly suggested to carefully pick age- and sex-matched controls as well as to precisely describe both factors in publications.

1.6.1 Pediatric Pain

In children, pain management is especially difficult. First of all, this is due to limited communication options in young children (O’Donnell & Rosen, 2014). But in addition, and more important in the context of this thesis, pain and nociceptive mechanisms in children differ from the same processes in adults. A common misperception was, that young human children feel less pain than adults. More current reports reveal that this is not true, in fact, studies even opposed this early assumption. Nociceptors reach functional maturity already before birth and do not differ between children and adults, but other structures involved in pain pathways vary greatly throughout maturation. Axonal structures, as well as synapses and junctions show a lack of organization in infants. Additionally, they are not able to differentiate properly between normal touch and nociceptive signals. Furthermore, the descending pain system is not fully established in newborns, and they often lack complete myelination of fibers. All of this leads to a higher pain sensitivity in children (Pancekauskaitė & Jankauskaitė, 2018) and clearly shows that pain perception develops and changes during maturation. In humans there are more and more studies suggesting an adjusted pain treatment in children (Fitzgerald, 2005; Friedrichsdorf et al., 2016). In addition, there are indications that inflammation in newborns, caused by infections, influences pain perception and tactile sensitivity and potential even impacts pain perception in adults (Cobo et al., 2022).

1.7 Aims of the Study

The molecular mechanisms underlying somatosensation and more specifically pain and its chronification are yet to be completely understood. This is of particular relevance given the high prevalence of chronic pain in human society coupled to the limited treatment options. Therefore, it is important to better understand mechanisms limited to chronic pain to be able to specifically target them in future medications. This thesis combines two different aspects of the role of proteins in murine studies in nociception and somatosensation. The role of one specific transmembrane protein, Tmem160, in the context of pain was characterized in depth. Additionally, the role of TRP channels in thermosensation and nociception as well as the overall proteome of the DRG, as one specific part of the pain neuraxis, was studied in mice throughout maturation.

1.7.1 Characterization and Effect of Tmem160 on Somatosensation

Membrane proteins are relevant for nociception and pain signaling. Previous to this study, proteomics revealed Tmem160 as a potential protein of interest in the DRG in the context of pain. This study seeks to characterize the role of Tmem160 in pain by using a global and a conditional (limited to around 80% of the PSN) KO mouse line. A battery of pain models, *in vivo* and *in vitro* experiments were performed to gain insights into the localization, function and action mechanisms of Tmem160 in the context of acute and chronic pain. This will reveal if Tmem160 has potential as a target for human pain treatment in the future. Adult mice of both sexes were compared to reveal potential sex differences.

1.7.2 Characterization of Age- and Sex-Differences in the DRG Proteome and Their Effect on Somatosensation

To specifically investigate the influence of maturation and sex on somatosensation, nociception and the composition of the DRG, *in vivo* and *in vitro* studies were applied to juvenile and adult mice of both sexes. The methods included studies of acute pain behavior and thermal sensitivity *in vivo*, as well as neuronal excitability and neuronal TRPV1 expression *in vitro*. Furthermore, mass spectrometry was applied to study the proteome and a commercially available array was applied to study cytokine and chemokine levels in DRG under naïve conditions.

2 Materials and Methods

2.1 Materials

Table 1: Antibodies

Reagent or Resource	Supplier/Source	Composition	Identifier
Chicken anti-peripherin, IgY, polyclonal	Abcam	1:100	RRID: AB_777207
Donkey anti-chicken, Alexa Fluor 488	Dianova	1:250	N/A
Donkey anti-goat, Alexa Fluor 488, IgG, polyclonal	Life technologies	1:250; 1:1000	RRID: AB_2534102
Donkey anti-rabbit, Alexa Fluor 488, IgG, polyclonal	Life technologies	1:250	RRID: AB_2535792
Donkey anti-rabbit, Alexa Fluor 680, IgG, polyclonal	Life technologies	1:250	RRID: AB_2534018
Donkey anti-mouse, Alexa Fluor 488	Life technologies	1:250	N/A
Donkey anti-mouse, Alexa Fluor 546, IgG, polyclonal	Life technologies	1:250	RRID: AB_2534012
Goat anti-chicken, Alexa Fluor 555, polyclonal	Life technologies	1:250	RRID: AB_2535858
Goat anti-chicken, Alexa Fluor 647, polyclonal	Life technologies	1:250	RRID: AB_2535866
Goat anti-rabbit, Alexa Fluor 488, IgG, polyclonal	Life technologies	1:250	RRID: AB_2576217
Goat anti-rabbit, Alexa Fluor 555	Life technologies	1:250	N/A
Goat anti-Tmem160 (N-19), IgG, polyclonal	Santa Cruz	1:10	N/A
Mouse anti-c-Myc, IgG1, monoclonal	Life technologies	1:100	RRID: AB_2533008
Rabbit anti-NDUFV2, IgG, polyclonal	Protein Tech	1:100	RRID: AB_2149048
Rabbit anti-NF200, IgG, polyclonal	Sigma Aldrich	1:200	RRID: AB_477272
Rabbit anti-Tmem160, polyclonal	Sigma Aldrich	1:10	RRID: AB_2682965
Rabbit anti-TRPV1	Alomone	1:100	RRID: AB_2313819
All antibodies directed against mitochondrial proteins employed for western blots	Generated in house by Sven Dennerlein		N/A

Table 2: Chemicals, peptides, and recombinant proteins

Reagent or Resource	Supplier/Source	Composition
Acetic Acid	Merck	
Acetone	Sigma Aldrich GmbH	
Acetonitrile	Thermo Fisher Scientific	
Ammonium bicarbonate	Sigma Aldrich GmbH	
Ammonium Sulfate	Merck	
Antimycine A	Sigma Aldrich GmbH	
Betadine®	Avrio Health L.P.	
Bovine Serum Albumine (BSA)	Sigma Aldrich GmbH	
Buprenorphine; TEMGESIC	Essex pharma GmbH	
Capsaicin	Sigma Aldrich GmbH	
Carprofen; Rimadyl	Zoetis	
Chloroform	Merck	
Collagenase	Gibco	

Complete Freund's adjuvant	Sigma Aldrich GmbH	
cOmplete ULTRA Tablets, Mini, EASYpack	Roche	
Coomassie Brilliant Blue G250	Serva	
Dimethylsulfoxide (DMSO)	Sigma Aldrich GmbH	99.9%
Dithiothreitol	Sigma Aldrich GmbH	1 M
DMEM (Dulbecco's Modified Eagle Medium)/F-12 (1:1) + GlutaMax-I	Gibco	
DMEM/F-12 (1:1) + GlutaMax-I + Serum	Gibco	+10% FBS
Donkey Serum	Dianova	
Dulbecco's Phosphate Buffered Saline (DPBS)	Gibco	
Ethanol	Sigma Aldrich GmbH	
FCCP	Sigma Aldrich GmbH	
Fetal Bovine Serum (FBS)	Life technologies	
FuGENE® HD Transfection	Promega	
Fura-2/AM Cell Permeant	Life technologies	
Formic Acid	Thermo Fisher Scientific	
Glycerol	Roth	
Glycerol	Thermo Fisher Scientific	
Hanks' Balanced Salt Solution; HBSS	Gibco	10x, [+] $CaCl_2$, $MgCl_2$
HEPES	Gibco	1 M
Horse Serum	Thermo Fisher Scientific	
Iodoacetamide	Sigma Aldrich GbmH	
IRDye 800CW Streptavidin	LI-COR	
Isoflurane	cp-pharma	
Laminin	Invitrogen	
Methanol	JT Baker	
Mustard Oil, AITC	Sigma Aldrich GmbH	95%
NaCl	Merck	
Novex Sharp Pre-Stained Protein Standard	Thermo Fisher Scientific	
NP40/Igepal	Sigma Aldrich GmbH	
NuPAGE LDS Sample Buffer	Life Technologies	4x
NuPAGE MOPS SDS Running Buffer	Life Technologies (Thermo Fisher Scientific)	4x
NuPAGE Antioxidant	Life Technologies	
NuPAGE Sample Reducing Agent	Life Technologies	10x
NuPAGE 4-12% Bis Tris Gel	Thermo Fisher Scientific	1.5mmx 10 well
Oligomycin B	Sigma Aldrich GmbH	
Opal 570 dye	Perkin Elmer	
Ovogest	MSD Animal Health	
Oxygen	Westfalen Gas	
Papain	Worthington	
PBS	Thermo Fisher Scientific	10x
PBS	Gibco	10x, pH7.4, [-] $CaCl_2$, $MgCl_2$
PFA	Electron Microscopy Sciences	16%, used as 4% in PBS
***ortho*-Phosphoric Acid**	Sigma Aldrich GmbH	
Pluronic F-127	Invitrogen	
Poly-D-Lysine (PDL)	Millipore	1mg/ml in H_2O
Potassium Chloride (KCl)	Roth	
Power SYBR Green PCR Master Mix	Thermo Fisher Scientific	

Pregmagon	IDT Biologika GmbH	
QIAzol Lysis Reagent	QIAGEN	
RNAscope probe Mm-Tmem160	ACD	
rhß-NGF	R&D Systems	
rhGDNF	R&D Systems	
rhNeurotrophin-3	R&D Systems	
rhNeurotrophin-4	R&D Systems	
Sera-Mag SpeedBead beads	Cytiva	1:1 mix
SlowFade Gold Antifade Mountant	Thermo Fisher Scientific	
SlowFade Gold Antifade Mountant with DAPI	Thermo Fisher Scientific	
Streptavidin (IRDye 800CW)	Li-COR	
Sucrose	Merck	30% in PBS
Tissue-Tek O.C.T.	Sakura	
TMRM	Invitrogen/Life technologies	
Tris	Accugene/Avantor	1 M
TRIS-HCl	Roth	
TritonX-100	Roth	
Trypsin	Serva	
Trypsin/Lys- C	Promega	
Tumour Necrosis Factor (TNFα)	Peprotech	
Water MS grade	Sigma Aldrich GbmH	

Table 3: Critical commercial assays

Reagent or Resource	Supplier/Source
Complex IV Rodent Enzyme Activity Dipstick Assay Kit	Abcam
Genomic DNA Isolation Kit for Tissue and Cells	Nexttec™
NucleoSpin RNA XS Kit	MACHEREY-NAGEL
P3 Primary Cell 4D-Nucleofector X Kit	Lonza
Proteome Profiler Mouse Cytokine Array Kit, Panel A	R&D Systems
QuantiTect Reverse Transcription Kit	QIAGEN
RNAscope Multiplex Fluorescent Reagent Kit v2	ACD
RNeasy Mini Kit	QIAGEN

Table 4: Proteome profiler - Mouse Cytokine Array Panel A (R&D Systems)

Reagent or Resource	Description
Mouse Cytokine Array Panel A	4 nitrocellulose membranes each containing 40 different capture antibodies printed in duplicate.
Array Buffer 4	A buffered protein base with preservatives.
Array Buffer 6	A buffered protein base with preservatives.
Wash Buffer Concentrate	25-fold concentrated solution of buffered surfactant with preservative.
Detection Antibody Cocktail, Mouse Cytokine Array Panel A	Biotinylated antibody cocktail. Lyophilized.
4-Well Multi-dish	Clear 4-well rectangular multi-dish.
Transparency Overlay Template	1 transparency overlay template for coordinate reference.

Table 5: Experimental models: cell lines

Reagent or Resource	Supplier/Source	Identifier
HEK293T	ATCC	CRL-3216

Table 6: Experimental models: organisms/strains

Reagent or Resource	Supplier/Source	Identifier
C57BL/6J (M. musculus)	Jackson Lab	RRID: IMSR_JAX:000664
EIIa-Cre (M. musculus)	Jackson Lab	B6.FVB-Tg(EIIa-cre)C5379Lmgd/J Stock No: 003724
***Tmem160* KO (M. musculus)**	generated in house	N/A – see methods for detail
Advillin-Cre (M. musculus)	Kind gift of Prof. Dr. Klaus-Armin Nave, MPIEM, Göttingen	(Zurborg et al., 2011) Tg(Avil-cre)1Phep MGI:5292346

Table 7: Oligonucleotides

Reagent or Resource	Supplier/Source	Composition
Primers for genotyping and qPCR	Generated in house	See below for details

Table 8: Primer for qPCR

Gene/Protein	Forward (always 5'-3')	Reverse (always 5'-3')
GAPDH	CAATGAATACGGCTACAGCAAC	TTACTCCTTGGAGGCCATGT
Iba-1	GGATTTGCAGGGAGGAAAA	TGGGATCATCGAGGAATTG
mt-Cox1	GAACCCTCTATCTACTATTCGG	CAAGTCAGTTTCCAAAGCCT
mt-Cytb	ATTCCTTCATGTCGGACGAG	GGGATGGCTGATAGGAGGTT
mt-ND2	CGCCCCATTCCACTTCTGATTACC	TTAAGTCCTCCTCATGCCCCTATG
Tmem160	TCTCCTTCATGCAGAGTGACAT	ATCCTCAGGCACCAGTTCCAC
Uqcr10	CGCAGAACTTCCACCTTTGC	CCACAGTTTCCCCTCGTTGA

Table 9: Primer for genotyping

Gene/Protein	Genotyping Primer (always 5'-3')
Advillin-Cre genotyping	TTTCCGGTTATTCAACTTGCACCA
Fragment size: 281 bp	GCAATGGCTCCCTGTTCACT
Tmem160 genotyping	ACTAGTACAAGTTTTGTTTCCTGGC
Fragment sizes: Tmem160 WT = 235 bp; Tmem160	GGCCAGAGTAAGGCAAGCATC
floxed = 269 bp; Tmem160 recombined, KO = 202 bp	CGGTCTCTCACCTAGGCAGT

Table 10: Recombinant DNA

Reagent or Resource	Supplier/Source
HyPer-mito-YFP	Kind gift from Prof. Dr. Michael Müller, UMG Göttingen
pCDNA3.1-myc-His	Invitrogen
pCMV6-TMEM160-Myc-DDK	Origene

Table 11: Software and algorithms

Reagent or Resource	Supplier/Source	Identifier
Adobe Illustrator®	https://www.adobe.com/de/products	RRID: SCR_010279
Adobe Photoshop	Adobe Systems	RRID: SCR_04199
Axiovision	Zeiss	RRID: SCR_002677
Boris	http://www.boris.unito.it/	RRID: SCR_021434

DIA-NN	https://github.com/vdemichev/DiaNN	RRID: SCR_022865; Version 1.8.0
GraphPad Prism	www.graphpad.com/scientific-software/prism	RRID: SCR_002798; Version 8 and 9
ImageJ	https://imagej.net/Fiji	RRID: SCR_003070
InkScape	https://inkscape.org/en/	RRID:SCR_014479
MaxQuant	Max Planck Institute of Biochemistry	RRID:SCR_014485; Version 1.6.17.0
Metafluor	Molecular Devices	RRID: SCR_014294
Microsoft 365®	https://www.microsoft.com/	RRID: SCR_014001
Mouse proteome database	Uniprot	Downloaded on 2021- 07- 08, 17070 entries
R	https://www.r-project.org/	Version 4.1.1
SPSS	IBM	RRID: SCR_002865

Table 12: Machines and equipment

Reagent or Resource	Supplier/Source	Identifier
5-0 PROLENE®	Ethicon	N/A
6-0 PROLENE®	Ethicon	N/A
Aurora Series UHPLC column	IonOpticks	N/A
Axio Observer Z1	Zeiss	RRID: SCR_021351
Bioruptor Pico	Diagenode	
CatWalk™ XT gait system	Noldus	RRID: SCR_021262
Cryostat	Leica	RRID: SCR_002865
FemtoJet	Eppendorf	
Hargreaves radiant heat apparatus	IITC Life Science	RRID: SCR_012152
Lightcycler 480	Roche	RRID: SCR_020502
Microsyringe	Hamilton	N/A
NanoElute	Bruker Daltonik	N/A
NanoPhotometer N60	Implen	N/A
4D- Nucleofector X Unit	Lonza	N/A
Odyssey Infrared Imaging System	LI-COR	N/A
Plantar Aesthesiometer	Ugo Basile	RRID: SCR_021751
Precellys Homogenisator	Bertin Instruments	N/A
Protein LoBind tube	Eppendorf	N/A
Seahorse XF Analyzer	Seahorse Bioscience	RRID: SCR_019540
SuperForstPlus™ slides	Thermo Fisher Scientific	N/A
timsTOF Pro	Bruker Daltonik	N/A
Von Frey filaments	Bioseb	N/A

2.1.1 Experimental Models

2.1.1.1 Mice

C57BL/6J mice were acquired from Charles River, further bred in house and subsequently used for experiments. Mice were group-housed in an age- and sex-matched manner using a 12h light/dark cycle. Individually ventilated cages were used in the animal facility of Max Planck Institute for Multidisciplinary Sciences (Göttingen, Germany) as well as in the University Medical Centre (Münster, Germany) while open housing was utilized at the University of Vienna (Austria). All mice were provided with water and food *ad libitum.* Experiments with mice within the Tmem160-section of the thesis were performed at an age between 10w and 14w in Göttingen and Münster, experiments within the aging-section were performed in Göttingen and Vienna with mice at an age of 4-5w and 12-15w. Mice of both sexes were used in most of the experiments as indicated. Housing, sacrificing and all experiments using mice were conducted in accordance with ARRIVE (Animal Research: Reporting of In Vivo Experiments) guidelines and the ethical guidelines for the investigation of experimental pain in conscious animals (Zimmermann, 1983). All experiments were approved by the institutional animal care and use committee (IACUC) of the Max Planck Institute for Multidisciplinary Sciences, the Animal Ethics Committee of the State Agency for Nature, Environment and Consumer Protection North Rhine-Westphalia (LANUV, Germany; registration number: 81-02.04.2017.A491), the Landesamt für Verbraucherschutz und Lebensmittelsicherheit of Lower Saxony (LAVES, Germany; registration number: Az 17/2501 und Az 13/1359) and/or the Bundesministerium für Bildung, Wissenschaft und Forschung, Refarat V/3b Tierversuchswesen und Gentechnik (BMBWF-V/3b, Austria).

2.1.1.2 Generation and Validation of Tmem160 Knockout Mice

KO mice for *Tmem160* were generated at the animal facility of the Max Planck Institute for Multidisciplinary Sciences (Göttingen, Germany) using CRISPR/Cas9 technology (Wang et al., 2013; H. Yang et al., 2014). Female C57Bl/6JRj mice (3 – 4w) were treated with pregnant mare serum gonadotropin (7.5 U, Pregmagon) and human chorionic gonadotropin (5 U, Ovogest) until superovulation and subsequently bred with C57Bl/6JRj males to collect inseminated eggs. *Tmem160* Exon 1 was flanked with loxP sites (Figure 3, Allele: *Tmem160* floxed) using in-house made CRISPR reagents (hCAS9_sgRNAs_HDR.DNA; 1 gRNA/loxP site; one long dsDNA as repair template) by microinjection (Femtojet) into the pronucleus and the cytoplasm of zygotes at the pronuclear stage. To reduce the probability for off-target effects, short-lived RNA-based reagents (Doench et al., 2016; Tycko et al., 2019) were used for anything gene-specific (i.e., signal guide RNAs (sgRNAs) and hCAS9) instead of plasmid-coded reagents. The cutting frequency determination (CFD) specificity was determined at 96 out of 100 (sgRNA1) and 92 out of 100 (sgRNA2), meaning low chance for off-target effects (Doench et al., 2016; Tycko et al., 2019). After genetic manipulation, zygotes were planted in both oviducts of pseudopregnant NMRI (Naval Medical Research Institute) foster mice. To cause a global (constitutive) *Tmem160* KO, floxed *Tmem160* mice were mated with an EIIa-Cre driver line (Holzenberger et al., 2000; Lakso et al., 1996) (recombination at E0.5). Genotypes (Allele: *Tmem160* recombined, KO) were confirmed using DNA from tail biopsies (performed with the Genomic DNA Isolation Kit for Tissue and Cells according to the manufacturer's protocol) in a PCR followed by quality control analysis on a 1% agarose gel (primers and fragment sizes are listed in Table 9), and quantitative reverse transcription PCR (qPCR with primers directed against exon 2 and exon 3 of Tmem160 mRNA; for detailed procedure and primers please see below). In addition, tissue sections were observed with in situ hybridization methods using RNAscope technology (Figure 5, RNAscope probe Mm-Tmem160 targets region 2-819 of Tmem160 mRNA). *Tmem160* KO mice were healthy and fertile.

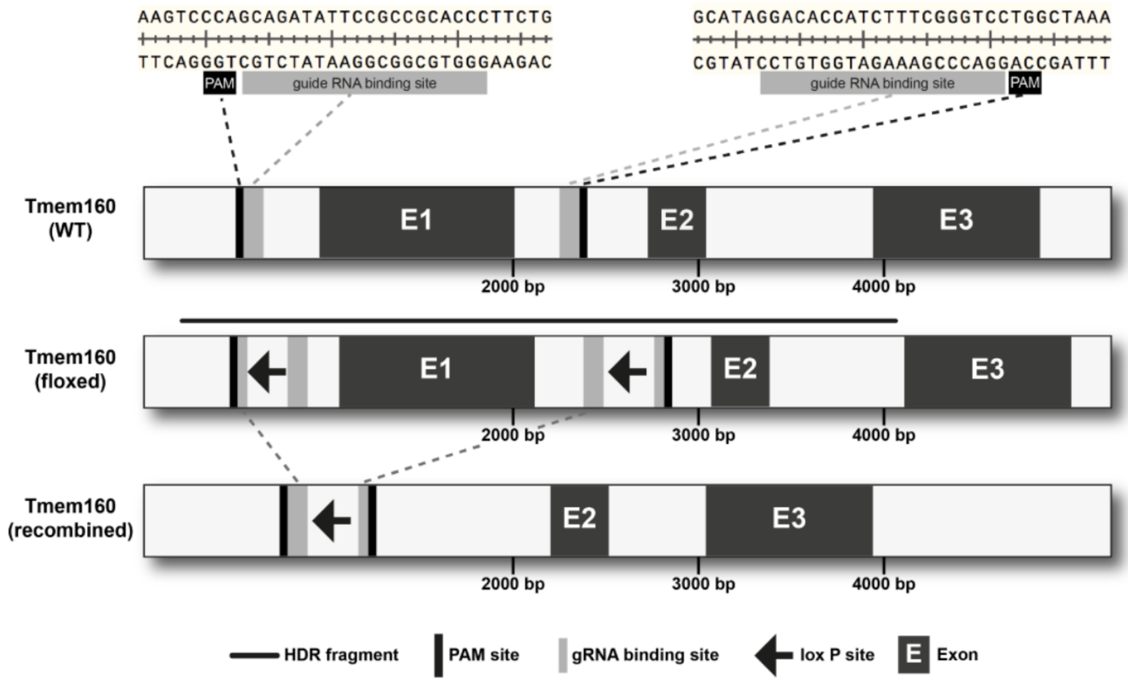

Figure 3: Schematic of the *Tmem160* gene and knockout, adapted from (Segelcke, Fischer, et al., 2021).

Schematic of the *Tmem160* gene and the generation of a global *Tmem160* knockout (KO, recombined) mouse line by CRISPR-Cas9 technology. The original gene (WT) consist of three exons and the binding sites for the gRNA used for CRISPR-Cas9 technology. loxP sites were integrated to generate the floxed gene. Recombination of mice with the floxed gene with EIIa-Cre driver line caused a newly recombined *Tmem160* gene lacking exon 1 and unable to generate the protein. Mice with a recombined *Tmem160* gene are considered *Tmem160* KO. Contributions: Figure was generated by Daniel Segelcke and adapted by me.

To observe potential sensory neuron-specific effects, *Tmem160* was deleted in around 80% of sensory neurons of dorsal root ganglia by mating floxed *Tmem160* mice (see above) with the Advillin-Cre driver line (Zurborg et al., 2011). The Advillin-Cre driver line causes an expression of the Cre-recombinase enzyme specifically in sensory neurons. The recombinase then recombines the DNA and removes Exon 1 of *Tmem160* in sensory neurons. Floxed littermates without expression of the Cre-recombinase and therefore with an intact *Tmem160* gene served as the appropriate control for experiments. These conditional KO mice (cKO) for *Tmem160* were healthy and fertile. Genotyping was performed as described above for the global KO mice, except that in situ hybridization was not executed.

2.1.1.3 Cell Lines

HEK293T (Human embryonic kidney cells) cells were acquired and verified from ATCC (American type culture collection). Cell line identity was confirmed regularly by morphological checks. No visible indications for mycoplasma contamination were detected, therefore, tests for mycoplasma contamination were not performed.

2.2 Methods

2.2.1 Pain Models

2.2.1.1 Spared Nerve Injury

The spared nerve injury (SNI) model of partial denervation causes neuropathic pain by transection of two out of three branches of the sciatic nerve (common peroneal and tibial nerves) (Decosterd & Woolf, 2000) while the sural nerve stays intact (and is therefore spared). It initiates tactile hypersensitivity in the dermatome of the sural nerve. Mice were treated with buprenorphine (0.07 mg/kg, s.c., TEMGESIC, 0.3 mg injection solution) to reduce acute pain (Richardson & Flecknell, 2005) thirty minutes prior to surgery. All mice received anesthesia initially with 5% isoflurane (in 100% oxygen) and were maintained with 1.5-2% isoflurane (1 ml/ml, veterinary) via a nose cone. The skin was incised above the biceps femoris muscle, and the muscle was bluntly dissected to reveal the trifurcation of the sciatic nerve. An 8-0 silk surgical knot ligated the common peroneal and tibial nerves. Both nerves were cut twice distally from the knot while removing 2 mm nerve section to avoid regeneration. The skin was closed using three single 5-0 PROLENE sutures and treated with Betadine. On day 5 post surgery, sutures were removed under short isoflurane anesthesia. The control group (Sham surgery) was treated in the same way without ligature and transection of the common peroneal and tibial nerves. Mice were given daily applications of carprofen (Rimadyl) for a maximum of three days (5 mg/kg, s.c.) as postoperative analgesic treatment.

2.2.1.2 Incision

The paw incision-model (INC) was performed by collaborators as described before (Pogatzki & Raja, 2003). In brief, the plantar hind paw of the mice was incised (0.5 cm) unilaterally under anaesthesia. Sham-treated mice were used as controls, in which no incision was performed, but anaesthesia was applied as for INC mice. INC models the pain that is developed post-surgery. For details, the reader is referred to the publication (Segelcke, Fischer, et al., 2021).

2.2.1.3 Complete Freund's Adjuvant

The complete Freund's adjuvant (CFA) model was performed by collaborators. In brief, CFA was injected unilaterally into the plantar hind paw of the mice. Sham treatment consist of injection of 0.9% saline. For details, the reader is referred to the publication (Segelcke, Fischer, et al., 2021).

2.2.1.4 Acute Pain

Mice were familiarized to the testing chamber for 1h. TRP-channel agonists were injected unilaterally into the hind paw of the mouse as described previously (Avenali et al., 2014; Sondermann et al., 2019). The following agonists and concentrations were applied to different cohorts: the TRPA1-agonist AITC (50 mM in 1x PBS (Phosphate buffered saline), volume:

10 µL) or the TRPV1-agonist Caps (0.5 mg in 5%EtOH/1x PBS, volume: 10 µL). Mice were sacrificed after the experiment.

2.2.2 Behavioral Assays

2.2.2.1 Mechanical Sensitivity

Tactile or mechanical sensitivity was tested using a Plantar Aesthesiometer within the acute pain model and naïve wildtype animals, whereas a set of calibrated von Frey filaments with a logarithmic force range from 0.07 g to 2 g was used to test the animals post SNI surgery and also in the INC and CFA models.

The Plantar Aesthesiometer was calibrated and set to the following parameters: increasing force up to 10g within 40s. The withdrawal latency and force were measured five times for each hind paw of each animal. For testing post TRP-agonist injection, mechanical testing was performed in 30-minute intervals until a maximum of 90 minutes post injection.

The von Frey filaments were applied 5 times (1Hz) to the plantar aspect of the ipsilateral hind paw. The ascending stimulus method determined the 60% paw withdrawal threshold as described by Mogil (Mogil, 2020). This means that the stimulus to which the mouse reacts at 3 out of the 5 times is recorded as withdrawal threshold.

In figures, mechanical sensitivity is either displayed as withdrawal latency in seconds (Plantar Aesthesiometer), or as 60% paw withdrawal threshold (von Frey filaments). For the longitudinal studies of mechanical sensitivity in pain models, pre-testing values (before intervention) are set to 0% and for post intervention time points, mechanical sensitivity is depicted as change in percentage.

2.2.2.2 Thermal Sensitivity

Thermal or heat sensitivity was tested in naïve animals, within the acute pain model in wildtype animals and post SNI surgery. Thermal testing was performed on a glass plate using the Hargreaves radiant heat apparatus. The withdrawal latency was measured by the test executioner 5 times for each hind paw of each animal. For that, the apparatus applied a thermal stimulus to the plantar surface of the paw. The cut-off time to prevent tissue damage was set to 40 s. In figures, thermal sensitivity is depicted as withdrawal latency in seconds.

2.2.2.3 Analysis

Analysis of mechanical and thermal behavioral testing was performed using Excel and displayed using GraphPad Prism. For statistical analyses, two-way ANOVA was applied as well as the Bonferroni post-hoc-test.

2.2.2.4 Motor Coordination

To test for motor coordination, a Rotarod has been used (Dunham & Miya, 1957). The setup consists of a rotating rod on which the mice are placed. Motor coordination is required to stay on the rod and the time is measured that the mice remain on the rotarod before falling off.

2.2.2.5 Gait Analysis

In addition to stimulus-evoked behaviors, such as mechanical and thermal hypersensitivity, another important aspect is the pain elicited by movement, e.g., walking. This is known as movement-evoked pain-related behavior and can be measured using the CatWalk^{TM} XT gait system. In this setup, the mice are placed on a walkway and recorded. Different static (stand time, print area) and dynamic (swing speed, duty cycle) gait parameters were analyzed based on the recordings. To detect unilateral antalgic gait in the pain models used during this study, the parameters were compared between ipsilateral (treated) and contralateral (non-treated) side and are depicted as ratios. For details, the reader is referred to the publication (Segelcke, Fischer, et al., 2021).

2.2.2.6 Non-evoked Pain Behavior

To assess the pain that the mice are experiencing without external stimuli, i.e., the non-evoked pain (NEP) behavior, the mean print area over ten minutes of both hind paws of the animals post SNI was determined as described previously (Pogatzki-Zahn et al., 2021; Segelcke, Pradier, et al., 2021). In short, animals were placed on a 1 cm thick plexiglass plate that was illuminated horizontally with green LEDs. For a better contrast, a second plexiglass illuminated with red LEDs was placed on top of the animal boxes. Videos were recorded from below the mice over a time frame of 10 minutes. Screenshots were acquired every 30 seconds blinded to pain model and genotype. Like this, 20 fixed images were generated for analysis with ImageJ Fiji (Schindelin et al., 2012). For each image, the contact surface of both hind paws of each mouse were measured. NEP is always displayed as a ratio between ipsilateral (ipsi, treated) and contralateral (con, non-treated) paw, to remove an increase in body weight as a confounder. The following exclusion criteria were applied for each mouse on each image: rearing, twisting, not all paws were on the ground, or excessive urination. Mice were excluded from the analysis if less than three images out of the 20 images were of good quality. The remaining average values per mouse were statistically evaluated using 2way ANOVA with Sidak's multiple comparison test (GraphPad Prism 8) to detect differences between genotypes and different time points post-surgery. In figures, NEP behavior is depicted as ratio, ipsi vs con, of footprint area as indicated by green coloring in the screenshots. In some figures, NEP behavior is shown as Change (%). In these cases, pre-testing values are set to 0% and an increase or decrease of the ratio is displayed as positive or negative change.

2.2.2.7 Grooming Behavior

As described previously (Segelcke, Fischer, et al., 2021), we were also interested in pain-related changes in self-grooming behavior. Bouts of wiping, licking or nibbling the fur with forepaws and tongue (Jirkof et al., 2012) is considered self-grooming behavior. This was analyzed in the NEP recording manually using the "Behavioral Observation Research Interactive Software" (BORIS). Two different experimenters analysed the data independently. Inter-rater reliability was determined by SPSS. The inter-rater reliability is the degree of agreement among different independent raters and is expressed as **κ**. **Κ** was interpreted according to guidelines from Cicchetti and Sparrow; (0.0=poor to 1.0=excellent) (Cicchetti & Sparrow, 1981). In figures grooming behavior is displayed using the total number of bouts (frequency) and the total time in seconds that the mice spent doing grooming behavior (duration) over a specific time frame.

2.2.2.8 Nocifensive Behavior

Nocifensive acute pain behavior was assessed with a stopwatch over the first 10 minutes post injection of the TRP-channel agonist. A lifting, licking, or flicking of the injected paw is considered nocifensive behavior. In figures, nocifensive behavior is shown in total seconds throughout this time frame.

2.2.3 Tissue Isolation

Mice were sacrificed using CO_2-inhalation, the head was cut off and the following tissues were collected in ice-cold PBS before flash-freezing in liquid nitrogen and storage at -80°C until further use.

2.2.3.1 Dorsal Root Ganglia

To collect dorsal root ganglia (DRG) the back skin was removed from the animal to get access to the vertebrate column. The vertebrate column was detached from the rest of the body and cut open under a binocular to reveal the spinal cord and the DRG. For further use in primary cell cultures, all DRG of the mice were collected in cell culture medium at room temperature, for other experiments only lumbar DRG 1-5 or 3-5 were collected and analysed further. To conduct cryo-embedding, lumbar DRG were collected in ice-cold 4% paraformaldehyde (PFA).

2.2.3.2 Spinal Cord

The vertebrate column was treated as described above. The lumbar spinal cord was collected in ice-cold PBS and snap-frozen for qPCR experiments.

2.2.3.3 Sciatic Nerve

After removal of the vertebrate column, the skin of the upper leg was removed, and the muscle was cut to reveal the sciatic nerve which was collected.

2.2.4 Cell Culture

2.2.4.1 Primary DRG Culture

Primary DRG cultures of mice were prepared according to the standard protocols of the laboratory as described previously (Sondermann et al., 2019). In short, coverslips were coated with poly-D-lysine (PDL) and laminin. DRG were collected and digested using collagenase and papain. A bovine serum albumin (BSA) column was used to remove cell debris. Neurons were kept in culture medium (DMEM/F-12 (1:1) + GlutaMax-I) with 10 % horse serum and NGF (100 ng/mL) and used for Calcium-imaging (Ca^{2+}-imaging) experiments or immunostainings at day 1 in vitro.

2.2.4.2 Nucleofection of DRG Neurons

Dissociated DRG neurons were nucleofected using the P3 Primary Cell 4D-Nucleofector X Kit in the 4D-Nucleofector X Unit as described before (Sondermann et al., 2019) using the following plasmids: 0.5 mg pCMV6-TMEM160-Myc-DDK or pCDNA3.1-myc-His (control transfection for anti-Myc labelling specificity, data not shown) in combination with 0.5 ug HyPer-mito-YFP. Nucleofected neurons were cultured in DMEM/F-12 + Glutamax + 10% horse serum + 100 ng/ml NGF + 50 ng/ml GDNF + 50 ng/ml NT-3, and 50 ng/ml NT-4. At day 2 in vitro neurons were fixed for immunocytochemistry.

2.2.4.3 HEK Cell Culture

Cell culture and transfection of HEK293T cells were executed as described previously (Sondermann et al., 2019). Shortly, HEK293T cells were cultured in the following medium constitution: DMEM + Glutamax + 10%FBS + 1%penicillin/streptomycin.

2.2.5 Ratiometric Calcium-Imaging

To display changes in the amount of intracellular Ca^{2+} and therefore assess cellular excitability in vitro, ratiometric Ca^{2+}-imaging was performed in primary DRG cultures at day 1 as described previously (Sondermann et al., 2019). Briefly, Fura-2/AM served as a Ca^{2+}-binding and cell-permeable dye. Cells were incubated for 30 minutes with Fura-2/AM and then transferred to the assay buffer solution. Solutions with different concentrations of the following substances were used as stimuli: AITC (TRPA1 agonist), Caps (TRPV1 agonist) and KCl (see Table 13 and Table 14 for concentrations). To perform Ca^{2+}-imaging a Zeiss Axio Observer Z1 and the MetaFluor software were used. Alternating excitation at 340 nm and 380 nm, and measuring the emission at 510 nm served the purpose of detecting the Ca^{2+} influx indirectly by measuring the intracellular Ca^{2+} level. The level can be determined using the absorption values for both wavelengths (340 nm and 380 nm) and calculating their ratio (Bootman et al., 2013).

A minimum of 3 different coverslips were measured per culture, a minimum of 4 cultures of different mice were used for each naïve condition. Coverslips were imaged over 10 minutes according to the following stimulation protocol:

Table 13: Stimulation protocol naïve, adapted from (Fischer, 2019)

Time (minutes)	Solution
0-2	Assay Buffer
2-3	Capsaicin (100 nM)
3-5	Assay Buffer
5-6	Capsaicin (1 µM)
6-8	Assay Buffer
8-9	KCl (60 mM)
9-10	Assay Buffer

Additionally, Ca^{2+}-imaging was used to assess excitability in DRG cultures pre-treated with TNFα (100ng/ml) as described elsewhere (Hanack et al., 2015; Willemen, Hanneke L. D. M. et al., 2018) or vehicle control (0.1% BSA in PBS) for 6 hours in cultures of male *Tmem160* KO and wildtype (WT) mice (Fischer, 2019). Multiple coverslips and cells from N=3 mice per genotype were used. The following stimulation protocol was used:

Table 14: Stimulation protocol TNFα, adapted from (Fischer, 2019)

Time (minutes)	Solution
0-1	Assay Buffer
1-3	AITC (30 µM)
3-5	Assay Buffer
5-7	Caps (100 nM)
7-9	Assay Buffer
9-10	KCl (60 mM)
10-11	Assay Buffer

2.2.5.1 Analysis

Analysis was performed using Microsoft Excel. All cells responding to at least one of the stimuli were identified as neurons. For all given stimuli, the share of neurons responding to it were calculated. In addition, all responding neurons were considered for an assessment of average response amplitude to the corresponding stimulus. The results were displayed using GraphPad Prism and compared between genotypes and experimental conditions. To test for statistical significance, t-tests were used, as well as Grubb's test to exclude outliers. For contingency tests, Fisher's exact test was used. In figures, the responding cells to the specific stimulus relative to total number of neurons are depicted as percentage values. The response amplitude is displayed as ratio of the fluorescent signal at 340 nm and 380 nm excitatory wavelength.

2.2.6 Cryo Embedding and Tissue Sectioning

Lumbar DRG (lDRG) were collected in 4% PFA (in PBS) and incubated for 24 hours at 4°C, afterwards the tissue was transferred to 30% Sucrose and incubated over night at 4°C. Tissue was embedded in Tissue-Tek O.C.T. (Optimal cutting temperature), and step-serial sections were cut (10 µm) at -20°C using a cryostat. Sections were mounted on SuperFrost Plus slides and stored at -80°C.

2.2.7 Staining

2.2.7.1 Immunohistochemistry

Immunohistochemistry (IHC) was performed as described previously (Segelcke, Fischer, et al., 2021). In summary, tissue sections were thawed, treated with blocking buffer for 1h and incubated with different primary (4°C, overnight) and secondary (room temperature, 2 hours) antibodies with dilutions as listed in Table 1.

2.2.7.2 Immunocytochemistry

At day 2 in vitro, immunocytochemical stainings were performed on HEK293T cells or nucleofected DRG cultures as described previously (Segelcke, Fischer, et al., 2021). In short, cells were washed, fixed in 4% PFA, blocked for 30 minutes and incubated with primary antibody (4°C, overnight) and secondary antibody (room temperature, 2h). Antibodies were used with dilutions as listed in Table 1. Two to three independent cultures were analysed.

2.2.7.3 In Situ Hybridization/RNAscope

To validate the global *Tmem160* KO and to assess the distribution of Tmem160 mRNA in WT DRG, the RNAscope Muliplex Fluorescent Reagent Kit v2 was used according to manufacturer's instructions for fixed frozen tissue. Tissue embedding and cryosectioning was performed as described above. Target retrieval was conducted manually, and an Opal 570 dye was used for the HRP-C1 signal. An IHC was added and performed as described above.

2.2.7.4 Image Acquisition and Analysis

For immunostainings and RNAscope, images were acquired on a Zeiss Axio Observer Z1 inverted epifluorescence microscope using Axiovision software. Acquisition parameters were not changed between experimental groups and controls, they were processed in parallel. Analyses were performed on raw images as described previously (Sondermann et al., 2019). Only for presentation purposes were brightness & contrast of matched images adjusted (always in parallel) with ImageJ Fiji (Schindelin et al., 2012) or Adobe Photoshop CC2017. In DRG sections, figures display the percentage of cells positive for the antigen relative to the total number of cells counted.

2.2.8 Mitochondrial Assays

2.2.8.1 TMRM Staining

TMRM staining was performed by colleagues. In summary, Tetramethylrhodamin methyl ester (TMRM) allows live labelling of mitochondria in cells. Carbonyl cyanide p-trifluoromethoxyphenylhydrazone (FCCP) was used as an uncoupler of the oxidative phosphorylation. After FCCP treatment, TMRM fluorescence intensities displays changes in mitochondrial membrane potential. Mitochondrial dysfunction can influence the membrane potential. For details, the reader is referred to the publication (Segelcke, Fischer, et al., 2021).

2.2.8.2 Complex IV Rodent Enzyme Activity Dipstick Assay

An activity assay for Complex IV was performed by colleagues. In short, dipsticks are used, on which capture antibodies for complex IV are immobilized. Complex IV is fixated on the dipstick in active form and its activity is determined by precipitation of di-amino bendizinetetrachloride (DAB). Signal intensity was compared between conditions. DRG were used to check for complex IV activity. For details, the reader is referred to the publication (Segelcke, Fischer, et al., 2021).

2.2.8.3 Seahorse Respiration of Isolated Mitochondria

Respiratory assays were performed by collaborators. In essence, mitochondria from the brain were isolated and used to study oxygen consumption rate (OCR) using the Seahorse XF analyser as published before (Dudek et al., 2016). For details, the reader is referred to the publication (Segelcke, Fischer, et al., 2021).

2.2.8.4 Tmem160 *Localization Assays in Isolated Mitochondria*

Submitochondrial localization of Tmem160 – as Tmem160^{FLAG} - was determined by collaborators in HEK293T cells. In brief, carbonate extraction was caused using Na_2CO_3 at different pH. Alternatively, detergent lysis was performed. Proteins known to be membrane-integrated as well as soluble and membrane-associated were used as controls. The “protease protection assay” combined with swelling assays served to show in which of the mitochondrial membranes Tmem160 is located, using controls representative for outer mitochondrial or inner mitochondrial membrane localization. For details, the reader is referred to the publication (Segelcke, Fischer, et al., 2021).

2.2.9 Cytokine Array

To study cytokine and chemokine levels in DRG lysates between different conditions, the Proteome Profiler Mouse Cytokine Array Kit, Panel A was used as described previously (Segelcke, Fischer, et al., 2021). In short, DRG samples were lysed, relative protein abundance was detected on the provided membrane with a spectrophotometer and compared between the different conditions. Higher fluorescence signal correlates with higher cytokine expression levels. Correction for total protein amount was performed using a Coomassie staining. Intensity analysis was completed using ImageJ Fiji. Data are displayed as ratio between *Tmem160* KO and the WT control from multiple experiments and as ratio between sexes and ages.

A

	1	2	3	4	5	6	7	8	9	10	11	12	13	14	15	16	17	18	19	20	21	22	23	24
A	Ref	Ref																					Ref	Ref
B	CXCL13	CXCL13	C5	C5	G-CSF	G-CSF	GM-CSF	GM-CSF	CCL1	CCL1	CCL11	CCL11	sICAM-1	sICAM-1	IFN-γ	IFN-γ	IL-1α	IL-1α	IL-1β	IL-1β	IL-1ra	IL-1ra	IL-2	IL-2
C	IL-3	IL-3	IL-4	IL-4	IL-5	IL-5	IL-6	IL-6	IL-7	IL-7	IL-10	IL-10	IL-13	IL-13	IL-12 p70	IL-12 p70	IL-16	IL-16	IL-17	IL-17	IL-23	IL-23	IL-27	IL-27
D	CXCL10	CXCL10	CXCL11	CXCL11	CXCL1	CXCL1	M-CSF	M-CSF	CCL2	CCL2	CCL12	CCL12	CXCL9	CXCL9	CCL3	CCL3	CCL4	CCL4	CXCL2	CXCL2	CCL5	CCL5	CXCL12	CXCL12
E	CCL17	CCL17	TIMP-1	TIMP-1	TNF-α	TNF-α	TREM-1	TREM-1																
F	Ref	Ref																					PBS	PBS

B

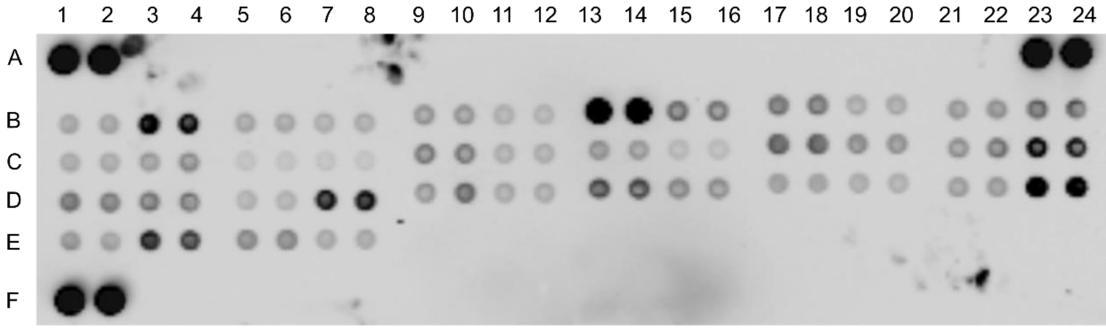

Figure 4: Membrane layout and exemplary membrane for cytokine array, adapted from (Segelcke, Fischer, et al., 2021).

The cytokine array allows a relative conclusion on protein levels of 40 different cytokines and chemokines within a tissue lysate. The array consists of a membrane on which the cytokines are spotted in duplicates. Higher fluorescent intensities correlate with a higher abundance of the cytokine in the sample. (A) Panel coordinates as given by the manufacturer (R&D Systems). (B) Exemplary original image of a membrane. Contributions: Figure was generated and adapted by me.

2.2.10 Gene Expression

Gene expression levels were compared using quantitative real-time polymerase chain reaction (qPCR) essentially as described previously (Sondermann et al., 2019):

2.2.10.1 RNA Isolation and Complementary DNA Synthesis

RNA was isolated from tissue lysates depending on the tissue type. For lumbar DRG the NucleoSpin RNA XS kit was applied according to manufacturer's instructions. For spinal cord and sciatic nerve samples, incubation with Qiazol, homogenization with a Precellys Homogenisator (5000 rpm, 3x10s), Chloroform extraction and application to the RNeasy Mini Spin Column from the RNeasy Mini Kit was performed. The isolated RNA was reverse transcribed to complementary DNA (cDNA) using the QuantiTect Reverse Transcription Kit according to manufacturer's instructions.

2.2.10.2 Quantitative Real-Time PCR

The final qPCR experiments were conducted using a Lightcycler 480 platform and the SYBR Green fluorescence detection method. In this context the Power SYBR Green PCR Master Mix was used. Analysis was performed as described previously (Sondermann et al., 2019). To summarize, the relative abundance was corrected to the housekeeping gene GAPDH and then compared between the different experimental groups. Sequences of the primers used can be found in Table 8.

2.2.11 Mass Spectrometry

All mass spectrometry experiments were performed by colleagues essentially as described earlier (Xian, Sondermann, Gomez Varela, & Schmidt, 2022), the main difference lying in the type of tissue used:

2.2.11.1 Protein Extraction

Shortly, lDRG were processed with lysis buffer and acetone precipitation. Proteins were then reduced and alkylated.

2.2.11.2 SP3-Assisted Protein Digestion and Peptide Clean-up

A version of the single-pot, solid-phase-enhanced sample preparation (SP3) method was used, relying on magnetic beads. Proteins were digested using Trypsin/Lys-C. Peptides were eluted from the beads using mass spectrometry (MS) grade water. Before storing them at -20°C, samples were acidified.

2.2.11.3 LC-MS/MS Data Acquisition

Nanoflow reversed-phase liquid chromatography (Nano-RPLC) was used to separate the peptides applying gradients of different solvents. A hybrid TIMS (Trapped ion mobility spectrometry) quadrupole TOF (Time of flight) mass spectrometer coupled to the Nano-RPLC acquired spectra of the eluted peptides. Data-independent acquisition (DIA) mode together with parallel accumulation serial fragmentation (PASEF) was used.

2.2.11.4 DIA-PASEF Data Processing

Data collected using the DIA-PASEF modes were processed using DIA-NN (Demichev et al., 2020) and compared to a precited spectrum library generated from a murine protein database. Theoretically calculated spectra were compared to the recorded spectra. The intensity for different gene groups was extracted using MaxLFQ (Cox et al., 2014).

2.2.11.5 Differential Expression Analysis and Reactome Pathways Analysis

The R package, ProTIGY[1] was used on quantitative data as generated by MaxLFQ. Quantified proteins presented in less than 75% of all replicates of the same condition were filtered out, and the averages between technical replicates were submitted to log2-transformation, and consequently, differential expression analysis after removing keratins. Age- and sex-dependent comparisons were performed using two-sample moderated t-tests. Of specific interest were protein identifications (IDs) with a high significance and a high fold change. Those were defined as differentially expressed proteins (DEPs). DEPs show an adjusted p-

[1] https://github.com/broadinstitute/protigy

value ≤ 0.05 (Benjamini and Hochberg, for multiple testing (Storey, 2002)) and an absolute log_2 fold change (FC) > 0.585 (indicative of a fold change of ± 50%). STRING (string-db.org; (Szklarczyk et al., 2021)) was used to create a reactome pathway analysis of DEPs (settings: high confidence (0.07); false discovery rate (FDR) < 0.05). Lists were compared using Venny (Oliveros, 2007-2015). Some IDs contained multiple protein names. For those, only the first was used to analyze reactome pathways and to compare with prior published -omic data sets in mouse DRG.

2.2.11.6 Statistics

Statistics were performed as described previously (Segelcke, Fischer, et al., 2021). In detail: Sample sizes were not a priori calculated. Data was analyzed using GraphPad Prism unless indicated otherwise. All data is represented as mean ± SEM (standard error of mean) unless indicated otherwise. All replicates are biological unless indicated otherwise. All statistical tests are two-sided, only performed on raw data, and indicated in the respective figure legend for each dataset. In all panels: not significant, ns $p > 0.05$; * $p < 0.05$; ** $p < 0.01$; *** $p < 0.001$; **** $p < 0.0001$. Five mice were excluded from the study because the sural nerve was touched – and potentially damaged – during the SNI surgery.

2.3 Contributions

Contributions of me and collaborators are shown in the respective figure legends and summarized in this section.

2.3.1 Characterization and Effect of Tmem160 on Somatosensation

The following experiments were performed and analyzed by me within the scope of my master thesis previous to this dissertation (Fischer, 2019): Cytokine Array experiments under naïve condition in male and female *Tmem160* KO as well as in male *Tmem160* cKO. Ca^{2+}-imaging experiments using only Caps as stimuli and after incubation with TNFα in male *Tmem160* KO. The following experiments were performed and analyzed by collaborators: All behavioral studies under naïve conditions and within the INC, CFA and SNI model were performed by collaborators from "Translational Pain Research" group, University Clinic Münster, Germany (PI: Esther Pogatzki-Zahn), mainly Daniel Segelcke. Submitochondrial localization and mitochondrial oxygen consumption rate on isolated mitochondria was investigated by Sven Dennerlein ("Mitochondrial protein biogenesis" group, University Medical Center Göttingen, Germany). *Tmem160* KO mice were generated by Fritz Benseler and Nils Brose and genotyped by Fritz Benseler ("Molecular Neurobiology" group, Max Planck Institute for Multidisciplinary Sciences Göttingen, Germany). Meike Hütte (previous member of the "Somatosensory Signaling and Systems Biology" group, Max Planck Institute for Multidisciplinary Sciences Göttingen, Germany) performed acute pain experiments related to the injection of Caps, *in vitro* costaining of *Tmem160* with mitochondrial markers, immunostainings for peripherin and NF200, qPCR for expression of mitochondrial markers in DRG, measurements of Complex IV activity and Tmrm-imaging. The following experiments were planned, performed and analyzed by me within the scope of this dissertation: expression levels of Iba1 mRNA in the ipsilateral and contralateral spinal cord at day 7 and day 28 post SNI in male and female *Tmem160* KO and male *Tmem160* cKO, Ca^{2+}-imaging experiments on female *Tmem160* KO and male *Tmem160* cKO DRG cultures, acute pain experiments related to the injection of AITC, RNAscope experiments to confirm *Tmem160* KO and the distribution of Tmem160 mRNA within DRG sections, Cytokine Array experiments at day 7 post SNI. Data were interpreted, including a further statistical analysis and interpretation of the data collected during my master thesis, and subfigures were generated by me.

Figures were generated by Daniel Segelcke and me and adapted by me for the purpose of display in this dissertation. The original publication (Segelcke, Fischer, et al., 2021) is based on conceptualization and direction of Manuela Schmidt, experimental design on mouse behavior was completed by Daniel Segelcke and Esther Pogatzki-Zahn. Esther Pogatzki-Zahn and Manuela Schmidt supervised all experiments and data analysis. The manuscript was written, discussed and revised by Manuela Schmidt, Daniel Segelcke, me, and Esther Pogatzki-Zahn. First authorship is shared between Daniel Segelcke and me.

2.3.2 Characterization of Age- and Sex-Differences in the DRG Proteome and Their Effect on Somatosensation

Measurements of naïve thermal hypersensitivity throughout maturation in male mice were carried out and analyzed by Niklas Michel (previous member of the “Somatosensory Signaling and Systems Biology” group, Max Planck Institute for Multidisciplinary Sciences Göttingen, Germany). Acute pain experiments were performed and analyzed by me, as well as TRPV1 stainings in DRG sections. Elisa Fernandez (lab rotation student, previous member of the “Somatosensory Signaling and Systems Biology” group, Max Planck Institute for Multidisciplinary Sciences Göttingen, Germany) performed and analyzed Ca^{2+}-imaging experiments within this section, taught and supervised by me. Sample preparation for mass spectrometry was conducted by Julia Sondermann (member of the “Systems Biology of Pain” group, University of Vienna, Austria), original analysis of the mass spectrometry data, including the generation of a list of fold changes and adjusted p-values, principal component analysis, comparison to ion channels and display of Pearson’s correlation for technical controls were carried out by Feng Xian (member of the “Systems Biology of Pain” group, University of Vienna, Austria). I performed further analysis and comparisons of the generated data to previously published databases and resources and interpreted the data accordingly. Cytokine Array experiments within this section were carried out by me together with David Steiner (former member of the “Systems Biology of Pain” group, University of Vienna, Austria), analyzed by me. All figures were generated by me, Feng Xian generated subfigures for Figure 24.

3 Results and Discussion

3.1 Characterization and Effect of Tmem160 on Somatosensation

CRISPR-Cas9 technology was used to create a global KO mouse line for *Tmem160*, depleting it in all cells of the body (Figure 3, see methods for detail). Genotyping and quantitative PCR were employed to determine the genotype of the mice and confirm a successful knockout in all cells. *Tmem160* KO and WT littermates of both sexes were used for all experiments in this section. All data of this section was published before at Cell Reports (Segelcke, Fischer, et al., 2021), if not indicated otherwise, figures were adapted.

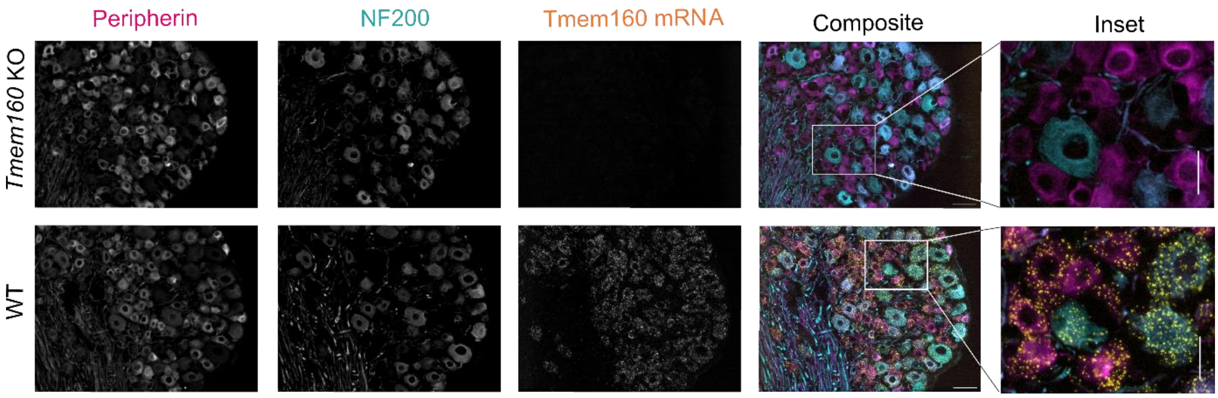

Figure 5: Tmem160 is expressed in mouse peripheral sensory neurons of DRG, adapted from (Segelcke, Fischer, et al., 2021).

Exemplary images of immunohistology for Peripherin and NF200 and a validation of *Tmem160* KO in whole DRG using RNAscope technology. Composite shows Peripherin[2] in magenta, NF200[3] in cyan and Tmem160 mRNA in yellow. Inset, magnification of indicated area. Scale bar, 50 µm. N = 3 mice/genotype. Contribution: Experiments were performed, and figures were selected and presented by me. Figure was generated together with Daniel Segelcke and adapted by me.

3.1.1 Tmem160 Expression in Mitochondria of Peripheral Sensory Neurons

To confirm *Tmem160* deletion in *Tmem160* KO DRG as well as to visualize Tmem160 expression in wildtype DRG, immunostainings and in situ hybridization was performed on cryo-embedded DRG tissue sections. Antibodies against Peripherin, a common marker for a subset of small unmyelinated DRG neurons, and NF200, a marker for medium- and large-diameter myelinated DRG neurons were used together with RNAscope technology to detect Tmem160 mRNA (see Methods for details). No expression of Tmem160 mRNA was found in *Tmem160* KO. In WT littermates, Tmem160 mRNA was present in both Peripherin and NF200 positive neurons, suggesting an even distribution across the different subpopulations (Figure 5). The processes in which a protein is conceivably involved depend on its subcellular localization, therefore we were interested to determine it for Tmem160. Looking at mRNA does not allow any conclusions on localization within the cell and all antibodies available for immunostainings lacked specificity (see Materials for details). Therefore, a Myc-tagged Tmem160 protein was

[2] Marker for a subset of small unmyelinated DRG neurons
[3] Marker for medium- and large-diameter myelinated DRG neurons

expressed (Tmem160-Myc) that could then be used in immunostainings for subcellular localization both in primary DRG cultures (Figure 6B) and in HEK293T cells (Figure 6C). The cells present in a primary DRG culture are equivalent to those found in cryo-embedded DRG tissue sections as used for Figure 5. HEK293T is a commonly used immortalized cell line derived from human embryonic kidney cells (see Methods for details). Stainings revealed a co-localization of Tmem160 with the mitochondrial markers HyPer-mito-YFP and Ndufv2, as observed by the overlap in the composite images. This indicates towards a localization of Tmem160 in mitochondria. In addition, the peptide sequence of Tmem160 hinted towards a mitochondrial import domain, as well as three transmembrane domains in *in silico* simulations (MitoProt II - v1.101[4], (Claros & Vincens, 1996), Figure 6A), supporting the experimental results. To discover Tmem160's submitochondrial localization, carbonate extraction and hypo-osmotic swelling experiments were performed (Aich et al., 2018; Dennerlein et al., 2015) in HEK293T cells expressing FLAG-tagged Tmem160 ($Tmem160^{FLAG}$) (Figure 6D-E). Carbonate extraction experiments detected $Tmem160^{FLAG}$ in isolated mitochondria and showed its integration into a mitochondrial membrane similar to MITRAC12 (cytochrome c oxidase assembly intermediate) (Figure 6D). The "protease protection assay" serves to determine localization within the two mitochondrial membranes. Here, $Tmem160^{FLAG}$ only became accessible upon destruction of the outer mitochondrial membrane (Figure 6E). If $Tmem160^{FLAG}$ localized in the outer mitochondrial membrane, it would have shown similar results as TOM20 which served as a marker for this purpose. Instead, the results for $Tmem160^{FLAG}$ resemble those for TIM23, which served as a control protein of the inner mitochondrial membrane, indicating the localization of Tmem160 in that same membrane. After we published our results (Segelcke, Fischer, et al., 2021) another group looked further into the subcellular localization and function of Tmem160 in HeLa (cervix cancer) and HepG2 (hepatoblastoma) cell lines (Yamashita et al., 2022). They verified the localization of Tmem160 in mitochondria in HeLa cells using TMEM160-Myc-DYKDDDDK and more specifically in the inner mitochondrial membrane in HepG2 cells (Yamashita et al., 2022). We performed the localization experiments in primary DRG cultures (mitochondrial localization) and HEK293T cells (mitochondrial and submitochondrial localization) so their experiments confirmed the localization in different cell lines and a different laboratory, providing even more validity to our results.

[4] https://ihg.gsf.de/ihg/mitoprot.html

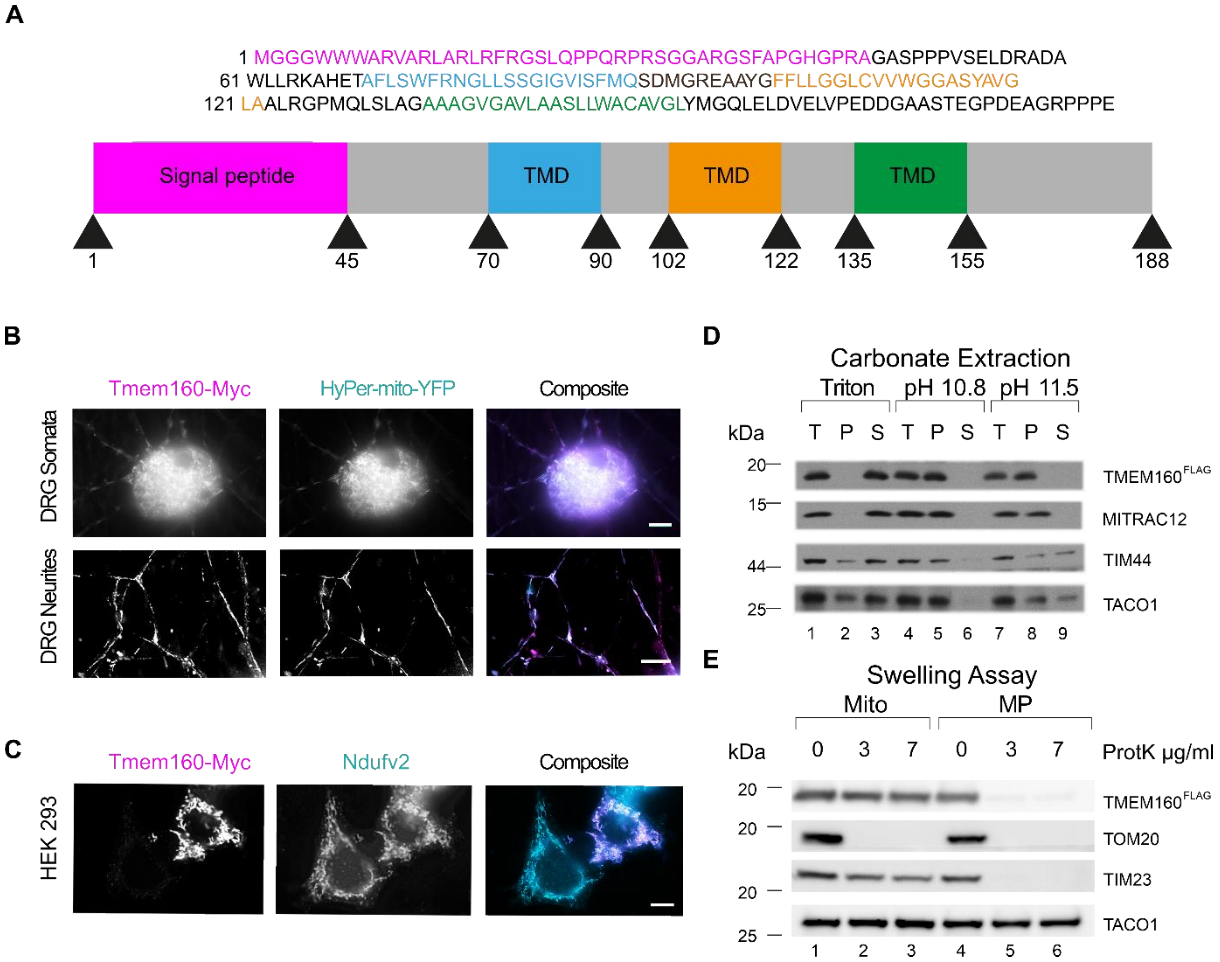

Figure 6: Tmem160 is localized to the inner mitochondrial membrane, adapted from (Segelcke, Fischer, et al., 2021).

(A) Tmem160 exhibits an N-terminal signal peptide (aa 1-45) for mitochondrial import (MitoProt II - v1.101[5]) and 3 transmembrane domains (TMD), predicted by *in silico* simulations. (B and C) Immunostainings were performed for Tmem160-Myc (magenta) and multiple mitochondrial markers (HyPer-mito-YFP, Ndufv2: cyan) *in vitro* in somata and neurites of DRG cultures (B) and in HEK293T cells (C). Composite represents the overlapping of both stainings. Scale bar, 10 µm. n = several coverslips from N = 4 independent DRG cultures (B) and N = 3 independent HEK293T cell cultures (C). (D and E) HEK293T cells were used to express Tmem160^{FLAG}. Mitochondria were collected from the cells and subjected to different analyses for submitochondrial localization. (D) During carbonate extraction the isolated mitochondria were subjected to detergent lysis (Triton) or carbonate extraction at different pH (as indicated). MITRAC12 was used as a positive control for a membrane-integrated protein, while the membrane-associated TIM44 (translocase of inner mitochondrial membrane) as well as the soluble TACO1 (translational activator of cytochrome c oxidase I) served as negative controls since they are known to dissociate from the inner mitochondrial membrane under higher pH-conditions. Tmem160^{FLAG} behaved like MITRAC12 and was resistant to carbonate extraction suggesting its integration into mitochondrial membranes. (T = total; P = pellet, S = soluble fraction). N = 2 independent mitochondria isolations. (E) During the “protease protection assay” Proteinase K (ProtK) was added to isolated mitochondria (Mito) and to hypotonically swollen mitochondria (swelling assay producing mitoplasts, MP). TOM20 served as a marker for localization to the outer mitochondrial membrane, TIM23 to the inner mitochondrial membrane, and TACO1 to the mitochondrial matrix. Accordingly, TOM20 signal disappeared upon ProtK treatment, while TIM23 was only accessible for ProtK upon hypo-osmotic swelling (in MP). As expected, the mitochondrial matrix marker TACO1 did not alter, even when the outer mitochondrial membrane was disrupted by PK treatment. Tmem160^{FLAG} only became accessible to ProtK treatment in MP, i.e., when the outer mitochondrial membrane was disrupted by hypotonic swelling, indicative of its localization at the inner mitochondrial membrane. N = 2 independent mitochondria isolations. Contributions: B and C: experiments were performed by Meike Hütte, who selected the pictures for display. D and E: experiments were performed by Sven Dennerlein, who provided pictures and analysis. A-E: Figures were generated by Daniel Segelcke and adapted by me.

[5] https://ihg.gsf.de/ihg/mitoprot.html

3.1.2 *Tmem160* KO Does Not Influence Basal Somatosensation, Acute Nociception, Mitochondrial Function, Incisional and Inflammatory Pain

During characterization of the *Tmem160* KO, immunostainings were performed on DRG sections for Neurofilament 200 (NF200) and Peripherin essentially as described above (without the use of RNAscope techonology). They showed only minor differences in expression patterns and frequencies between genotypes (*Tmem160* KO and WT) (Figure 7A-B). Fisher's exact tests revealed significant differences in the percentages of Peripherin and NF200 positive neurons between genotypes. This is most likely due to the very high number of neurons counted during the experiment. The percentage change is small and most likely does not have a biological consequence. Additionally, experiments were performed by my colleague that revealed no hint of a myelination deficit upon deletion of *Tmem160* (Hütte, 2019). *Tmem160* KO showed normal health and fertility except for a very low number of mice showing blindness at birth. Blind mice were not used for the experiments. To test for deficits in motor function, a Rotarod was used as well as several aspects of gait analysis on the freely walking mouse (Figure 7C). Moreover, basal somatosensation was investigated regarding tactile and heat stimuli (Figure 7D). To do this, the withdrawal latency to a stimulus was measured. This is also known as a somatosensory threshold. A lower withdrawal latency indicates a higher sensitivity to the stimulus. No differences between genotypes were observed under naïve conditions regarding motor behaviors and basal somatosensory function. This indicates, that Tmem160 is dispensable for a normal motor function and somatosensory behaviors. In this study, naïve always equals treatment-naïve, i.e., not in a pain model.

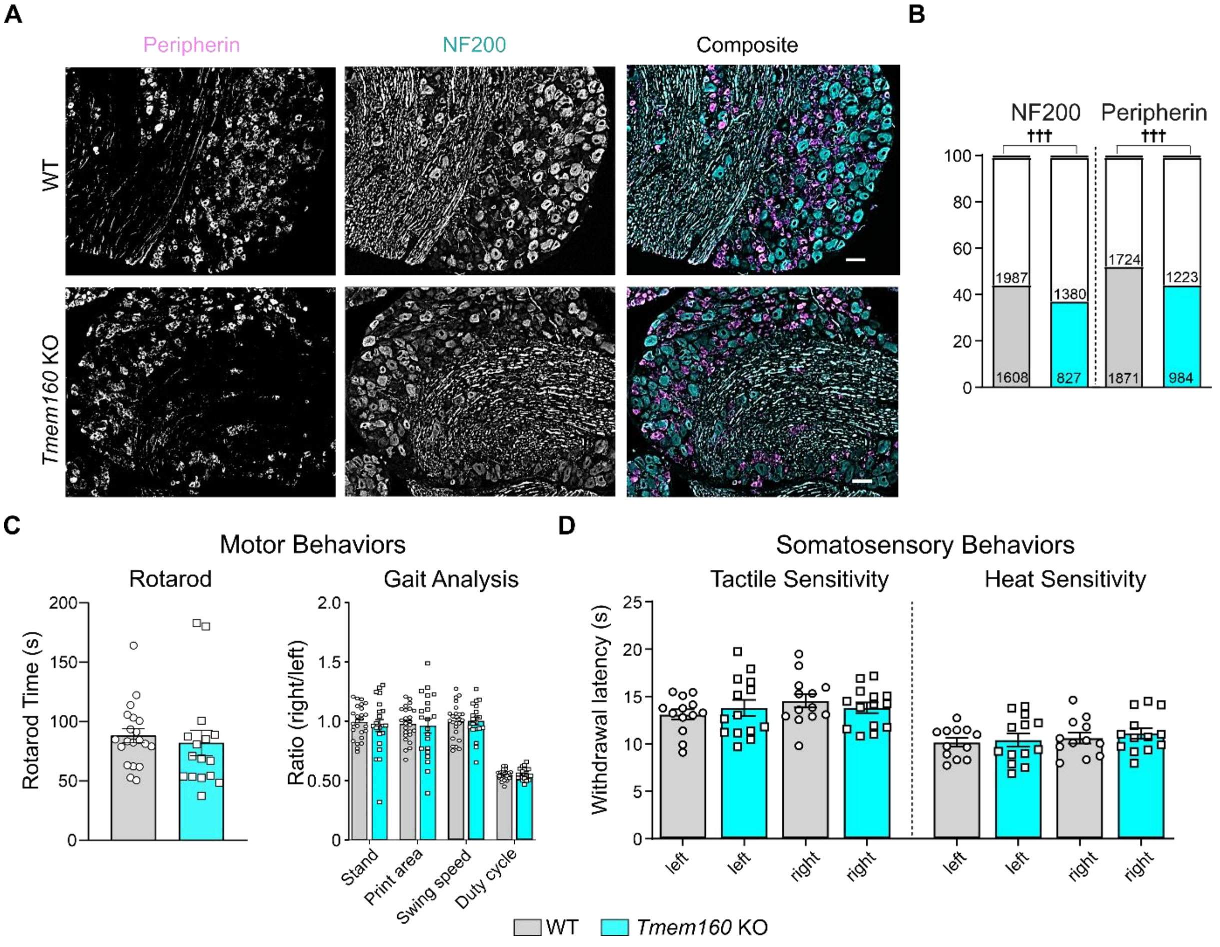

Figure 7: Tmem160 is dispensable for motor function and basal somatosensation, adapted from (Segelcke, Fischer, et al., 2021).

(A and B) Expression of Peripherin and NF200 as assessed by immunohistology in cryosections of DRG. N = 5 (WT) and N = 3 (*Tmem160* KO) mice. (A) Exemplary images of the staining in *Tmem160* KO and WT. The composite image shows Peripherin in magenta and NF200 in cyan. (B) Fraction of neurons as calculated across multiple experiments from images like those in (A). Significant difference was observed overall in the fraction of neurons positive for Peripherin and NF200 between *Tmem160* KO and WT. Fisher's exact test. † for comparison between genotypes. ††† $p \leq 0.001$. Scale bar, 50 µm. Numbers indicate the number of neurons quantified (color/grey: positive label for respective marker; white: no label for respective marker). (C) *Tmem160* KO displayed unaltered motor functions regarding coordination (Rotarod, time in seconds) and locomotion without external stimulus (gait analysis, ratio right/left hind paw) compared with WT littermates. N = 20 (WT) and N = 16 (*Tmem160* KO). (D) *Tmem160* KO presented WT-like somatosensory thresholds to tactile and heat stimuli. N = 13 (WT) and N = 14 (*Tmem160* KO). (C and D) Data are represented as mean ± SEM in a scatter bar plot. Two-way ANOVA followed by Holm-Sidak's multiple comparison tests, ns. Contributions: A and B: experiments were performed and analyzed, and images were presented by Meike Hütte, C and D: experiments were performed and analyzed by Daniel Segelcke. A-D: Figures were generated by Daniel Segelcke and adapted by me.

Acute pain fulfills important physiological functions, therefore we wanted to confirm experimentally, that these functions were not impaired upon deletion of *Tmem160*. To study the role of Tmem160 in acute nociception, chemically induced nociception in the hind paw was compared in *Tmem160* KO and WT. TRPV1 activation by unilateral injection of the agonist Caps was performed and in a different cohort, TRPA1 was activated by unilateral injection of AITC (Figure 8). Nocifensive behavior was analysed as well as hypersensitivity to tactile stimuli. Nocifensive behavior was defined as the time the mouse spent lifting, licking, or flicking the paw withing the first 10 minutes post injection. *Tmem160* KO mice behaved similar to the

WT littermates, both revealing a prominent nocifensive behavior and an ipsilateral hypersensitivity to tactile stimulation. Therefore, we assumed no influence of Tmem160 on acute nociception.

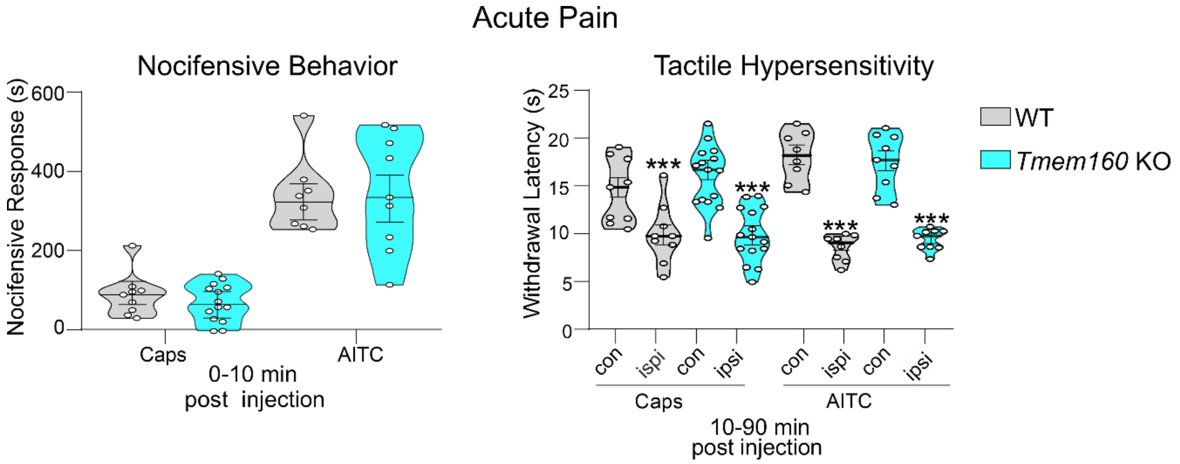

Figure 8: Acute pain behavior is not affected upon *Tmem160* deletion, adapted from (Segelcke, Fischer, et al., 2021).

Unilateral injection of Capsaicin (Caps) or Allyl Isothiocyanate (AITC) was performed in *Tmem160* KO and WT to model acute pain. Nocifensive behavior is the total time the mouse spent lifting, licking, or flicking the paw immediately after injection (left), the observation was followed by the measurement of withdrawal latency in response to tactile stimulation (right) in the ipsilateral, injected, paw (ipsi) and the contralateral, non-injected, paw (con). Both *Tmem160* KO and WT showed similar results, namely a pronounced nocifensive response and an ipsilateral hypersensitivity to tactile stimulation. Caps: N = 9 (WT) and N = 15 (*Tmem160* KO) mice. AITC: N = 8 (WT) and N = 9 (*Tmem160* KO) mice. Two-tailed unpaired t-test for comparison between ipsi- and contralateral paws. *** $p \leq 0.001$. Unpaired t-tests for comparisons between genotypes regarding the nocifensive behavior. Contributions: Caps: data generated and analyzed by Meike Hütte, AITC: data generated and analyzed by me. Figure generated by Daniel Segelcke and adapted by me.

Due to the mitochondrial localization of Tmem160 (Figure 6C and E) and the increasing awareness of the role of mitochondrial dysfunction in pathological pain (G. J. Bennett et al., 2014; Flatters, 2015; J. Li et al., 2020; Y. Yang et al., 2018) we next sought out to study the mitochondrial function in *Tmem160* KO. Quantitative PCR was performed on DRG samples for multiple components of the ETC and showed a reduction in expression levels in the *Tmem160* KO for some components (Nd2 (Subunit of NADH dehydrogenase, complex), Cox1 (Cytochrome c oxidase 1, complex IV)) (Figure 9A). Studies of mitochondrial function did not reveal any influence of this reduction on basal mitochondrial function: Three different assays were performed investigating mitochondrial function in *Tmem160* KO and WT. (1) The activity of complex IV of the ETC in DRG lysates was studied with a commercially available enzymatic activity assay (Figure 9C). (2) The mitochondrial oxygen consumption rate (OCR) in brain lysates was examined using the Seahorse assay (Duggett et al., 2016) (Figure 9B). (3) The mitochondrial membrane potential integrity in primary DRG cultures was investigated after incubation with FCCP using the mitochondrial dye TMRM (Cannino et al., 2012; Nicholls & Budd, 2000) (Figure 9D). FCCP is an uncoupler of the mitochondrial electron transport chain and causes a disruption of the mitochondrial membrane potential (Dispersyn et al., 1999). This can be visualized by a reduction in fluorescence intensity of TMRM. None of the experiments regarding mitochondrial function revealed a difference upon *Tmem160* deletion.

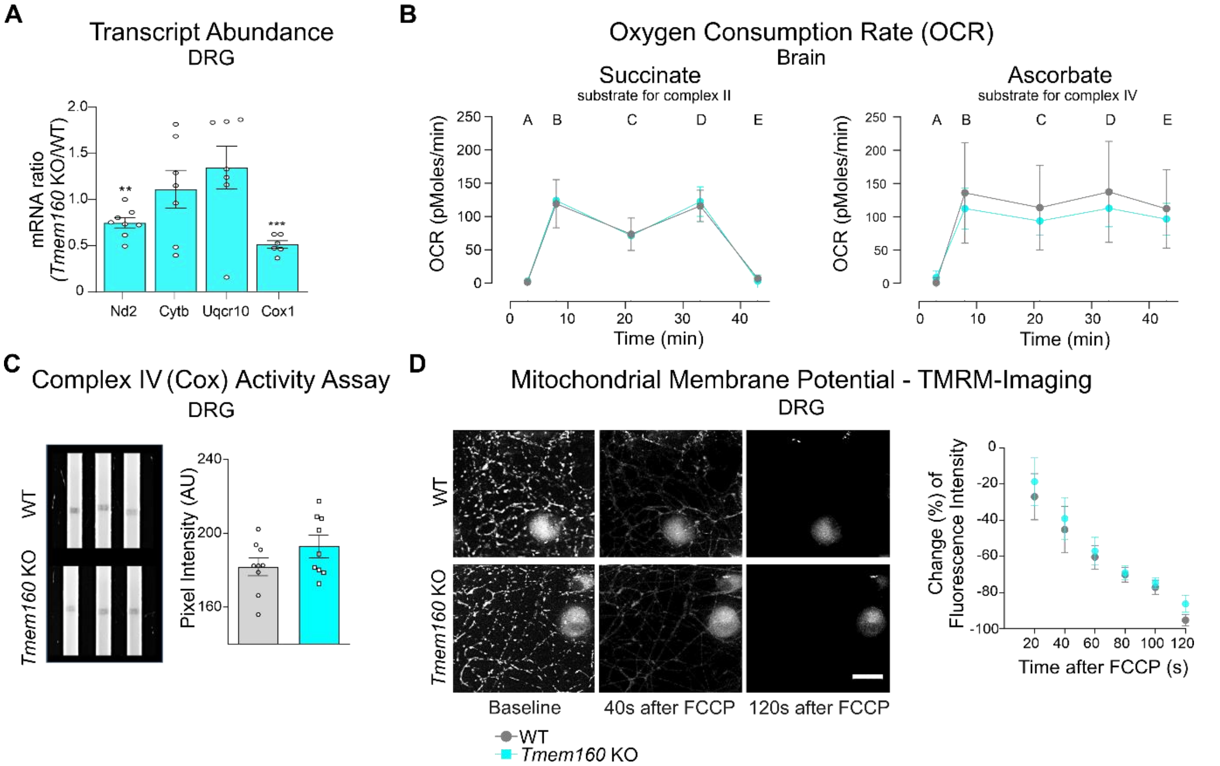

Figure 9: Mitochondrial function appears to be unaffected by *Tmem160* deficiency, adapted from (Segelcke, Fischer, et al., 2021).

(A) Normalized transcript levels of several mitochondrial proteins, components of the electron transport chain (ETC), in lDRG of *Tmem160* KO mice relative to WT littermates as measured by qPCR. Data are represented as mean ± SEM in a scatter bar plot. One-sample t-tests against a hypothetical value of 1.0 (i.e., normalized to WT littermates). P-Values: ** ≤ 0.01, *** ≤ 0.001. N = 4-7 (WT) and N = 6-8 (*Tmem160* KO). (B) Oxygen consumption rate of isolated mitochondria from brains of *Tmem160* KO and WT mice after incubation with succinate (left, a substrate for complex II) or ascorbate (right, a substrate for complex IV). Within each graph: A, calibration; B, substrate (basal respiration); C, Oligomycin (ATP-linked respiration + proton leak); D, FCCP (maximal respiratory capacity); E, Antimycin A + Rotenone + KCN (spare reserve capacity). Data are represented as mean ± SEM. 2-way ANOVA followed by Holm-Sidak's multiple comparison tests, ns. N = 2-3 mice/genotype in 3 independent experiments. (C) Enzyme activity dipsticks for cytochrome c oxidase (Cox, Complex IV) revealed no difference of Cox activity in DRG lysates (both lDRG and total DRG) of *Tmem160* KO and WT mice. (left) Representative images of 3 technical replicates of dipsticks in each genotype, and (right) quantification (depicted as Pixel intensity) across all experiments. Data are represented as mean ± SEM in a scatter bar blot. Unpaired student's t-test, ns. N = 6 in 3 independent experiments with DRG of 2 mice/genotype/experiment; 3 technical replicates/genotype/experiment. (D) TMRM-imaging to monitor the mitochondrial membrane potential upon addition of FCCP. (left) Representative images of the TMRM signal at baseline and two time points after FCCP addition in DRG cultures of either genotype. (right) Quantification of the TMRM signal normalized to the baseline intensity for each genotype. Data are represented as mean ± SEM. Scale bar, 20 µm; 2-way ANOVA followed by Holm-Sidak's multiple comparison tests, ns. Several coverslips from N = 3 mice/genotype for n = 3 independent cultures. Contributions: A, C and D: experiments were performed and analyzed, and pictures were provided by Meike Hütte. B: experiments were performed and analyzed by Sven Dennerlein. A-D: Figure generated by Daniel Segelcke and adapted by me.

Since Tmem160 was originally discovered as a possible protein of interest showing a decreased expression in multiple models of longer lasting pain (Rouwette et al., 2016) we were interested in studying both acute but especially chronic pain behaviors of the *Tmem160* KO.

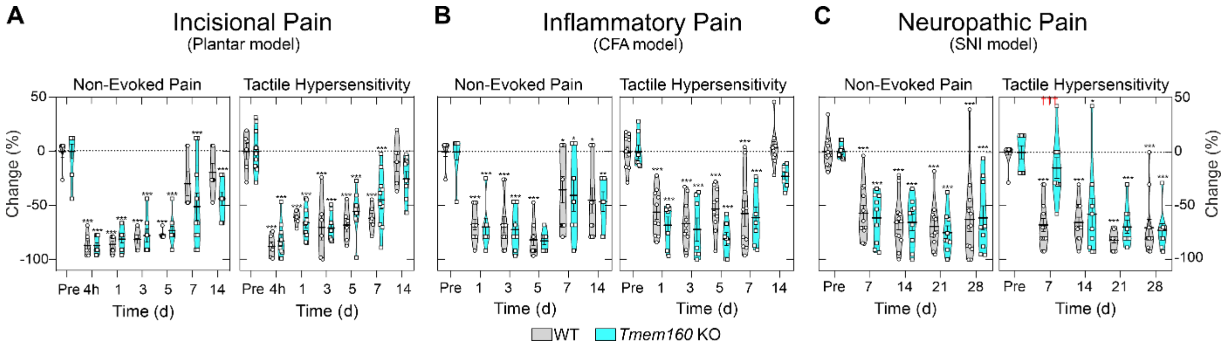

Figure 10: *Tmem160* deficiency delays the establishment of tactile hypersensitivity during neuropathic pain in male mice, adapted from (Segelcke, Fischer, et al., 2021).

Behavioral data of multiple murine pain models. Data are displayed as change in percentage (mean ± SEM) relative to the mean pre-value in a scatter violin plot. Non-evoked pain behavior is depicted as a ratio between treated (ipsilateral) and non-treated (contralateral) paw. Tactile hypersensitivity was measured using Von Frey filaments. (A) Unilateral plantar incision (plantar model of incisional pain) induced similar non-evoked pain behavior and tactile hypersensitivity in *Tmem160* KO and WT littermates over the entire observation period (up to 14 days). N = 6 (WT) and N = 10 (*Tmem160* KO) mice. (B) Unilateral injection of complete Freund's adjuvant (CFA; model of inflammatory pain) into one hind paw induced similar non-evoked pain behavior and tactile hypersensitivity in both genotypes over the entire observation period (up to 14 days). N = 10 (WT) and N = 7 (*Tmem160* KO) mice. (C) Unilateral spared nerve injury (SNI) resulted in similar non-evoked pain in both genotypes over the entire observation period (up to 28 days). In *Tmem160* KO mice, tactile hypersensitivity was significantly attenuated (ꜟꜟꜟ $p \leq 0.001$) 7 days post SNI. N = 10 (WT) and N = 7 (*Tmem160* KO) mice. (A–C) Statistics was performed on raw data, which can be found in Figure 11 and Figure 12. Two-way ANOVA followed by Holm-Sidak's multiple comparison tests. * for comparison between ipsi- and contralateral paws. * $p \leq 0.05$, ** $p \leq 0.01$, ***$p \leq 0.001$. ꜟ for comparison between genotypes; ꜟꜟꜟ $p \leq 0.001$. Contributions: A-C: Data was generated and analyzed by Daniel Segelcke. A-C: Figure generated by Daniel Segelcke and adapted by me.

To model post-operative pain, a unilateral incision was performed at the plantar aspect of the hind paw (Pogatzki & Raja, 2003). No significant differences between *Tmem160* KO and WT could be discerned when considering non-evoked pain behavior (NEP; hind paw footprint analysis, see Methods for detail) and evoked pain behavior (stimuli-evoked pain, tactile and thermal hypersensitivity) (Figure 10A, for additional and raw data Figure 11A, C). Multiple different gait-characteristics, namely print area, stand, swing speed and duty cycle, were investigated using the CatWalk XT gait analysis system (Noldus, NL) to simulate clinically relevant movement-evoked pain behavior (Cunha et al., 2020; Pitzer et al., 2016; Segelcke, Pradier, et al., 2021) (Figure 11A, C). No differences were found between genotypes regarding the gait characteristics post incision, both *Tmem160* KO and WT showed a significant reduction in print area while stand and duty cycle remained unchanged. Overall, this indicates a certain specificity for differences in Tmem160 expression levels in DRG to the more chronic context studied earlier (Rouwette et al., 2016).

To model inflammatory pain CFA was injected unilaterally into the hind paw (McCarson & Fehrenbacher, 2021). The same behavioral battery was used as described before for the incision model (Figure 10B, Figure 11B, D) and did not reveal differences between *Tmem160* KO and WT.

Neuropathic pain was initiated using the SNI model of unilateral transection of two branches of the sciatic nerve. The testing battery was applied as described above for the other pain models (Figure 10C, Figure 12). Sham-treated mice, in which the surgery was performed in the same way omitting nerve transection, served as a control to ensure that the influence is specific for the nerve injury (Figure 12).

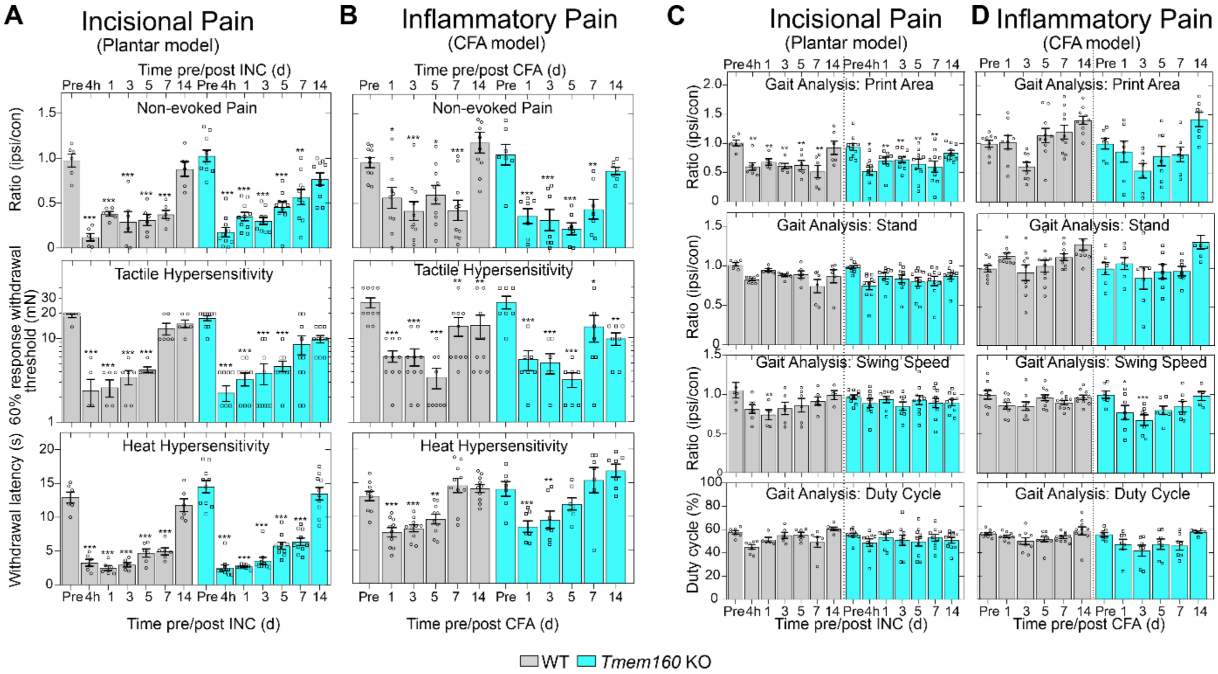

Figure 11: Raw data of behavioral assays in the plantar model of incisional pain and the CFA-model of inflammatory pain, adapted from (Segelcke, Fischer, et al., 2021).

(A and C) Unilateral plantar incision induced non-evoked pain behavior, tactile, and heat hypersensitivity. Non-evoked pain behavior and tactile hypersensitivity are displayed in Figure 10A (A). Moreover, gait analysis showed a reduction of the print area during movement while other measured parameters were largely unchanged, except for a slight reduction in swing speed in WT at day 1 post incision (C). No major differences could be discerned between *Tmem160* KO compared to WT littermates. N = 6 (WT) and N = 10 (*Tmem160* KO) mice. (B and D) Unilateral injection of complete Freund's adjuvant (CFA) into one hind paw induced non-evoked pain behavior, tactile, and heat hypersensitivity. Non-evoked pain behavior and tactile hypersensitivity are displayed in Figure 10B (B). However, gait analysis was largely unchanged, except for a slight reduction in swing speed in *Tmem160* KO at ay 1 and 3 post CFA injection (D). No major differences could be discerned between *Tmem160* KO mice compared to WT littermates. N = 10 (WT) and N = 7 (KO). Data are represented as mean ± SEM in a scatter bar plot. 2-way ANOVA Holm-Sidak's multiple comparison tests. * for comparison relative to pre-values. P-Values: * ≤ 0.05, ** ≤ 0.01, *** ≤ 0.001. Contributions: A-D: Data was generated and analyzed by Daniel Segelcke. A-D: Figure generated by Daniel Segelcke and adapted by me.

3.1.3 Behavioral Differences Upon *Tmem160* Deletion Specific to Day 7 Post SNI

The neuropathic pain model by unilateral sciatic nerve injury (SNI model) (Decosterd & Woolf, 2000) is well-described to cause an effect over at least 28 days. During this time the same behavioral data was collected every 7 days as described above for incisional and inflammatory pain (Figure 10C, Figure 12). Both genotypes showed a largely similar non-evoked pain behavior over the 28-day period. However, testing of tactile hypersensitivity revealed a significant difference between genotypes: WT littermates showed pronounced tactile hypersensitivity at day 7 post surgery as described in the SNI model. In contrast, tactile hypersensitivity was reduced in the *Tmem160* KO mice who did not show a differential behavior compared to the pretesting values (Figure 10C, Figure 12B). This significant influence of *Tmem160* deletion was limited to the specific time point. At later time points in the observation period (14-28 days post SNI) again no significant difference between genotypes was visible and both genotypes showed a hypersensitivity to mechanical stimulation. The data of the control sham surgery showed no difference between *Tmem160* KO and WT (Figure 12).

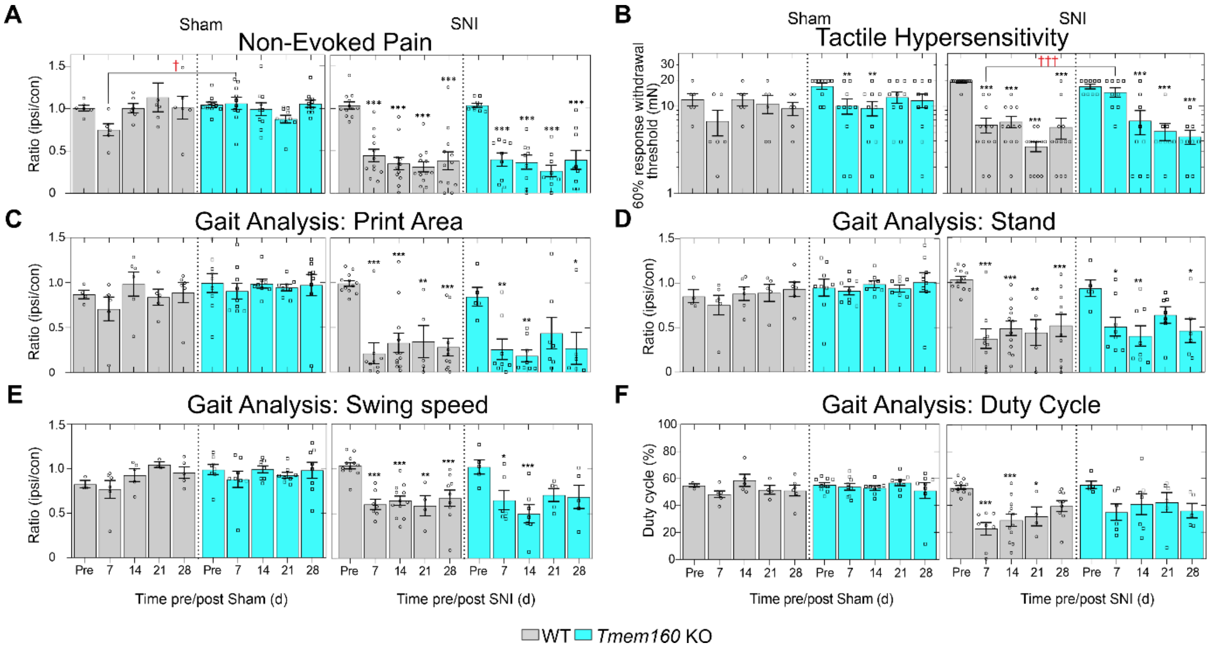

Figure 12: Raw data of behavioral assays in the spared nerve injury (SNI) model of neuropathic pain and sham-operated controls, adapted from (Segelcke, Fischer, et al., 2021).

(A-F) Non-evoked pain behavior as well as multiple parameters of gait analysis are displayed as a ratio between ipsilateral and contralateral side. Tactile hypersensitivity was measured ipsilaterally using Von Frey filaments and is depicted as withdrawal threshold (B). Duty cycle is represented as percentage (F, see Methods for details). No pain-related behavior was observed in Sham-operated mice in either genotype, except for non-evoked pain at 7d in WT (A) and slight tactile hypersensitivity at 7d and 14d in *Tmem160* KO (B). Unilateral spared nerve injury (SNI) induced non-evoked pain behavior (A), tactile hypersensitivity (B), and alterations in static (C, D) and dynamic (E, F) gait parameters in WT littermates and *Tmem160* KO. A strongly attenuated tactile hypersensitivity in *Tmem160* KO at day 7 post SNI (B, as shown in Figure 10C) was the only difference in pain behavior observed between genotypes. Sham: N = 6 (WT) and N = 9 (*Tmem160* KO) mice; SNI: N = 12 (WT) and N = 9 (*Tmem160* KO) mice. Data are represented as mean ± SEM in a scatter blot. Two-way ANOVA followed by Holm-Sidak's multiple comparison tests. * for comparison relative to pre-values. † for comparison between genotypes. P-Values: */† ≤ 0.05, **/†† ≤ 0.01, ***/††† ≤ 0.001. Contributions: A-F: Data was generated and analyzed by Daniel Segelcke. A-F: Figure generated by Daniel Segelcke and adapted by me.

Gait parameters were almost similar between *Tmem160* KO and WT with both showing antalgic gait post-surgery. Nevertheless, *Tmem160* KO mice showed a slightly smaller antalgic gait effect when comparing to pretesting values. While WT revealed a significant effect in all aspects of gait analysis at all time points, except for duty cycle at 28 days, in *Tmem160* KO multiple aspects and time points were insignificant compared to pre-testing. Still, the trend for antalgic gait was visible at all time points upon *Tmem160* deletion. Sham-treated controls from both genotypes served as a control and confirmed that the effects observed during gait analysis where indeed specific to the nerve injury. Non-evoked pain behavior showed a significant difference between genotypes in sham-treated animals at day 7 post surgery.

Additionally, a trend for hypersensitivity can be found in WT at day 7 post injury and in *Tmem160* KO at day 7 and 14 post injury.

Our behavioral data (Figure 8, Figure 10, Figure 11, Figure 12) suggests that a global depletion of *Tmem160* delays the establishment of tactile hypersensitivity in SNI-induced neuropathic pain while neuropathic pain maintenance as well as other pain-related behaviors (non-evoked pain behavior and antalgic gait) and other pain models (acute pain, plantar incision, CFA) show no influence of a lack of Tmem160.

3.1.4 *Tmem160* Deletion Reduces Cytokine/Chemokine Levels in Naïve Mice

To better understand the underlying molecular mechanisms of the *Tmem160* KO phenotype, neuroimmune and inflammatory signaling processes were investigated. These processes have been described to play a role in driving tactile hypersensitivity in the early phase of the SNI model (Cobos et al., 2018; Peng et al., 2016). We used a commercially available cytokine and chemokine array (Liu et al., 2019) to simultaneously assess the relative protein abundance of 40 cytokines in DRG lysates of naïve *Tmem160* KO and WT mice (Figure 13A, Figure 4). Overall, a downregulation of both pro- and anti-inflammatory cytokines/chemokines was observed in DRG lysates of male *Tmem160* KO compared to WT littermates using corrections with multiple testing. Many pro-inflammatory cytokines appeared significantly reduced, such as IFNγ, several interleukins (ILs; e.g. IL1β, IL6 and IL17 (the latter two being downstream factors of IL23, which shows a non-significant tendency ($p = 0.071$) for downregulation)). Also, TNFα shows a tendency ($p = 0.069$) for downregulation which gets significant when only individual significances are observed without any multiple testing option (Figure 13A). Given the complexity of inflammatory signaling (Ji et al., 2016) a simple interpretation or prognosis of the effect of the changes is difficult. Since many of the downregulated proteins are pro-inflammatory our results may nevertheless hint at a shift to an anti-inflammatory state in naïve male *Tmem160* KO DRG. A change compared to our publication from 2021 (Segelcke, Fischer, et al., 2021) is the new option of using multiple testing for the cytokine array experiments, that is by now provided by the newest version of GraphPad Prism (GraphPad Prism9). This allowed us to correct for potential significant results that occur only due to the higher number of cytokines/chemokines compared. This reduced the number of significant changes for the cytokine array experiments but did not change the overall conclusions. Nevertheless, it must be pointed out that the reduction of TNFα upon *Tmem160* deletion in male mice is no longer statistically significant. Still, we did observe a clear change upon addition of TNFα to our primary neuronal cultures prior to Ca^{2+}-imaging experiments. This shows the risk of losing biologically relevant results to statistical insignificance by using multiple testing. It should always be considered whether it is more important not to miss any potential difference or whether to focus on a higher likelihood of all reported changes to be caused by actual differences between the biological samples.

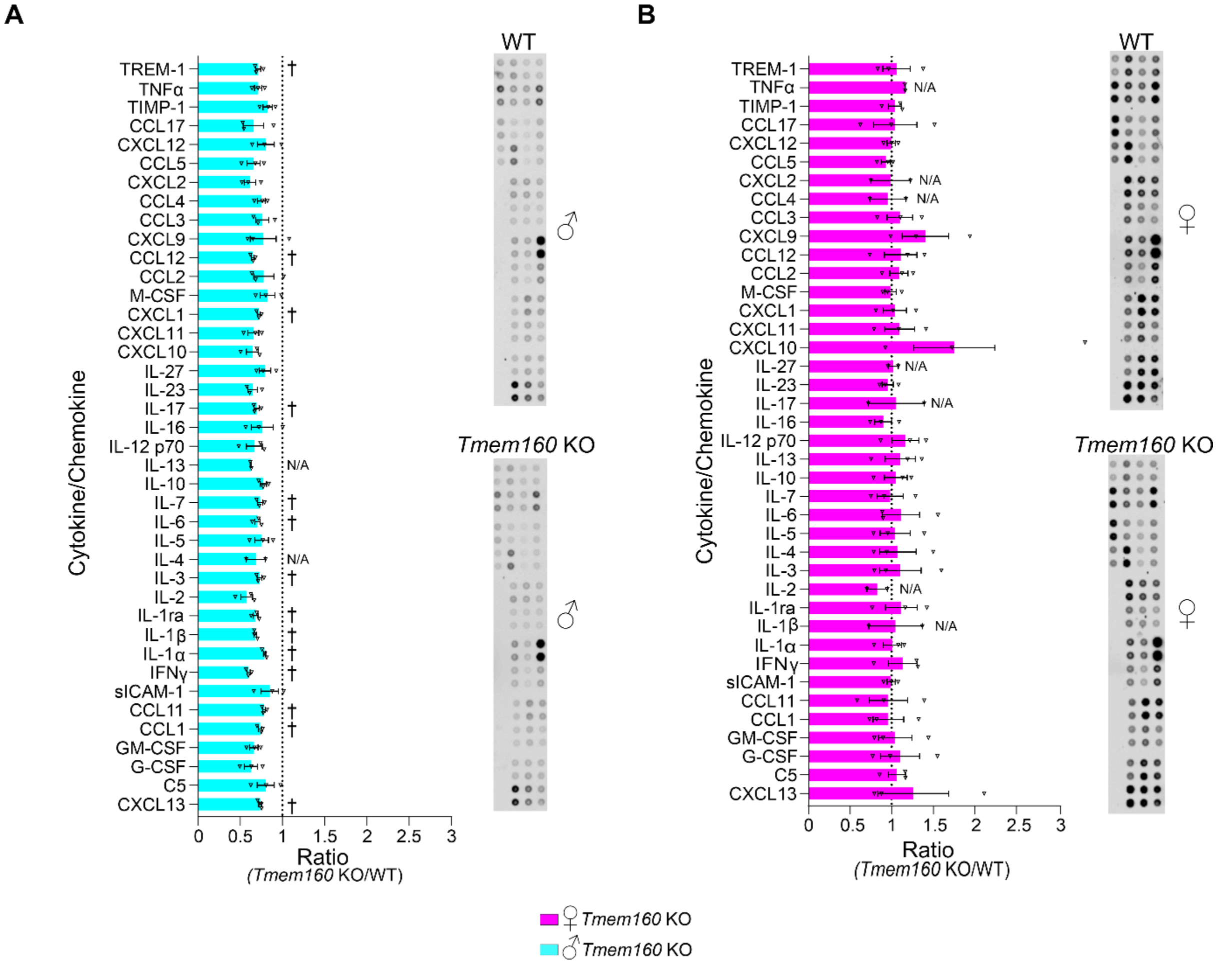

Figure 13: *Tmem160* deficiency alters the DRG cytokine/chemokine levels in a sexually dimorphic manner, adapted from (Segelcke, Fischer, et al., 2021).

Cytokine/chemokine levels in DRG lysates of *Tmem160* KO and WT mice were compared. (A) Pronounced downregulation of diverse pro- and anti-inflammatory cytokines and chemokines in naïve male *Tmem160* KO compared with WT littermates. (B) No overt changes in cytokines and chemokines in naïve female *Tmem160* KO compared with WT littermates. (A and B) Exemplary images of the membranes for WT (top) and *Tmem160* KO (bottom). Data are depicted as mean ± SEM in a scatter bar plot displaying the ratio of the abundance of each cytokine/chemokine between male *Tmem160* KO and WT mice, ratio *Tmem160* KO/WT. Multiple testing using ratio-paired t-tests. † for comparison between genotypes. † $p \leq 0.05$, †† $p \leq 0.01$. If ≤ 2 values/genotype were obtained per cytokine/chemokine, the significance could not be assessed (N/A). N = 6 (WT) and N = 6 (*Tmem160* KO) mice per sex. n = 3 membranes/genotype. Contributions: Data were generated and analyzed, and pictures were provided by me. Figures were generated by Daniel Segelcke and adapted by me.

3.1.5 Cytokine Expression Post SNI Might Depend on Tmem160

In male tissue at day 7 post SNI ipsilateral and contralateral lDRG of both *Tmem160* KO and WT animals were compared (Figure 14). The non-operated contralateral side served as control. In male WT animals an upregulation of sICAM-1 and IL-1ra on the ipsilateral side compared to contralateral control was found, that loses its significance upon the use of multiple testing. Despite this loss of significance, I would like to give a brief overview on possible interpretations of the experimental results, specifically since TNFα also showed a loss of significance under naïve conditions but turned out relevant within the course of the study. Our observations in WT are similar to observations of Lindborg et al. after axotomy in comparison to the sham-operated contralateral side reporting an ipsilateral increase of the pro-inflammatory cytokine sICAM-1 (Lindborg et al., 2018). In the contrary, IL-1ra is a commonly known anti-inflammatory cytokine which upon central injection may lead to analgesia (Webster et al., 2017). In our case this could implicate that the body is acting by counter measures.

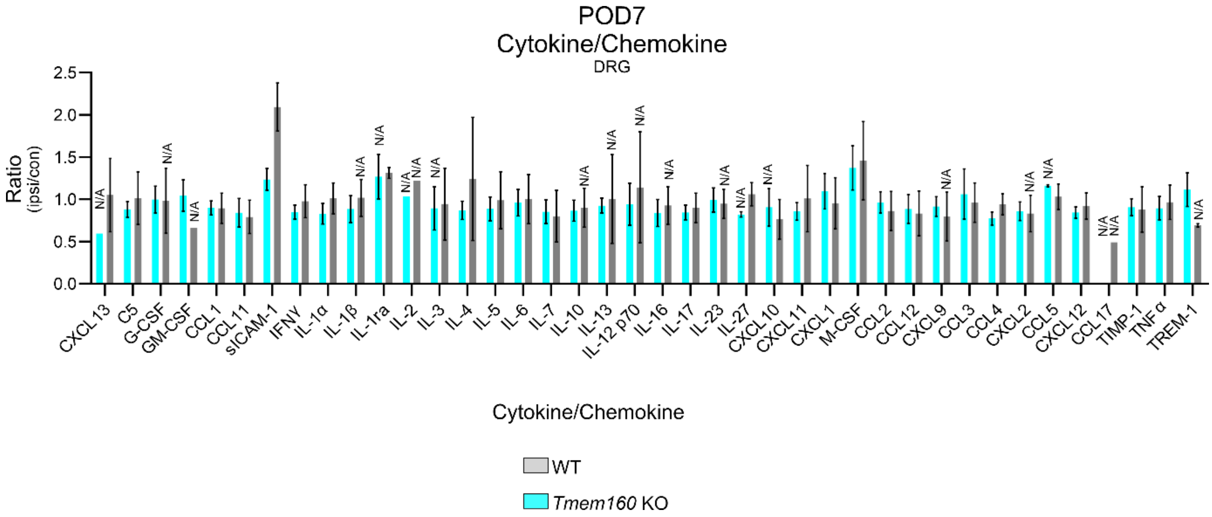

Figure 14: *Tmem160* deficiency alters the DRG cytokine/chemokine levels at day 7 post SNI in male mice.

Cytokine/chemokine levels in DRG lysates of ipsilateral versus contralateral *Tmem160* KO and WT mice were compared. Data are depicted as mean ± SEM in a scatter bar plot displaying the ratio of the abundance of each cytokine/chemokine between ipsi and con, ratio ipsi/con. Multiple testing using ratio-paired t-tests. If ≤ 2 values/genotype were obtained per cytokine/chemokine, the significance could not be assessed (N/A). N = 3 (WT) and N = 4 (*Tmem160* KO) mice. n = 3-4 membranes/genotype/side. Contributions: Data were generated and analyzed, and pictures were provided by me. Figure was generated by me.

In *Tmem160* KO animals, no elevation of sICAM-1 could be observed when comparing ipsi and con, IL-1ra levels could not be assessed. MIP-1β (also known as CCL4) showed a tendency for downregulation on the ipsilateral side (p=0.0733, before multiple testing). This is interesting since the pro-inflammatory cytokine has been described to be upregulated upon peripheral nerve injury and to play a role in inducing tactile allodynia (Saika et al., 2012). In our behavioural experiments we observed impaired tactile allodynia in the male *Tmem160* KO ipsi post SNI. An ipsilateral downregulation of CCL4 in the *Tmem160* KO could therefore contribute to the delayed establishment of tactile hypersensitivity in male *Tmem160* KO. The differential expression levels that were observed between KO and WT after SNI support the differential pain phenotype but are not able to fully explain them.

3.1.6 Tmem160 Acts Sexually Dimorphic: No Significant Changes to Wildtype Observed in Female Mice

All results described so far were generated only in male adult mice. In the context of pain and neuroimmune interactions the importance of the sex of the subjects has gained further attention and behavioral and mechanistical differences between male and female get reported frequently (Lopes, Malek, et al., 2017; Mapplebeck et al., 2016; Mogil, 2012; Rosen et al., 2017) (see Introduction). Since we observed differences in our male *Tmem160* KO mice in both the pain behavioral response and neuroimmune interactions (Figure 10C, Figure 13A) we decided to repeat the previous studies for females, where differences between *Tmem160* KO and WT were observed in male.

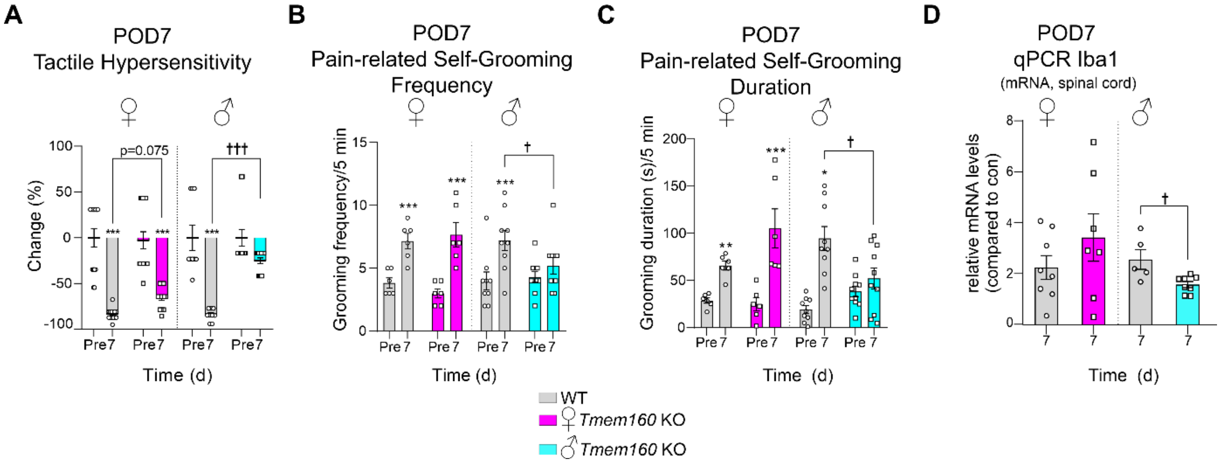

Figure 15: *Tmem160* deficiency alters neuropathy-related pain behaviors in a sexually dimorphic manner at day 7 post SNI, adapted from (Segelcke, Fischer, et al., 2021).

(A-C) Seven days after SNI, at post operative day 7 (POD7), different behavioral aspects were analyzed. (A) Tactile hypersensitivity as measured using Von Frey filaments is displayed as the percentage change relative to the mean pre-value of withdrawal threshold in a scatter bar plot. *Tmem160* KO males (independent cohort from data in Figure 10C, but same experimental design), but not females, exhibited reduced tactile hypersensitivity. (B and C) Pain-evoked self-grooming is expressed by frequency (B) and duration in seconds (C) over a 5 min observation period. Data are displayed as mean ± SEM in a scatter bar plot. Self-grooming is increased in male WT and female *Tmem160* KO and WT at POD7 compared to the pretesting values. No significant increase in self-grooming was observed in male *Tmem160* KO. (A-C) Two-way ANOVA followed by Holm-Sidak's multiple comparison tests on raw data. (A) Females: N = 14 (WT) and N = 16 (*Tmem160* KO) mice. Males: N = 9 (WT) and N = 15 (*Tmem160* KO). (B and C) κ = 0.852 for frequency and κ = 0.785 for duration. Females: N = 6 (WT) and N = 6 (*Tmem160* KO) mice. Males: N = 9 (WT) and N = 15 (*Tmem160* KO). (D) At 7 days post SNI, Iba1 mRNA levels were upregulated in the ipsilateral spinal cord (compared with the contralateral side) in female WT and *Tmem160* KO mice as well as in male WT mice, but the upregulation was significantly smaller in *Tmem160* KO males than in WT males. Data are depicted as mean ± SEM in a scatter bar plot. Mann-Whitney test between genotypes within sex. Females: N = 8 (WT) and N = 7 (*Tmem160* KO) mice. Males: N = 5 (WT) and N = 8 (*Tmem160* KO) mice. (A-D) * for comparison relative to pre-values/sex. † for comparison between genotypes/sex. */ † p ≤ 0.05, **p ≤ 0.01, ***/ ††† p ≤ 0.001. Contributions: A-C: Experiments were performed and analyzed by Daniel Segelcke. D: Experiments were performed and analyzed by me. A-D: Figures were generated together with Daniel Segelcke and adapted by me.

In contrast to the male *Tmem160* KO (Figure 15A and Figure 10C), the female *Tmem160* KO mice did not show a significant delay in onset of tactile hypersensitivity but rather showed a WT-like behavior (Figure 15A and Figure 16B). It remains noteworthy, that even though female *Tmem160* KO mice show tactile hypersensitivity at day 7, they show a tendency (p = 0.075) for smaller changes in tactile sensitivity to pretesting as compared with the female WT mice (Figure 15A). All other behaviors described above (NEP, locomotion) did not show a significant difference between female *Tmem160* KO and WT mice (Figure 10C, Figure 12A and Figure 12C-F). Within the SNI studies an additional example of rodent-specific behavior was observed, namely changes in self-grooming behavior post SNI (Cunha et al., 2020). Increases in self-grooming behavior under pain conditions have been reported to be used as distractions and might even cause hypoalgesia (Callahan, 2008). Self-grooming also led to a better well-being of the mice (Callahan, 2008). The exact molecular mechanisms underlying this process are unclear, a hypothesis would be that self-grooming acts hypoalgesic via spinal inhibitory interneurons. The interneurons could be influenced by A-fibers in the skin activated directly by grooming (Beyer et al., 1985). When examining grooming frequency and duration (Figure 15B-C) in male and female *Tmem160* KO and WT mice, we see a significant elevation in its frequency and duration in both WT groups at day 7 post SNI compared to pretesting values. While female *Tmem160* KO mice also showed this elevation, male *Tmem160* KO mice revealed weakened self-grooming at this time point. Our data suggest that the aforementioned phenotype of attenuated tactile hypersensitivity and changes in self-grooming behavior is specific to males 7 days post SNI and therefore sexually dimorphic. Next, we compared the cytokine/chemokine levels of the female KO mice with their WT counterpart (Figure 13B). Also, there we could not see the same effect as observed in the male *Tmem160* KO mice (Figure 13A). To further look at the immune response in the spinal cord qPCR for the microglia-activation marker Ionized calcium binding adaptor molecule 1 (Iba1) on spinal cord tissue from day 7 post SNI was performed (Figure 15D). Iba1 showed higher transcript levels in the ipsilateral spinal cords of WT mice of both sexes (compared to the contralateral side), indicating an ipsilateral activation of microglia in the spinal cord. This increase was significantly reduced in male *Tmem160* KO mice (Figure 15D). This could mean, that the reduction in tactile hypersensitivity is linked to a reduced ipsilateral microgliosis. Spinal Iba1 transcript level did not differ between genotypes anymore at the later time point of 28 days post SNI (Figure 16G), meaning that the microgliosis did not differ anymore between genotypes in males, in parallel with the behavioral phenotype (reduced tactile hypersensitivity) of male KO mice being specific to the early time point of the SNI model. Since the behavioral differences observed in male mice upon *Tmem160* deletion did not occur at later time points, studies using the SNI model in female *Tmem160* KO mice were only conducted until day 7 post surgery, the day most differences in males were observed. This was done to reduce the burden on the mice.

In conclusion, the results in female *Tmem160* KO mice strongly support a sexually dimorphic role of *Tmem160* in neuroimmune signaling, specifically during the early phase of neuropathic pain as represented by the SNI model (Figure 15).

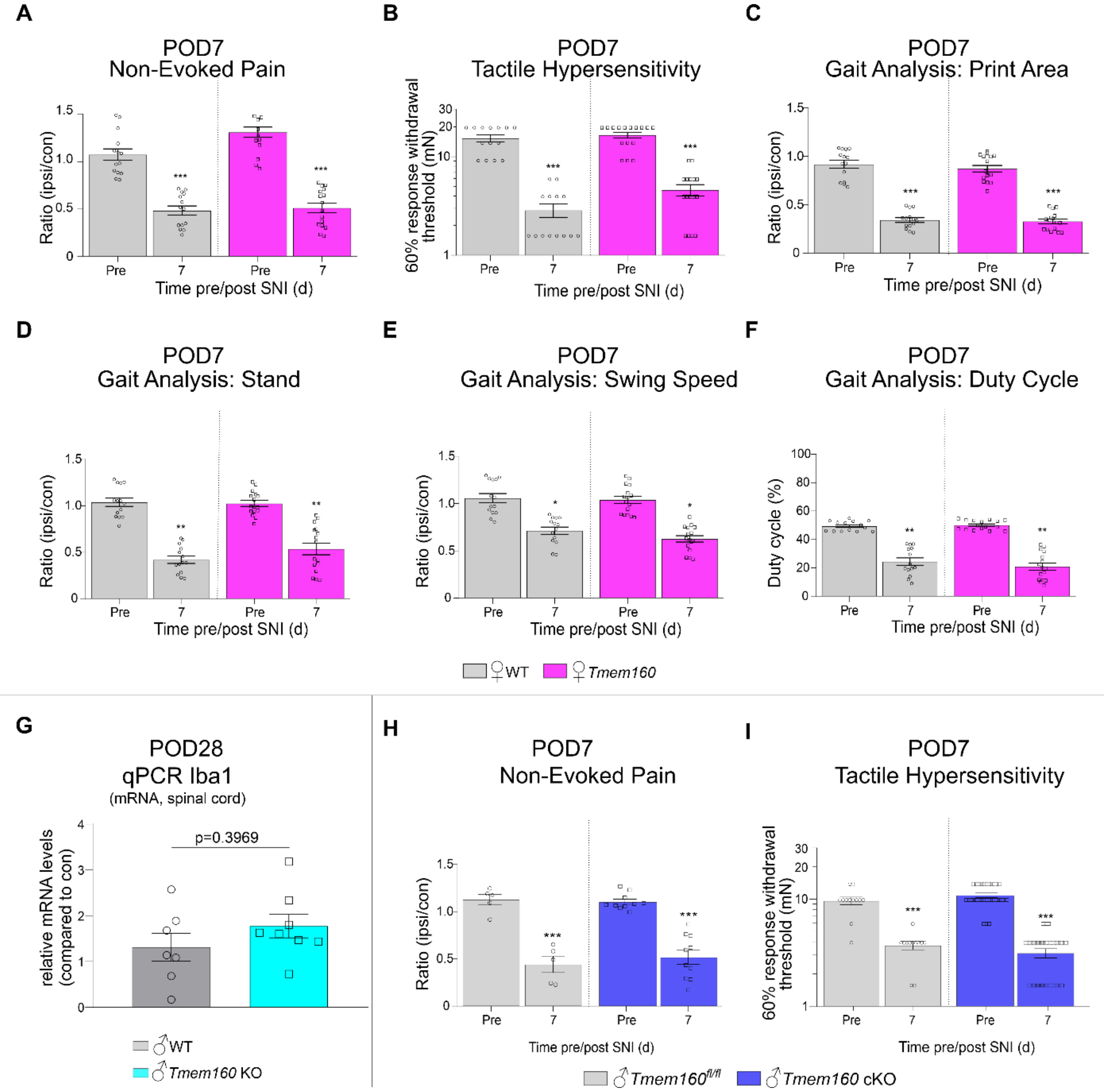

Figure 16: Raw data of behavioral assays in the SNI model of neuropathic pain 7d post SNI and Iba1 levels 28d post SNI, adapted from (Segelcke, Fischer, et al., 2021)

(A-F) Female global *Tmem160* KO mice: Unilateral spared nerve injury (SNI) induced non-evoked pain behavior (A), tactile hypersensitivity (B), and alterations in static (C, D) and dynamic (E, F) gait parameters in female *Tmem160* KO and WT littermates. (G) 28d post SNI Iba1 mRNA levels were upregulated in the ipsilateral spinal cord (compared to the contralateral side). Data are depicted as mean ± SEM in a scatter bar plot. Mann-Whitney test between genotypes, p = 0.39, ns. N = 7 (WT) and N = 8 (*Tmem160* KO) mice. (H-I) Male Advillin-Cre *Tmem160* KO (*Tmem160* cKO) mice: Unilateral SNI induced non-evoked pain behavior (H) and tactile hypersensitivity (I) in both floxed littermate controls (*Tmem160*$^{fl/fl}$) and *Tmem160* cKO male mice. (H) N = 5, *Tmem160*$^{fl/fl}$; N = 10, *Tmem160* cKO. (I) N = 12 *Tmem160*$^{fl/fl}$; N = 22 *Tmem160* cKO. (A-F, H, I) Data are represented as mean ± SEM in a scatter bar blot. 2-way ANOVA followed by Holm-Sidak's multiple comparison tests. * for comparison relative to pre-values. p-Values: * ≤ 0.05, **≤ 0.01, *** ≤ 0.001. Contributions: A-F, H-I: Experiments were performed and analyzed by Daniel Segelcke. G: Experiments were performed and analyzed by me. A-G: Figures were generated together with Daniel Segelcke and adapted by me.

3.1.7 Understanding the Action Mechanisms of Tmem160 by means of the sexual dimorphism

Our behavioral experimental results in female mice show, that for them, as opposed to the males, Tmem160 is not necessary to initiate tactile hypersensitivity and changes in grooming behavior in the early phases of 7 days post-surgery in the SNI model. This can be concluded since female *Tmem160* KO mice did not reveal significant differences compared to WT regarding tactile hypersensitivity and self-grooming behavior (Figure 15). What does this teach us about potential action mechanisms for Tmem160? To answer this question, it is important to know that many physiological and pathological processes differ between males in females both in rodents and in humans. Similar differences have already been reported in the context of pathological pain (Lopes, Malek, et al., 2017; Mapplebeck et al., 2016; Mogil, 2012; Rosen et al., 2017; Sorge et al., 2015). It has been reported, that pain pathways in males are noticeably influenced by microglia and macrophages (Lopes, Denk, & McMahon, 2017; Sorge et al., 2011; Sorge et al., 2015; X. Yu et al., 2020), while in females, these pathways were influenced by a T-cell response (Laumet et al., 2019; Mapplebeck et al., 2016; Sorge et al., 2015). Peng and colleagues also observed a sexual dimorphism in a spinal nerve transection model for neuropathic pain, that was specific to tactile hypersensitivity but only in the maintenance and not in the initiation phase post injury (Peng et al., 2016). The sexually dimorphic results that were observed indicate a role of Tmem160 in neuroimmune signaling, specifically in neuropathic pain.

3.1.8 Conditional KO in Sensory Neurons Alone is Insufficient to Produce Changes *in Vivo* and *in Vitro*

As described above, there is a well-described sexual dimorphism in neuroimmune signaling during pain (Lopes, Malek, et al., 2017; Rosen et al., 2017). Since we did find sex-dependent differences, we were further wondering, whether Tmem160 fulfils its function in neuroimmune signaling in early neuropathic pain. Tmem160 could act either in DRG sensory neurons, in immune cells or both. A recent study of spinal microglia populations within the SNI model in WT (Tansley et al., 2022) reported the expression of Tmem160 specifically in one of their microglia populations (referred to as “cluster 9” microglia). This population showed an inflammatory profile and is mainly lacking under naïve conditions (0.035% of total microglia) while in the early phase post SNI (day 3 post surgery) the percentage rises to 4.9% of total. The increase of this cluster was only detected in male but not in female mice. This showed many parallels to our here described experimental observations in the global *Tmem160* KO mice, namely an influence in the early phase post SNI that was observed in male but not in female, in our case on mechanical hypersensitivity behavior. It would be of interest to further study the role of these microglia (cluster 9), or more specifically Tmem160 in these microglia, but since they are so rare, this was not possible. Due to the inability to directly target *Tmem160* in the immune system, instead, neuronal *Tmem160* was targeted specifically. This also allowed conclusions about neuroimmune signaling and therefore generated indirect knowledge on the role of Tmem160 in immune cells. To achieve this, conditional KO (cKO) mice (Advillin *Tmem160* KO) were generated with the Advillin-Cre driver line (see Methods for detail). This deleted *Tmem160* in approximately 80% of DRG sensory neurons (Zurborg et al., 2011). For the experiments in this section, floxed littermates were chosen as appropriate controls, equivalent to WT littermates for the *Tmem160* KO (see Methods for detail). cKO was validated using genotyping and qPCR of DRG tissue (remaining Tmem160 transcript level = 11% ± 1% of floxed littermate controls (*Tmem160*$^{fl/fl}$), N = 8 mice/genotype). This value might seem high compared to the global *Tmem160* KO but is influenced by non-neuronal cells of the DRG as well as a remaining expression of Tmem160 in approximately 20% of the primary sensory neurons.

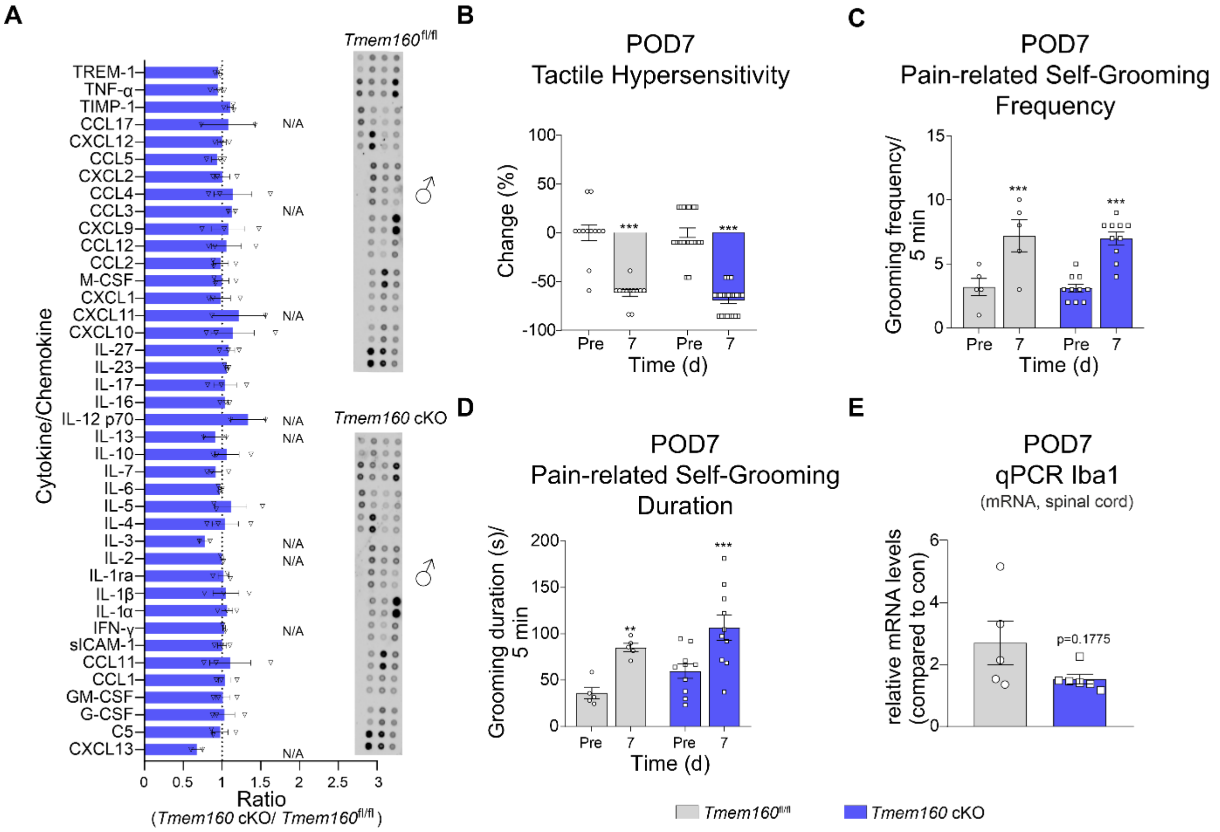

Figure 17: Conditional *Tmem160* deficiency in Advillin-positive sensory neurons reveals no alterations of the DRG cytokine profile or neuropathy-induced behaviors or spinal Iba1 mRNA levels in male mice, adapted from (Segelcke, Fischer, et al., 2021).

(A) Cytokine/chemokine levels were compared between DRG of naïve Advillin-Cre *Tmem160* cKO (*Tmem160* cKO) males and floxed male littermate controls (*Tmem160*$^{fl/fl}$). Exemplary images of the membranes for *Tmem160*$^{fl/fl}$ (top) and *Tmem160* cKO males (bottom). Data are represented as mean ± SEM in a scatter bar plot. Multiple testing using ratio-paired t-tests, ns. If ≤ 2 values/genotype were obtained per cytokine/chemokine, the significance could not be assessed (N/A). N = 6 (WT) and N = 6 (cKO) mice. n = 3 membranes/genotype. (B–D) Pronounced tactile hypersensitivity and pain-related self-grooming in both floxed male littermate controls (*Tmem160*$^{fl/fl}$) and *Tmem160* cKO 7 days post SNI. Tactile hypersensitivity is displayed as the percentage change (± SEM) relative to the mean pre-value in a scatter bar plot (B). Pain-evoked self-grooming is expressed by frequency (C) and duration in seconds (D) over a 5 min observation period (κ = 0.882 for frequency, κ = 0.815 for duration). Self-grooming data are displayed as mean ± SEM in a scatter bar plot (C and D). Two-way ANOVA followed by Holm-Sidak's multiple comparison tests on raw data. * for comparison relative to pre-values. *$p \le 0.05$, **$p \le 0.01$, ***$p \le 0.001$. (C and D) N = 5 (*Tmem160*$^{fl/fl}$) and N = 10 (*Tmem160* cKO). (E) 7 days post SNI, Iba1 mRNA levels were upregulated in the ipsilateral spinal cord (compared with the contralateral side) in both floxed male littermate controls (*Tmem160*$^{fl/fl}$) and cKO (*Tmem160* cKO) males. Data are depicted as mean ± SEM in a scatter bar plot. Mann-Whitney test between genotypes, p = 0.1775. N = 5 (*Tmem160*$^{fl/fl}$) and N = 6 (*Tmem160* cKO). Contributions: A and E:

Experiments performed and analyzed by me. B-D: Experiments performed and analyzed by Daniel Segelcke. Figures generated together with Daniel Segelcke and adapted by me.

The following experiments in which differences were observed between male *Tmem160* KO and WT mice were repeated with male *Tmem160* cKO mice and floxed controls to study the cKO and gain further insights: cytokine and chemokine array (Figure *17*A), SNI model and pain-related behaviors at day 7 post SNI (Figure *17*B-D, Figure *16*) and spinal Iba1 levels at day 7 post SNI (Figure *17*E). Cytokine levels, as well as pain behavior in the cKO were largely similar to the floxed littermate controls showing no expression of Advillin-Cre. Spinal Iba1 levels increased in *Tmem160* cKO and floxed controls (ipsi compared to con), slightly less so in the cKO ($p = 0.1775$, not significant, Figure *17*E), indicating an ipsilateral activation of microglia, i.e., a microgliosis. Overall, none of the experiments revealed significant differences between *Tmem160* cKO and floxed controls, suggesting that the differences in the global *Tmem160* KO mice relative to wildtype are not based on only sensory neurons. We cannot be completely sure that sensory neurons are not involved in this process, since around 20% of the DRG sensory neurons are spared in cKO mice using the Advillin-Cre driver line (Zurborg et al., 2011). Nevertheless, it is most likely that in male mice, in the early phase of neuropathic pain post SNI, Tmem160 does not play its role in neuronal cells but rather in non-neuronal cells, possibly in immune cells or indeed in the “cluster 9” microglia population mentioned above (Tansley et al., 2022).

3.1.9 *Tmem160* Deletion Modulates TRPA1-Mediated Neuronal Excitability *in Vitro*

As a final step in our study of Tmem160 and its KO mouse lines, we wanted to better understand the mechanisms leading from an altered naïve cytokine/chemokine profile to the observed behavioral phenotypes. One option is that this would happen via changes in neuronal excitability. Intriguingly, TNFα, one of the cytokines demonstrated to be downregulated in the DRG of male *Tmem160* KO mice in the cytokine array, has previously been shown to influence TRPA1 and TRPV1 membrane trafficking and channel activity (Meng et al., 2016). Additional other cytokines also regulate the TRP channels (Guan et al., 2016), but the decision was made to further investigate the potential role of TNFα in our puzzle. Ratiometric Ca^{2+}-imaging was performed in primary DRG cultures from naïve mice to detect potential changes in TRPA1 (stimulated with 30 µM AITC)- or TRPV1 (stimulated with 100 nM Caps)-induced neuronal response (Bautista et al., 2006). To control for general neuronal health and activity, KCl stimulation was performed at the end of the experiment (Figure 18) leading to membrane depolarization in all neurons (Y. Chen & Huang, 2017) and consequently activating voltage-gated calcium channels (Catterall, 2011; Schor et al., 2009). In order to compensate for the lower level of TNFα in male *Tmem160* KO DRG (Figure 13A), cultures were incubated with exogenous TNFα (100 ng, 6h) or vehicle control. Afterwards, the conditions were compared using ratiometric Ca^{2+}-imaging (Figure 18A-C). Indeed, we did see differences in the vehicle control conditions between *Tmem160* KO and WT: While the cultures lacking *Tmem160* showed WT-like response amplitudes to AITC (Figure 18A and C) the percentage of cells responding to AITC stimulation was significantly reduced upon *Tmem160* deletion (Figure 18A-B). The exogenous addition of TNFα "rescued" the reduced response to AITC in the *Tmem160* KO culture returning the response to the WT level (Figure 18A-B). The response to KCl was largely similar across all conditions, and the TRPV1 response differed only in the response amplitude in the *Tmem160* KO condition incubated with TNFα (Figure 18A-C). This reveals a certain specificity of the effect to the TRPA1 response. Since TRPV1 is prone to desensitization, Ca^{2+}-imaging was performed again in primary DRG cultures of naïve mice omitting the AITC stimulation and prior incubation with TNFα. Instead, two different concentrations of Caps stimuli were given (Figure 19A-C). Under these conditions, no significant difference was visible between *Tmem160* KO and WT.

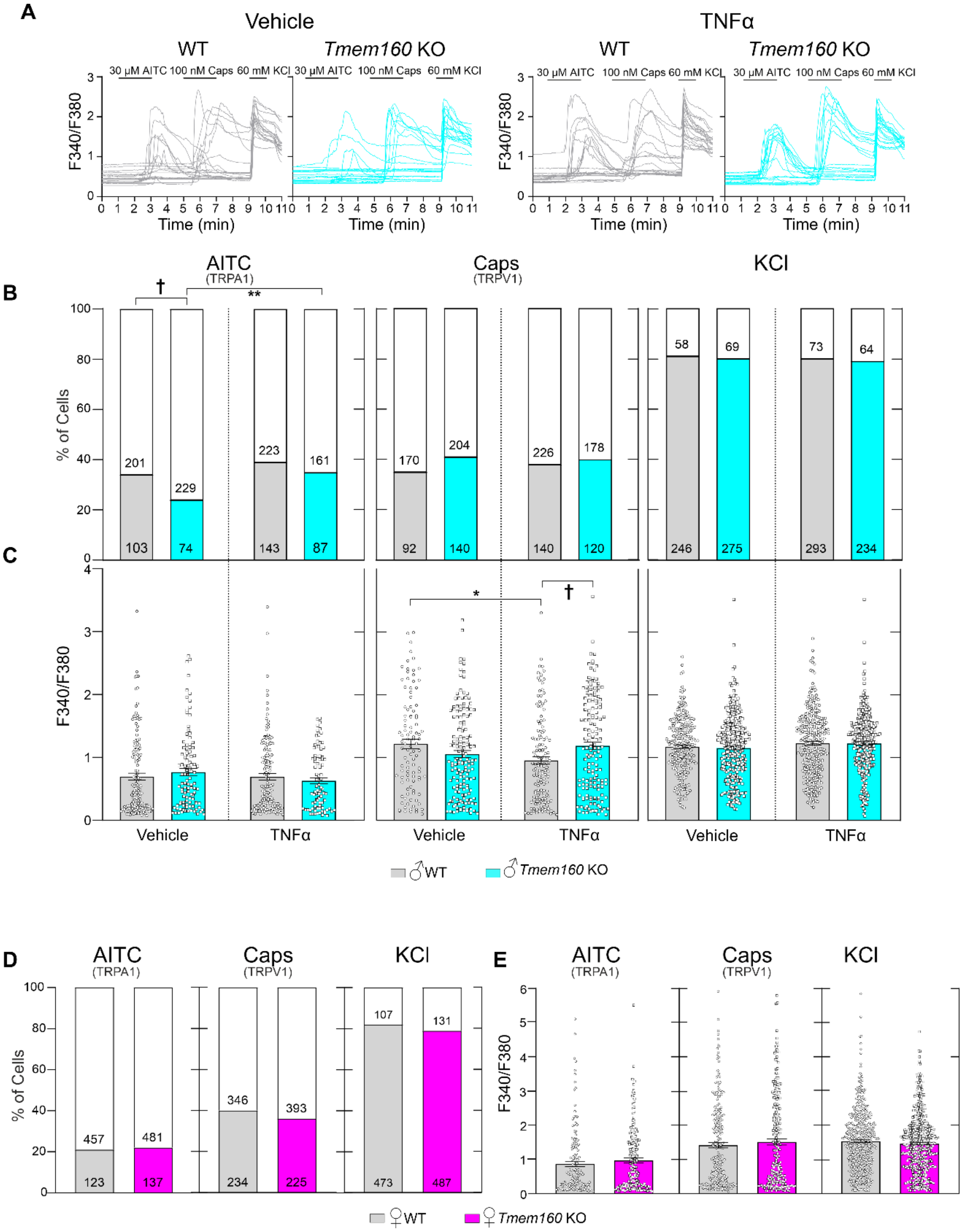

Figure 18: Tmem160 modulates TRPA1-mediated neuronal activity in males, adapted from (Segelcke, Fischer, et al., 2021).

(A–C) Ratiometric Ca^{2+}-imaging was performed in cultured DRG neurons of naïve *Tmem160* KO and WT males. After incubation with exogenous TNFα (100 ng) or vehicle (0.1% BSA in PBS) for 6 h, stimuli were applied from minute 1 to 3 (AITC, 30 µM), 5 to 7 (Caps, 100 nM), and 9 to 10 (KCl, 60 mM) (see black bars in (A)). (A) Representative traces and stimulation protocol. (B) Percentage of responding (colored part) and non-responding (white part) cells to indicated stimuli. Numbers represent the total number of neurons responding or non-responding to the stimuli. (C) Scatter bar plots represent the maximum fluorescence amplitudes (F340/380, mean ± SEM) of responding neurons to indicated stimuli. (D–E) Ratiometric Ca^{2+}-imaging was performed in cultured DRG neurons of naïve *Tmem160* KO and WT females exactly as described above for males yet without incubation with TNFα/vehicle. (D) Percentage of responding (colored part) and non-responding (white part) neurons to indicated stimuli. Numbers represent the total number of neurons imaged. (E) Scatter bar plots represent the maximal amplitudes (mean ± SEM) of responding neurons to indicated stimuli. (B and D) Fisher's exact test. (C and E) Mann-Whitney Test. All tests: * for comparison to vehicle control. ⫯ for comparison between genotypes. */⫯ $p \leq 0.05$, ** $p \leq 0.01$. For both genotypes and sexes, multiple coverslips from N = 3 mice were used. Contributions: A-C: Experiments were performed and analyzed by me, during my master thesis. D-E: Experiments were performed and analyzed by me. A-E: Figures were generated together with Daniel Segelcke and adapted by me.

To complete our data sets and gain further mechanistic insights, we performed Ca^{2+}-imaging experiments with MO, Caps and KCl stimuli but without incubation with TNFα using DRG cultures from female *Tmem160* KO and WT mice (Figure 18A-E), as well as male cKO and floxed control mice (Figure 20A-B). None of those comparisons revealed any differences or any effect of the *Tmem160* KO in females and the *Tmem160* cKO in males on any neuronal activity tested, indicating that the main action mechanism of Tmem160 – conceivably via downregulation of TNFα – most likely does not take place in neuronal cells and is somewhat specific to males.

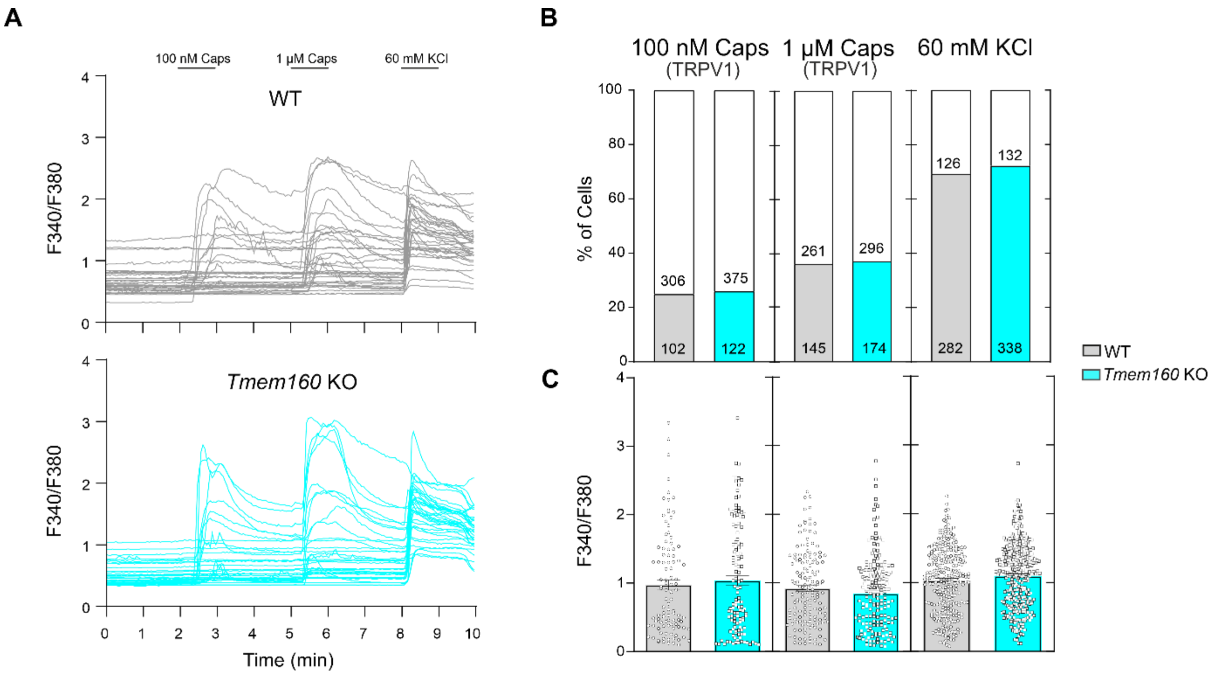

Figure 19: Tmem160 does not significantly affect TRPV1-mediated neuronal activity, adapted from (Segelcke, Fischer, et al., 2021).

Ratiometric Ca^{2+}-imaging was performed in cultured DRG neurons of naïve *Tmem160* KO and WT males, measuring Ca^{2+} influx by the ratio of fluorescence emitted from different excitatory wavelengths (F340/380). (A) Representative traces and stimulation protocol. (B) Percentage of responding neurons (colored part) to indicated stimuli are displayed, the total number of neurons assessed is depicted in the respective bars. Fisher's exact test was performed between genotypes. (C) Average response amplitudes to indicated stimuli are displayed as mean ± SEM in a scatter bar plot. Mann-Whitney test was applied to compare between genotypes. (A-C) Multiple coverslips from N = 3 mice/genotype were imaged. Contributions: A-C: Experiments were performed and analyzed by me, during my master thesis. Figures were generated together with Daniel Segelcke and adapted by me.

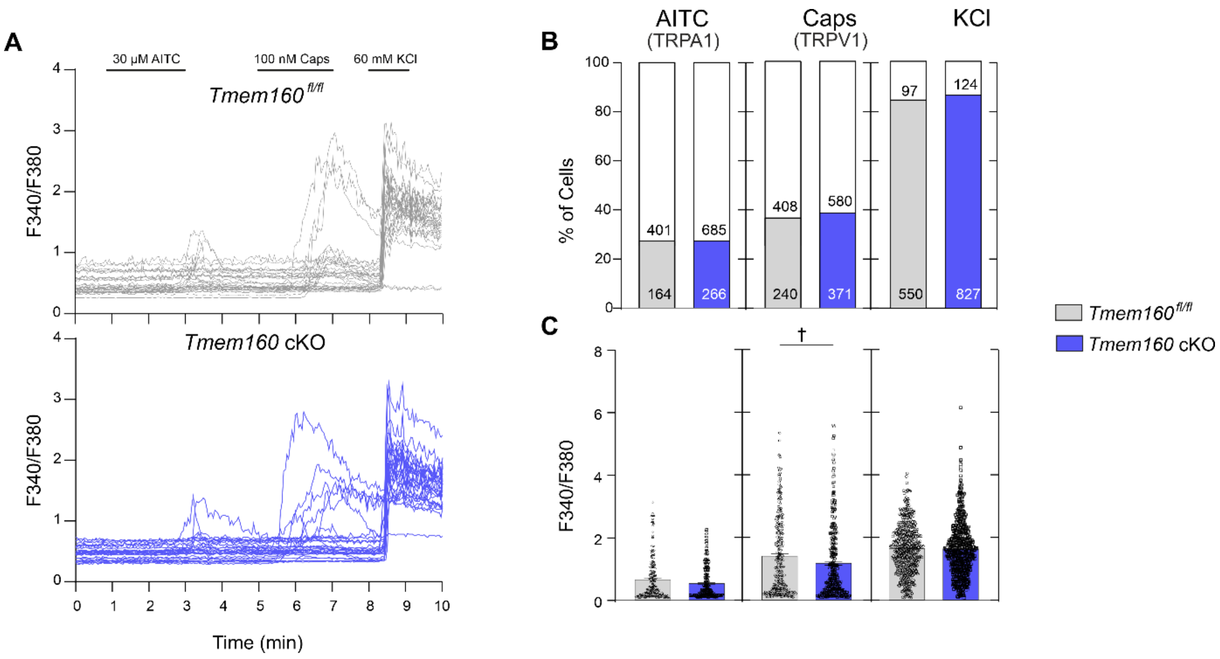

Figure 20: Neuronal Tmem160 does not alter TRPV1-mediated neuronal activity, adapted from (Segelcke, Fischer, et al., 2021).

Ratiometric Ca^{2+}-imaging was performed in cultured DRG neurons from Advillin-Cre *Tmem160* cKO (*Tmem160* cKO) and male *Tmem160*$^{fl/fl}$ littermates, measuring Ca^{2+} influx by the ratio of fluorescence emitted from different excitatory wavelengths (F340/380). (A) Representative traces and stimulation protocol. (B) Percentage of responding versus non-responding neurons are displayed, the total number of neurons assessed is depicted in the respective bars. Fisher's exact test was performed between genotypes. (C) Average response amplitudes to indicated stimuli are displayed as mean ± SEM in a scatter bar plot. Mann-Whitney test was performed. (A-C) Multiple coverslips from N = 3 mice/genotype were imaged. Contributions: Experiments were performed and analyzed by me. Figures were generated together with Daniel Segelcke and adapted by me.

3.1.10 Summary of Experiments and Results of Behavioral Phenotyping of *Tmem160* KO

Two different lines of *Tmem160* KO mice were used: a global KO and a conditional cKO limited to around 80% of the primary sensory neurons. In addition, mice of both sexes were used for all experiments. This gave deeper insights compared to using only one mouse line and sex. Also, a broad spectrum of pain models and behavioral testing methods were used. This was, to achieve a comprehensive understanding of the effect of the *Tmem160* deletion under different conditions. Both classical reflexive-based assays (withdrawal to thermal and mechanical stimulations) have been applied, as well as newer methods focused on a better translational potential from rodents to humans, as it has been discussed in pain related research (Gereau, 2014; Mogil, 2009; Mogil, 2020). Movement-evoked pain using gait analysis was performed as well as non-evoked pain equivalents without any stimuli (Segelcke, Pradier, et al., 2021). Rodent-specific behavioral observations (Mogil, 2020; Turner et al., 2019) were added including self-grooming (Callahan, 2008). These observations prevent anthropomorphizing preclinical results (Du Percie Sert & Rice, 2014; Vasconcelos et al., 2012). To reduce influences of the experimenter on results (Mogil, 2020; Sorge et al., 2014), many of the behavioral experiments were video-recorded and analyzed afterwards (NEP, locomotion, self-grooming behavior).

Overall, it stood out specifically, that *Tmem160* deletion caused a very concise phenotype limited to pathological chronic pain while leaving physiological acute pain functions intact. Furthermore, the changes were not only limited to the modality of neuropathic pain - in contrast to incisional and inflammatory pain - but also to a specific early timepoint within the neuropathic pain model of SNI. Additionally, differences were uniquely observed in tactile hypersensitivity as well as self-grooming behavior. Finally, the phenotype was sexually dimorphic and only occurred in male *Tmem160* KO mice, while female *Tmem160* KO mice showed a WT-like behavior. The behavioral differences described so far were only observed in male global *Tmem160* KO mice and not in conditional *Tmem160* cKO mice, where the deletion was limited to sensory neurons.

3.1.11 Potential Action Mechanisms of Tmem160

Hypotheses regarding the action mechanisms of Tmem160 involved (1) developmental abnormalities or a malfunction of the nociceptive system (2) mitochondrial dysfunction or (3) neuroimmune modulations and subsequently changes in neuronal excitability. In the following, all hypotheses will be discussed, and it will be demonstrated why an action of Tmem160 in neuroimmune modulations can be supported.

(1) First of all, several experiments and observations were performed, to assure that development, general health, and basal functions of the mice were not affected by a deletion of *Tmem160*. Indeed, *Tmem160* KO mice were fertile and revealed normal motor functions. The only abnormality observed in *Tmem160* KO regarding general health was a slightly elevated risk to be born blind in both sexes. Basal sensitivity to thermal and mechanical stimulation was also unchanged compared to WT littermates. Immunohistochemistry stainings confirmed a lack of morphological changes or neuronal loss in DRG sections upon *Tmem160* deletion. Additionally, no hints for myelination deficits could be observed (Hütte, 2019). Acute pain experiments performed by injecting agonists of the TRP channels into the hind paw of the animals revealed an in general normally functioning nociceptive system. This led to the overall conclusion that the phenotypical changes most likely were not caused by developmental abnormalities or a general malfunction of the somatosensory system.

(2) An involvement of Tmem160 in the cause of mitochondrial (dys)function should be investigated due to several reasons. It is known that mitochondria influence neuropathic pain (G. J. Bennett et al., 2014; Flatters, 2015; J. Li et al., 2020; Y. Yang et al., 2018) and we detected an influence of *Tmem160* depletion under neuropathic conditions. This suggests a role of Tmem160 in mitochondria and plausibly their dysfunction. Considering the protein sequence of Tmem160 using *in silico* methods, it is most likely, that Tmem160 consists of

three transmembrane domains as well as carrying a mitochondrial import sequence (MitoProt II - v1.101[6], (Claros & Vincens, 1996), Figure 6A). Mitochondrial localization of Tmem160 was indeed confirmed by immunostainings (Figure 6B-C). Mitochondrial dysfunction was investigated upon *Tmem160* deletion. mRNA expression levels of different parts of the ETC were measured as well as the activity of complex IV of the ETC and mitochondrial oxygen consumption rates in different organs. Neither of the activity assays indicate an influence of *Tmem160* deletion on mitochondrial function (Figure 9). Overall, our data suggest that ETC-dependent mitochondrial function, if at all, plays a minor mechanistic role for the observed phenotype in *Tmem160* KO.

(3) Multiple *in vitro* experimental results complementing the behavioral observations implicate a role of Tmem160 in altering neuroimmune signaling and interactions. The first hint towards this is an overall reduced level of cytokines and chemokines in DRG lysates of naïve male *Tmem160* KO mice (Figure 13A). In addition, the microglia response in the ipsilateral spinal cord at day 7 post injury was decreased compared to the WT control as measured by the Iba1 mRNA level relative to the contralateral side (Figure 15D), implying a reduced spinal microgliosis upon neuropathic injury. Moreover, DRG cultures of the male *Tmem160* KO showed a reduced response to the TRPA1-agonist AITC, but an addition of external TNFα reversed this and equalized the responses between genotypes indicating that the neuronal response itself remained intact. Finally, the conditional KO (Advillin *Tmem160* KO) limited to 80% of the sensory neurons in DRG did not show to be sufficient to elicit similar experimental results, both *in vitro* and *in vivo* (Figure 17, Figure 20). This was an indication that Tmem160 does not perform its main action in neuronal cells. Nevertheless, it is still highly likely that Tmem160 contributes to neuroimmune signaling. The other main option for Tmem160 to act on this, but not in the neurons, is a likely role in immune cells.

When comparing the phenotypical time course post SNI observed in this study to other publications, it seems to resemble a publication from Cobos et al. highlighting the role of neuroimmune interactions post SNI (Cobos et al., 2018). Peripheral monocytes and central microglia (Peng et al., 2016; Vicuña et al., 2015) are described to be relevant for the initiation but not the maintenance of mechanical hypersensitivity in models for neuropathic pain. The overall reduced cytokine and chemokine levels upon *Tmem160* deletion as discovered in the cytokine array experiments included both pro- and anti-inflammatory cytokines. Examples for non-significantly downregulated anti-inflammatory cytokines are IL2 and IL10 (Figure 13A). The interactions between the soluble messengers and the cellular receptors are complex. Pro-inflammatory cytokines can even cause sensitization in sensory neurons (Ji et al., 2016). Specifically in the context of neuropathic pain a balancing has shown to be beneficial for the

[6] https://ihg.gsf.de/ihg/mitoprot.html

pain outcome (Grace et al., 2014; Kiguchi et al., 2015; Lees et al., 2013; Niehaus et al., 2021), therefore, the data cannot be easily interpreted. In addition, the specific mechanisms leading to the downregulation of cytokines/chemokines upon *Tmem160* deletion in male mice are so far not understood. The association of many down-regulated proteins with a pro-inflammatory state nevertheless hints at a more anti-inflammatory condition in naïve male KO DRG.

One of the pro-inflammatory cytokines showing a tendency for downregulation was TNFα. TNFα has been described to be involved in pain-related behaviors credibly acting via IL1β, CXCL1 or GM-CSF(Granulocyte-monocytes-colony stimulating factor) (Vicuña et al., 2015). All of those were found downregulated in the male *Tmem160* KO DRG compared to WT (significantly for IL1β and CXCL1, non-significantly for GM-CSF). This suggests that the reduced TNFα levels observed in DRG of male *Tmem160* KO mice also has a high potential to influence changes in pain behavior. Furthermore, TNFα was described to increase the response of TRP channels to their agonists among other mechanisms by increasing membrane trafficking (Meng et al., 2016; Zhao et al., 2019). We suggest therefore, that the reduced response to the TRPA1 agonist AITC in the Ca^{2+}-imaging experiments could be caused directly by the lack of TNFα found under naïve conditions in the male *Tmem160* KO. This is supported by the fact, that, possibly as a compensation for the endogenous reduction, an addition of exogenous TNFα “rescued” the response back to the WT level. This effect was specific to TRPA1 in our experiments and not visible in response to TRPV1 activation or general neuronal excitability. Considering the complex nature of sensitization processes in peripheral sensory neurons like those of the DRG in the context of neuropathic pain (Costigan et al., 2009; Paldy et al., 2017; Wetzel et al., 2017) it seems highly unlikely, that this is the only effect on neuronal receptors and signaling levels upon deletion of *Tmem160*. Nevertheless, it is the most prominent hypothesis based on the results gathered so far.

It is also important to keep in mind that primary cultures of DRG, as they were used for the Ca^{2+}-imaging experiments, not only include sensory neurons but also non-neuronal cells, e.g. satellite glia, macrophages and fibroblasts (Cook et al., 2018; Ji et al., 2016; Krames, 2014; Price & Gold, 2018; Thakur et al., 2014) and it is not possible to identify in which of these cell types Tmem160 performs its action in this *in vitro* context. Also, one cannot equate a primary DRG culture to a naïve condition since the preparation of the cultures involved dissection of axons. It has been described earlier, that due to this nerve injury, primary cultures are more representative of a neuropathic phenotype, when considering markers for an immune or inflammatory reaction (Lopes, Denk, & McMahon, 2017; Ono et al., 2012; Wangzhou et al., 2020). So, in this case, the Ca^{2+}-imaging experiments rather provide additional insights on the processes during an ongoing inflammation or neuropathic response resembling pathological chronic pain states, as opposed to representing a naïve state or physiological acute pain state.

This goes in hand with the fact, that we did not see changes in naïve mice or in the acute pain model after injection of the TRPA1 agonist AITC (Figure 8) *in vivo*.

To find out if the influence of Tmem160 on neuroimmune signaling is due to its action in neurons or immune-cells or both, another mouse line was generated. Conditional *Tmem160* KO mice (Advillin *Tmem160* cKO) reveal a depletion of *Tmem160* limited to around 80% of sensory neurons (Zurborg et al., 2011). These mice showed none of the differences that were observed in the global *Tmem160* KO. They showed a control-like mechanical hypersensitivity at day 7 post SNI, as well as a control-like increase in self-grooming behavior. Additionally, no differences were observed in naïve cytokine/chemokine levels in DRG and in neuronal excitability studies *in vitro*. Around 20% of the DRG sensory neurons still express Tmem160 in the *Tmem160* cKO and a contribution of this neuronal Tmem160 cannot be ruled out. But nevertheless, the experimental results imply that the neuronal Tmem160 is most likely not solely responsible to cause the phenotype observed. Instead, Tmem160 in this context rather acts in non-neuronal cells, possibly in immune cells or more specifically in the "cluster 9" microglia population published earlier (Tansley et al., 2022). All of the experimental results described in this section indicate, that indeed the third hypothesis is most likely, describing Tmem160 to cause neuroimmune modulations and consequently changes in neuronal excitability.

3.2 Characterization of Age- and Sex-Differences in the DRG Proteome and Their Effect on Somatosensation

In addition to studying the function of one specific protein in pain (Tmem160, see previous section), we were interested to investigate the role of age and maturation on nociception and thermosensation. It has been discovered recently, that mechanosensation is highly dependent on maturation in male mice with a decreasing mechanosensitivity between 4w of age and 12w of age (Michel et al., 2020). In addition, it has come to attention lately, that in humans, children and adults differ in their pain perception (see Introduction for more information on pediatric pain). This raises the question, whether similar developmental effects can be observed in other aspects of somatosensation or even in pain perception in the mouse.

3.2.1 Behavioral Response to Thermal Stimuli and Acute Pain Stimuli Depends on Maturation in Naïve Male Mice

In line with the decrease in mechanical sensitivity (Michel et al., 2020), thermal sensitivity also decreased between 4w and 12w (Figure 21B) (Michel, 2020) under naïve conditions in male mice. Based on these previous findings, it was decided to further investigate the mechanism behind the behavioral differences. All experiments in this section were performed exclusively in male mice, if not indicated otherwise, for better comparability to the previously published studies (Michel et al., 2020; Michel, 2020) and according to the 3R principles for animal research, replacement, reduction and refinement. The thermosensation, or more specifically the response to a heat stimulus investigated above, is among others mediated by TRPV1. This channel also plays a role in the context of pain. One stimulus that can cause nociception via activation of this TRPV1 channel is Caps, the pungent substance in chili. Injection of Caps, or other chemicals, into one hind paw of the mouse is a commonly used model for acute pain (see above, also used in the Tmem160 study). To check for a general influence on TRPV1 by age, this unilateral model of Caps-elicited acute pain was applied to mice at 4w and 12w. Their nocifensive response was measured as well as their sensitivity to the same thermal stimulation used above for naïve animals, but this time after the injection. The nocifensive response is defined as the time the mouse spent lifting, licking, or flicking the injected paw and is also described as a short-term acute pain behavior. In this case, we observed the mouse within the first 10 minutes post injection and added up the total time (in seconds, s) during which the mouse performed nocifensive behavior of the injected paw. To our surprise, we found significantly lower values for the length of nocifensive response in the 4w mice than in the adult mice (Figure 21A). This contrasts the aforementioned results regarding thermosensitivity under naïve conditions (Figure 21B). Thermal sensitivity is displayed as a withdrawal latency, that is the time (s) that the mouse takes to withdraw its paw in response to the stimulus. The lower the value for withdrawal latency, the higher the sensitivity for the stimulus used. After measuring the nocifensive response we then tested for thermal hypersensitivity for further 10 minutes (10-20 minutes post Caps injection, Figure 21C) using the same method with which data were generated under naïve conditions (Figure 21B). It is well described that thermal hypersensitivity develops in adult rodents upon Caps injection (Gilchrist et al., 1996). Despite this, we were not able to detect a significant thermal hypersensitivity in the ipsilateral paw compared to the contralateral paw in the adult mice during this experiment (Figure 21C). Nevertheless, the trend (p = 0.0695) still shows an ipsilateral thermal hypersensitivity in the adult mice. This trend for hypersensitivity was not visible in the 4w old mice where both paws showed a very similar mean withdrawal latency with a higher spread of the ipsilateral data (Figure 21C).

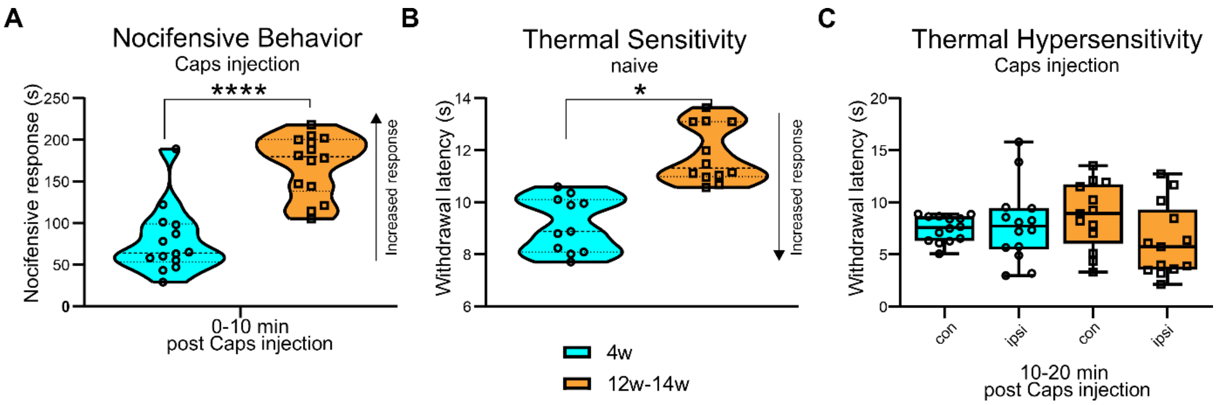

Figure 21: Age influences nocifensive behavior post capsaicin injection and thermal hypersensitivity under naïve and acute pain conditions.

(A) Injection of capsaicin (Caps) into the left hind paw resulted in reduced acute nocifensive responses in 4w compared to 13w old male mice. Two-tailed unpaired t-test for comparison between age groups. N = 14 (13w) and N = 15 (4w) mice. (B and C) Thermal (hyper)sensitivity was assessed using a Hargreaves Apparatus. The withdrawal latency of the hind paws in response to thermal simulation by a light ray was measured repeatedly. (B) Violin blots[7] show the median in a straight line, dashed lines show the quartiles. Pooled values per mouse are depicted in the graph, one-way ANOVA with Tukey's HSD (honestly significant difference) test on grand means with pooled and weighted SEM of means per mouse and time point; no differences between paws, two-way ANOVA on grand means per paw and time point; differences between individual mice were neglected, since no outliers were detected, according to the ROUT method, with Q set to 1%. N = 12 mice were measured at 4w and 12w of age. (C) Within the first 20 minutes post injection of Caps thermal hypersensitivity was measured as described above. Means were calculated per paw per mouse. Pre-testing was performed one day before testing on the same animals. N = 14 (13w) and N = 15 (4w) mice. No significant differences between both paws in both age groups were detected but a tendency (p = 0.0695) for an ipsilateral hypersensitivity is visible for 13w old mice. Ratio-paired t-tests were performed within each age group between paws to account for inter-individual variability. (A-C) * $p \leq 0.05$, **** $p \leq 0.0001$. Contributions: A , C: Data generated, analyzed and figure generated by me. B: Data generated and analyzed by Niklas Michel (Michel, 2020), figure generated by me.

Several factors could have contributed to this high variability in the data collected and to why ipsilateral hypersensitivity remained insignificant in adult mice. Within the study the laboratory moved from the Max Planck Institute for Experimental Medicine in Göttingen, Germany to the

[7] Violin plots are similar to box plots as they show the median and quartiles. Additionally, their width depends on the data density at the Y-value. The more data points show a certain Y-value, the more width the violin plot shows at that value.

University of Vienna, Austria where the study was continued. While most of the experiments were performed in Göttingen, the Caps injection was performed in Vienna as well as the tissue collection for the proteomics study. Differences between the two laboratories lay in the animal housing type (individually ventilated cages (IVCs) in Göttingen versus open cages (OC) in Vienna), the laboratory, the experimental room, the animal caretakers and even the sex of the experimenter. All of those factors can potentially contribute to the higher variability in data and differences in the results. The experimental setup was moved, and parts had to be replaced. While we tried to keep the experimental conditions consistent, similar settings and light intensities could not be guaranteed. The sex of the experimenter also influences experimental results (Georgiou et al., 2022). It was reported that the susceptibility to stress increased in mice that were handled and tested by a male experimenter compared to a female scientist (Georgiou et al., 2022). Regarding Figure 21 this revealed the following situation: the experiments underlying Figure 21B were performed in Göttingen by my colleague Niklas Michel (male), while I (female) performed the acute pain experiment with unilateral Caps injection in Vienna (Figure 21A+C). During pre-testing experiments for the thermal hypersensitivity post Caps (day 0) data were recorded by me in Vienna in the same way as for Figure 21B in Göttingen. My recordings (data not shown) differed from the data collected in Göttingen. While my data showed a trend towards lower withdrawal times at the juvenile age this did not gain significance, most likely due to a high variability of the data (larger range of 7-10 seconds) compared to the previous experiment in Göttingen (range of approximately 3 seconds). We also observed a high variability in the thermal sensitivity post Caps injection (Figure 21C) measured in Vienna, leading to no significant difference between ipsilateral and contralateral paw even in adult wild type mice where this change was well documented before. This could similarly be explained by all factors described above. It is likely, that the difference in housing and the change of laboratory in one way or another led to the higher variability in the recordings in Vienna, preventing us from discovering significant results. It will be interesting to investigate whether future experiments in Vienna will also show this high data variability or whether the variability will decrease over time. In addition, it will be interesting to record and study the sex of the experimenter as a potential covariate influencing further data.

3.2.2 Percentage of TRPV1-Postive Cells in the DRG Decreases with Maturation in Naïve Male Mice

To better understand the underlying mechanisms of the decrease in thermal sensitivity and the increase in nocifensive behavior, we further decided to study the role of TRPV1 during maturation. TRPV1 is a highly relevant thermoreceptor and also the direct target of Caps stimulation (see Introduction for details). First, we assessed the fraction of TRPV1-positive neurons within the DRG in cryosections of 4w and 12w, to detect, how the share of cells theoretically being able to respond to TRPV1-stimulation, differs with age. In line with, and possibly even explanatory for, the decrease with maturation in thermal sensitivity under naïve conditions (Figure 21B), the fraction of TRPV1-positive neurons in the DRG sections decreased with maturation (Figure 22) from around 32% at 4w to 26% at 12w. After this result, it was of interest to find out, whether the missing link between the percentage of TRPV1-postive neurons in DRG and the sensitivity to thermal stimulation *in vivo* could be provided by different excitatory responses both in average response amplitude and in percentage of cells actually responding to a TRPV1-activating stimulus of Caps.

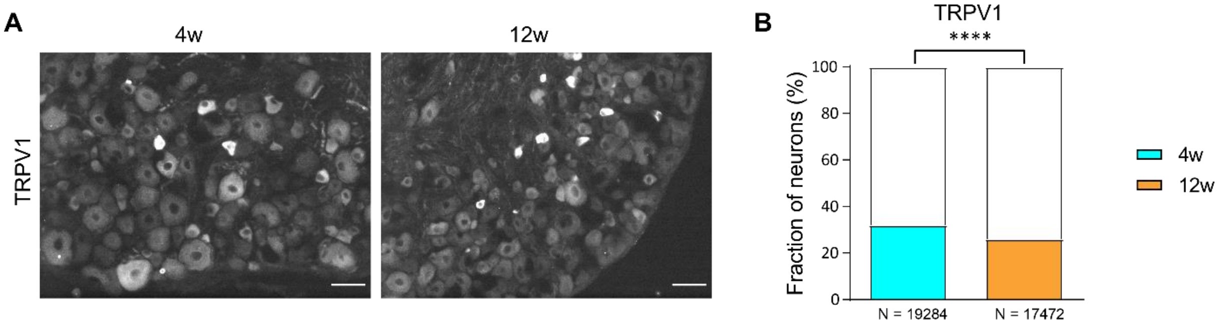

Figure 22: Age modulates the share of TRPV1⁺ DRG neurons

Expression of TRPV1 as assessed by immunohistology in cryosections of lumbar DRG of 4w and 12w old mice. (A) Exemplary images comparing 4w and 12w. Scale bar, 50 µm. (B) Fraction of neurons with a positive label for TRPV1. Numbers indicate the number of neurons quantified (color: positive label for TRPV1; white: no label for TRPV1). n = 6 (4w) and n = 6 (12w) mice in 3 independent rounds of experiments. Fisher's exact test. **** $p \leq 0.0001$. Contributions: Data generated, analyzed and figure generated by me.

3.2.3 Percentage of DRG Neurons Responding and Response Amplitude to TRPV1-Stimulation *In Vitro* Decreases with Age in Naïve Male Mice

As described above, some of the most relevant ion channels involved in pain signaling and other parts of somatosensation belong to the group of TRP channels (see Introduction for details). In addition to TRPV1 that was already investigated above, TRPA1 is another channel of interest in the context of pain perception. TRPA1 is activated by mechanical stimulation, low temperatures and the pungent substance in mustard oil, AITC. To gain insights on neuronal excitability to different stimuli *in vitro* that are known to elicit pain *in vivo*, ratiometric Ca^{2+}-imaging experiments were performed in primary DRG cultures comparing 4w and 12w. AITC and Caps were used as stimuli to activate the respective channel while a potassium chloride (KCl) solution allowed identification of functional neurons within the culture by a depolarization of the neurons, followed by an activation of voltage-gated calcium channels (Figure 23). The experiments revealed a significant difference between 4w and 12w in percentage of neurons responding to Caps stimulation with a larger share of responders in the 4w old DRG (Figure 23B). The response amplitude also shows a trend to a higher value in the juvenile cell culture (Figure 23C). No significant differences were observed in the response to AITC. It is noteworthy, however, that we see a significant difference in the percentage of responding neurons to the "control" stimuli of KCl, which will be discussed below.

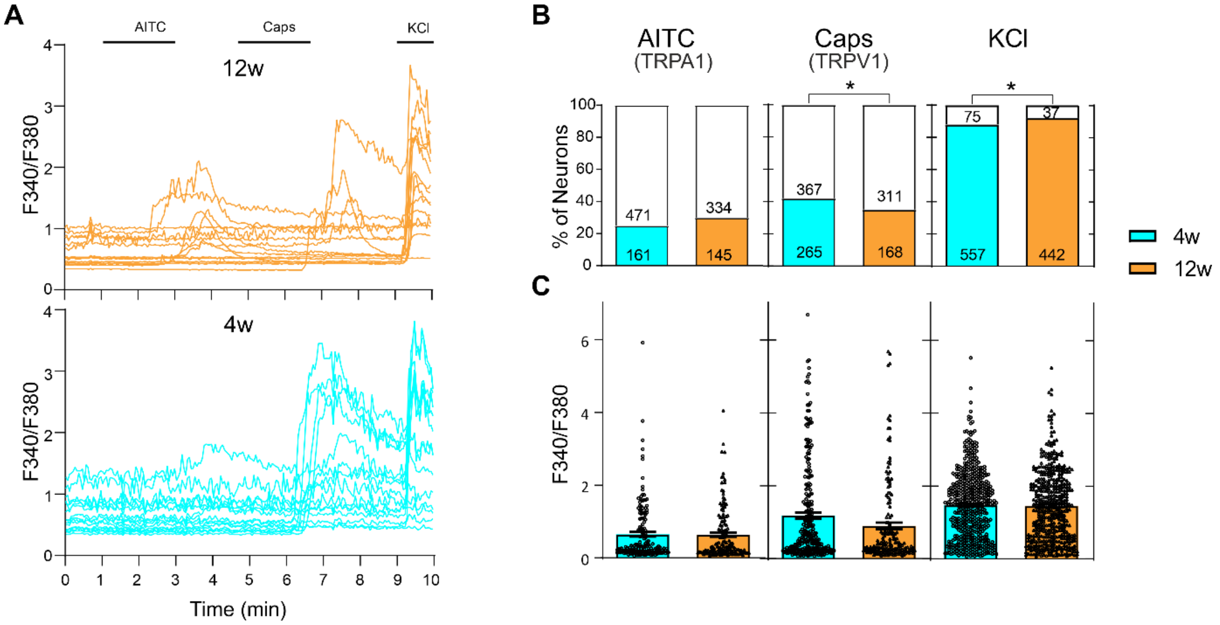

Figure 23: Age modulates the share of responders to Caps and KCl stimulation.

Ratiometric Ca^{2+}-imaging was performed in cultured DRG neurons of different aged mice. After incubation with Fura-2 dye, stimuli were applied from minute 1 to 3 (MO, 30 µM), 5 to 7 (Caps, 100 nM), and 9 to 10 (KCl, 60 mM). (A) Representative traces and stimulation protocol. (B) Percentage of responding (colored part) and non-responding (white part) neurons to indicated stimuli. Numbers represent the total number of neurons imaged. Fisher's exact test. (C) Scatter bar plots represent the maximum fluorescence amplitudes (F340/380, mean ± SEM) of responding neurons to indicated stimuli. Mann-Whitney Test. (A-C) * $p \leq 0.05$. For both ages, multiple coverslips from N = 3 mice were used. Contributions: Data generated and analyzed by my lab rotation student, Elisa Fernández, taught and supervised by me and figure generated by me.

3.2.4 Differences in TRPV1 Expression and TRPV1-Dependent Responses *in Vivo* and *in Vitro* Through Maturation

Summarizing the experimental results on pain, nociception and theromosensation in 4w and 12w male mice the following observations have been made: *in vivo*, thermal sensitivity decreased with age under naïve conditions while in an acute pain situation, the nocifensive response increased with age and younger mice did not develop a thermal hypersensitivity in response to Caps injection. *In vitro* studies in DRG tissue sections revealed a lower percentage of TRPV1-positive neurons at 12w compared to 4w and primary DRG cultures showed a decreased TRPV1-dependent response in adult mice both regarding the percentage of responders (significant) and the average response amplitude (trend).

Thermal sensitivity depends among others on the TRPV1 channel. Previous experiments with naïve mice revealed a reduction in withdrawal latency to thermal stimulation at 4w compared to adult mice (Figure 21B), i.e., younger mice were more sensitive to high temperatures.

This can most likely be explained by the higher number of TRPV1-positive cells present in DRG at the younger age (Figure 22). As described above, the share of TRPV1-positive neurons is higher in juvenile than in adult male mice (Figure 22), it decreases from 32% to 26% of total neurons. To further investigate neuronal excitability, specifically in response to different stimuli, Ca^{2+}-imaging experiments were performed on primary DRG cultures from mice of different ages using AITC and Caps as well as a “control” stimulus of KCl. AITC activates TRPA1 channels (Bautista et al., 2006) whereas KCl leads to membrane depolarization in all neurons (Y. Chen & Huang, 2017; J. Xie & Black, 2001) and consequently activates voltage-dependent calcium channels (Catterall, 2011; Schor et al., 2009). The stimulation protocol (Figure 23A) included first a stimulation with AITC, then a stimulation with Caps and as a last step with KCl. Between stimuli neurons were washed. The percentage of responders to AITC and Caps were largely similar in adult WT mice compared to the male adult WT mice studied within the Tmem160 (Figure 18). The response to AITC showed no significant changes between ages, neither in percentage of cells responding (Figure 23B), nor in mean response amplitude (Figure 23C). Since AITC is an agonist for TRPA1, it was concluded that TRPA1 was not affected by age as much as TRPV1. Therefore, TRPA1 was not studied further. As expected from the fluorescent stainings (Figure 22), the percentage of cells responding to Caps was higher at 4w than at 12w (Figure 23B). In addition, the mean response amplitude showed a trend to be higher at the younger age as well, representing a feasibly stronger influx of Ca^{2+}-ions during the process. As described above, this ion influx causes a desensitization of not only the TRPV1 channel itself (L. Luo et al., 2019; Sanz-Salvador et al., 2012; Touska et al., 2011; Vyklický et al., 2008) (see Introduction for details) but also a downregulation of voltage-dependent calcium channels (Wu et al., 2006). Since the response to KCl depends on those voltage-gated calcium channels (Catterall, 2011; Schor et al., 2009), this could potentially explain why we observed a lower percentage of neurons responding to the KCl stimulus at 4w of age (Figure 23B) while the response amplitude remained similar (Figure 23C). In this context it is important to keep in mind, that the KCl stimulation happens after the Caps stimulation. The explanatory hypothesis would be that at 4w more neurons express TRPV1 and within those neurons expressing TRPV1, a higher percentage could show a higher expression level at 4w compared to 12w. Upon Caps stimulation this would lead to more influx of Ca^{2+}-ions and hence a downregulation of voltage-gated calcium channels. Those would then be no longer able to get activated by extracellular KCl, causing less cells to respond to the KCl stimulus.

Acute pain reaction (nocifensive response) to unilateral injection of Caps into the hind paw of male mice was less prominent in juvenile (4w) than in adult mice (13w) (Figure 21A). The juvenile mice revealed a higher percentage of TRPV1-positive cells in DRG (Figure 22) and Caps is a specific agonist of the TRPV1 channel (Lumpkin & Caterina, 2007; Vriens et al., 2014). Therefore, it would have been expected that the juvenile mice would display more capsaicin-induced pain compared to the adults. There could be several reasons why instead a lower nocifensive response was observed in the juvenile mice. One possible explanation for the observations could be related to the fact that we only recorded the total time of nocifensive behavior over the observational period of 10 minutes. So contingently, the time course of the pain response could differ between 4w and adult mice. If that was true, this could for example be explained by the following mechanisms: as discovered during Calcium-imaging experiments the sensory neurons of the younger mice show a tendency for a stronger Ca^{2+} influx post stimulation with capsaicin (Figure 23C). Caps stimulation is known to cause a desensitization of TRPV1 (L. Luo et al., 2019; Sanz-Salvador et al., 2012; Touska et al., 2011; Vyklický et al., 2008) as well as a downregulation of voltage-dependent calcium channels (Wu et al., 2006), as described in the introduction and above. Both TRPV1 and voltage-dependent calcium channels are relevant for the afferent pain axis, since an influx of Ca^{2+}-ions contributes to the propagation of a signal. A hypothesis connecting the experimental results could be, that in younger mice more TRPV1-positive neurons contain more TRPV1 channels, leading to a greater Ca^{2+} influx and consequently to more desensitization against capsaicin. This would lead to a high pain response in the beginning that would be relieved quickly. To test this hypothesis, one could repeat the study using a video-based experimental set up. In the video recordings, one could easily trace the time course of the nocifensive behavior and compare it between the age groups, using analysis software such as BORIS, already applied by our collaboratos in the project of Tmem160 characterization. Another explanatory hypothesis relies on differences between thermosensation and Caps/TRPV1-mediated heat nociception. This hypothesis will be further discussed below.

As reported earlier, unilateral injection of Caps leads to a strong ipsilateral hypersensitivity compared to the contralateral paw in male adult WT mice (Figure 8) (Hütte, 2019; Segelcke, Fischer, et al., 2021). This hypersensitivity post Caps injection occurred in response to both thermal and mechanical stimulation (Gilchrist et al., 1996), with the thermal reaction being dependent on a voltage-gated calcium channel (DuBreuil et al., 2021). Based on this information, it was no surprise to see a trend ($p = 0.0695$) of this ipsilateral thermal hypersensitivity in adult mice (Figure 21C). It was in line with the aforementioned hypothesis of a pronounced desensitization in 4w, that those mice did not show a trend for ipsilateral thermal hypersensitivity after caps injection. Indeed, for 4w no difference could be discerned between the ipsilateral and the contralateral paw. This could potentially be similarly explained by the desensitization of the sensory neurons post stimulation with Caps caused by a higher Ca^{2+} influx. In this context, even after the first 10 minutes this would prevent an ipsilateral increase in sensitivity in the younger mice as compared to the adults. This depends on the experimental setup of first observing the nocifensive response for 10 minutes and thereafter testing for thermal hypersensitivity for further 10 minutes. A start of observations regarding thermal hypersensitivity directly after the injection could solve this problem but would also prevent the collection of the nocifensive response.

3.2.5 Thermosensitivity and Heat Nociception Might Not Develop in Parallel

Another possible interpretation for the differential changes in maturation comparing thermosensitivity under naïve conditions and the acute pain response would be to suggest that thermosensation and capsaicin/TRPV1-mediated heat nociception do not develop in a parallel way in male mice between 4w and 12w of age. Under naïve condition, younger mice showed a lower withdrawal latency to thermal stimulation compared to adult mice, meaning they were more sensitive at 4w (Figure 21B). This changed upon ipsilateral capsaicin injection into the hind paw of the animal. The acute nocifensive behavior was lower in young versus adult mice, they spent less time licking, lifting, or flicking the injected paw (Figure 21A). The adult mice showed a tendency for an ipsilateral thermal hypersensitivity after capsaicin injection which was not observed in the younger mice (Figure 21C).

Caps is a specific agonist of the TRPV1 channel, the main heat sensor in the nociceptive neurons (Lumpkin & Caterina, 2007; Vriens et al., 2014). But TRPV1 is not the only detector of warmth or heat described in mammals that possibly contributes to the thermal sensitivity under naïve conditions (Figure 21B). Further channels have been discovered in that context, most of them belonging to the families of the transient receptor potential (TRP) channels (Dhaka et al., 2006). TRPV2 is activated by temperatures larger than 52°C mediating painfully hot sensations. TRPV3 and TRPV4 are described in the context of warmth perception with a detection threshold of 27-39°C. Those channels show a prominent expression in non-neuronal cells including the keratinocytes of the skin (Lee et al., 2005; Lumpkin & Caterina, 2007). More recently Vandewauw et al. identified a combination of three TRP channels responsible for detection of noxious heat, namely TRPV1, TRPA1 and TRPM3 (Vandewauw et al., 2018). TRPA1 also mediates cold sensation (<17°C) and responds to AITC (Dhaka et al., 2006). Its expression mainly colocalizes with a subset of the TRPV1-expressing nociceptors (Vriens et al., 2014). TRPM3 is also expressed in small unmyelinated neurons mediating “slow pain” (Vriens et al., 2014). Other channels mediating heat in nociceptors or more general in sensory neurons are ANO1 (Anoctamin-1) and K2P (Two-pore domain potassium) channels (Vriens et al., 2014). Since no differences were observed in Ca^{2+}-imaging experiments, regarding TRPA1 activation and also TRPA1 is responsible for lower temperatures not investigated in our experiments, it is not unlikely that TRPA1 plays a role in causing the differences we observed.

A possible hypothesis regarding an unparallel development of thermosensitivity and heat nociception could be, that skin keratinocytes expressing TRPV3 and/or TRPV4 could be more prominent in earlier stages of development in male mice (4w) compared to adulthood leading to a higher sensitivity to innocuous thermal stimulation. Solinski et al. (Solinski & Hoon, 2019) described that TRPV1 is not needed for a response to heat in mammals, but also found that the neurons expressing TRPV1 nevertheless play an important role in eliciting a behavioral heat response. It will be interesting to confirm whether TRPV3/TRPV4-positive keratinocytes might further act on the population of TRPV1-positive neurons described by Solinski et al (Solinski & Hoon, 2019). A staining for TRPV3 and TRPV4 in DRG and skin sections could reveal more insights on their role in thermosensation specifically throughout maturation. In that case higher levels of TRPV3 and TRPV4 in the skin keratinocytes could lead to more signalling directed at TRPV1-positive neurons. Continuous high levels of signalling directed at TRPV1-positive neurons could potentially cause the higher percentage of TRPV1-positive neurons in the DRG of 4w versus 12w old male (Figure *22*).

If we now elicit an acute pain stage by unilateral capsaicin injection the response will predominantly be TRPV1 based and further processed only by nociceptors. Considering the results of our behavioral experiments, showing a stronger nocifensive response at 12w compared to 4w, the response to direct TRPV1 activation seems to increase with development in male mice. Potential lower levels of TRPV1 in the skin could lead to an increase of TRPV1 in the somata in the DRG as a countermeasure. Another plausible option would be an additional system interacting with the TRPV1-mediated pain in younger mice leading to less pain-susceptibility in general compared to adults. We checked if we could find hints for this crosstalk (likely with the immune systems), performing quantitative proteomics in skin and DRG or skin samples of mice of different ages. Using analysis of gene ontology – biological processes, in the comparisons of paw skin samples of juvenile (4w) and adult (14w) mice, female mice showed a higher expression of proteins connected to the “cellular response to heat” at younger ages (Xian, Sondermann, Gomez Varela, & Schmidt, 2022). To further interpret the nocifensive behavior, it is important to be aware that even though the injected Caps will mainly act on TRPV1, further processes may happen in the central nervous system to integrate the signal and cause the pain response in the mouse. The primary somatosensory cortex (S1) is known to integrate the sensory-discriminative component of pain (Vierck et al., 2013) whereas the anterior cingulate cortex (ACC) plays a role in the affective-motivational part of pain (Bushnell et al., 2013; Fuchs et al., 2014; Sewards & Sewards, 2002; Vogt, 2005).

3.2.6 Mass Spectrometry Reveals Differences in Protein Expression in Naïve DRG

So far, multiple differences in the context of pain, nociception and thermosensation were observed between 4w and 12w. Namely, thermal sensitivity under naïve conditions decreased with age, while the acute nocifensive response revealed an increase with age, and also the younger mice failed to develop a thermal hypersensitivity post injection of Caps. *In vitro* studies showed a decrease with age in the percentage of TRPV1-positive neurons as well as the percentage of neurons responding to TRPV1-dependent stimuli in DRG. The response amplitude to Caps stimulation also demonstrated a trend of a decrease throughout maturation. As described above, DRG play a pivotal role for somatosensation and pain perception. To gain a deeper insight into the underlying mechanisms that could influence the experimental results observed, the proteome of DRG was investigated as a whole. It is common knowledge, that proteins do not act independently, but instead, most processes in the body depend on interactions of proteins and therefore on the proteome as a whole. Mass spectrometry experiments allowed a quantitative comparison of the proteome in different samples. While so far, only male mice were investigated, for these experiments female samples were collected additionally. Recently published data explored similar comparisons between ages in samples of skin and sciatic nerve (SCN) and also studied female mice (Xian, Sondermann, Gomez Varela, & Schmidt, 2022). Here, we want to add to providing a resource of all steps within the neuraxis – skin/periphery, SCN, DRG, spinal cord- in juvenile and adult mice of both sexes. In addition, as described above, a sexual dimorphism has been shown recently in studies of pain, including the study of Tmem160 (Segelcke, Fischer, et al., 2021). Tmem160 was suggested as a promising pain-related candidate by another study of mass spectrometry, supporting the relevance of mass spectrometry as a hypothesis-generating resource. Therefore, quantitative mass spectrometry experiments were performed on lDRG tissue from four different experimental groups (4w female, 4w male, 14w female, 14w male) using 4 mice/group. Each sample was measured in two technical replicates.

A total of 9900 protein identifications (IDs) were quantified across all four experimental groups (Figure 24B). Of those, 8811 were detected in the overlap of all four groups and used for further analyses regarding relative expression levels. Relative expression levels are shown as fold change (FC) within the specific comparisons (4w male vs 14w male, 4w female vs 14w female, 4w male vs 4w female, 14w male vs 14w female). To get a first overview about the data and to determine whether a software without prior knowledge of the samples and their affiliation to the groups can group them accordingly, principal component analysis (PCA) was applied (Figure 24C). PCA was able to separate between age groups and – at the young age – between sexes. This was in line with the study in skin and SCN, also showing a separation by age in the PCA (Xian, Sondermann, Gomez Varela, & Schmidt, 2022). This supports the hypothesis, that the proteome of mice highly depends on their maturational state. To confirm the relevance of the generated data in the pain context, it was important to show that a list of ion channels, which play a crucial role in pain, were detected in our samples. Protein intensity for each replicate for each ion channel was log2-transformed and displayed in a heatmap (Figure 24D). Many different channels were detected in the majority of our replicates, for example multiple TRP channels including TRPA1 and TRPV1 as well as voltage-gated sodium channels, e.g., Voltage-gated sodium channel (Scn10a and Scn11a). Their presence in the data set and our ability to detect and identify them allowed to draw conclusions on their fold change in the different comparisons.

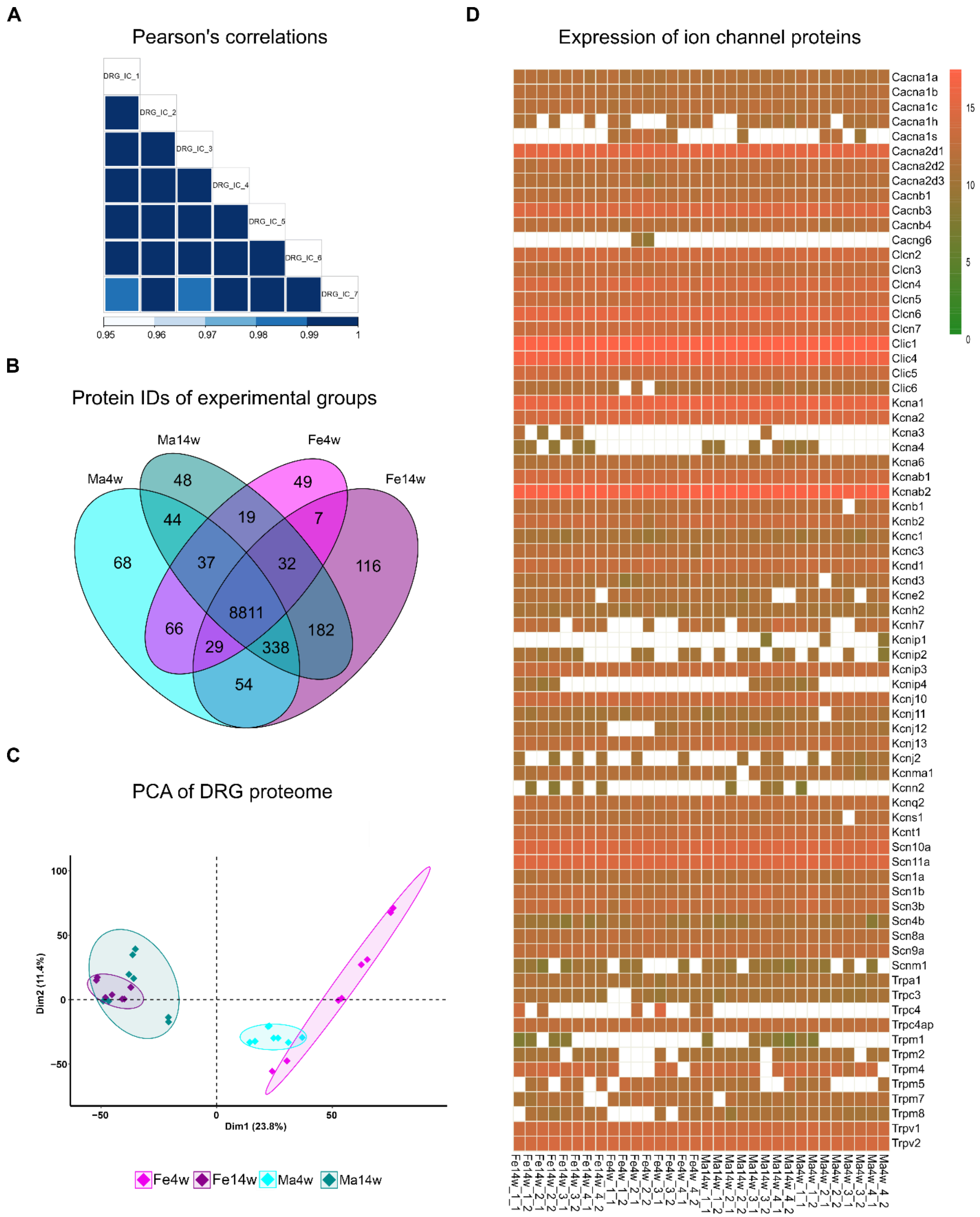

Figure 24: Technical details of mass spectrometry samples.

(A) Pearson's correlations of technical controls of DRG acquired over the total run time on a timsTOF Pro. A high value, indicated by the dark blue color code, shows a good comparability of the data collected throughout the total run time. (B) Protein IDs detected in ≥ 75% of samples within each group were subjected to a Venn diagram. This shows unique and overlapping protein IDs detected across age and sex groups in DRG samples. Only protein IDs detected in all four (4w female, 4w male, 14w female, 14w male) experimental groups were used for further analysis. A list of all IDs between the experimental groups is given in Supplemental Table 1. (C) Principal component analysis (PCA) reveals that age is an influencing variable in DRG tissue. (D) Heatmap shows the expression of ion channel proteins across all DRG samples based on log2-transformed protein intensities. The redder a sample appears at the ion channel of interest, the more of this ion channel is contained in the sample. (A-D) 2 technical replicates of 4 biological replicates/ group (4w female, 4w male, 14w female, 14w male). Contributions: Experiments were performed by Julia Sondermann and Feng Xian, analysis was performed by me together with Julia Sondermann and Feng Xian. Figures were generated together with Feng Xian and adjusted by me.

The quality of our mass spectrometry experiments was confirmed using Pearson's correlation on technical controls (Figure 24A). All values were >0.98, verifying a good comparability of the data independent on when they were run on the machine. All IDs containing a keratin were defined as potential contaminations, due to their association with other tissue types, and removed completely from further analyses. In this context, 19 IDs detected in all four groups were removed, 8811 IDs without keratins remained.

To further understand the differences between sexes and ages, that allowed the separation in the PCA, for all aforementioned 8811 IDs the FC was calculated in all relevant comparisons. Expression levels were compared using two-sample moderated t-tests, p-values were adjusted accordingly (Benjamini and Hochberg, for multiple testing (Storey, 2002), see Methods for detail). IDs were identified as differentially expressed proteins (DEPs) for a FC ≥ ±50% and an adjusted p-value ≤ 0.05, revealing both a biological relevance and a statistical significance. All IDs quantified in the relevant comparisons are depicted in volcano plots (Figure *25*A, C, Supplemental Table 2). FC is displayed as $\log_2$ FC, adjusted p-value is displayed as $-\log_{10}$ (adjusted p-value). High absolute values on the X-axis represent a high difference in expression level and high values on the Y-axis represent a high significance. DEPs in all comparisons are highlighted in the appropriate colors (cyan for male comparisons or DEPs with a higher expression in males in the age comparisons, magenta for female comparisons or DEPs with a higher expression in females in the age comparisons). Exemplary DEPs showing high significance and high FC are labelled with their names. Male mice, as they were used in the behavioral experiments, revealed 154 IDs to be differentially expressed between 4w and 14w of age (Figure 25B), including genes involved in pain signaling as will be discussed below (Figure 28A). Considering the age comparison in females, there was an even higher number of DEPs detected (733 in total), similarly including genes involved in pain signaling (Figure 25A). All DEPs and their overlap (120 IDs) between the age comparisons shown in Figure 25A are depicted in a Venn diagram (Figure 25B) including examples of DEPs unique for each sex. The same comparisons were performed between sexes within age groups. As expected from previous studies on the proteome of SCN and skin at the same ages, these comparisons revealed significantly less DEPs. For SCN they reported a total of 1557 age-dependent DEPs and 33 sex-dependent DEPs. In skin, a total of 282 age-dependent and 58 sex-dependent DEPs were identified (Xian, Sondermann, Varela, & Schmidt, 2022). In DRG, only 2 DEPs at 4w of age and 9 DEPs at the 14w age group (Figure 25C). A Venn diagram of the DEPs of the age-based comparisons from Figure 25C is depicted in Figure 25D including all DEPs. Interestingly, in connection to all previous experiments performed within this thesis, neither Tmem160, nor TRPA1, nor TRPV1 were DEPs in any of the comparisons made. To summarize the results shown in the Volcano Plots and Venn Diagrams in Figure 25, we report a significant alteration of the DRG proteome in mice mainly by age (4w vs 14w) and less so by sex. When looking at Figure 25A,B it does become obvious, that there still is a prominent difference between sexes when considering the age-based comparisons (i.e. (male 4w vs 14w) vs (female 4w vs 14w)) with significantly more DEPs being present in the female comparison (Figure 25B). This indicates that, while the proteome does not differ much between sexes within age groups, nevertheless, the changes in the proteome during maturation differ greatly between male and female. Even though the number of DEPs between sexes within age groups was low compared to the age-related differences between age groups within sexes, it is remarkable, that in SCN, skin and DRG, the number of DEPs at 4w was lower than at 14w (SCN: 0 DEPs vs 33 DEPs, skin: 26 DEPs vs 42 DEPs, DRG: 2 DEPs vs 9 DEPs) (Xian, Sondermann, Gomez Varela, & Schmidt, 2022). This could be explained by the fact that 4w mice are not yet sexually mature, so they are influenced less by sexual hormones including estrogen and testosterone.

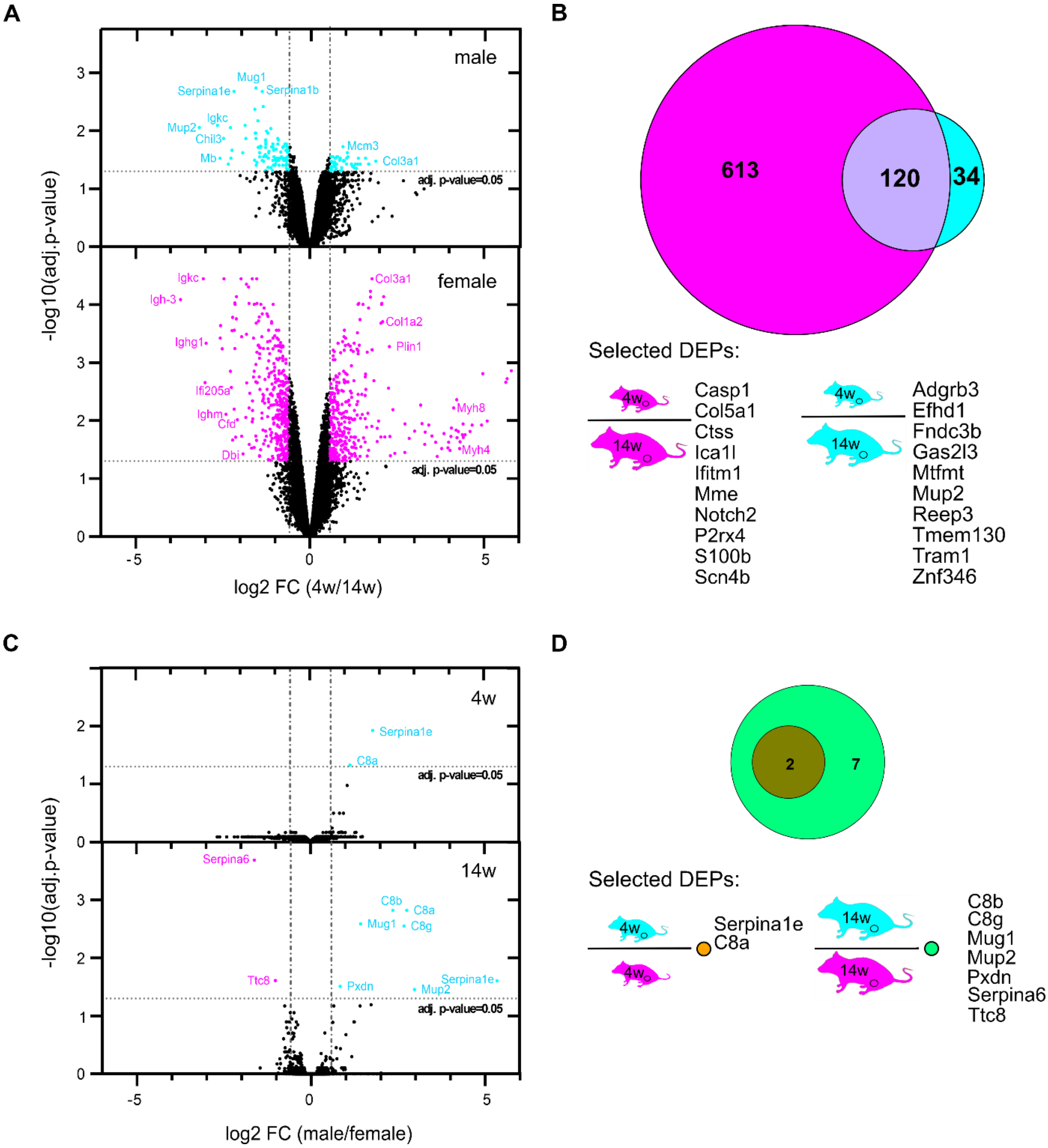

Figure 25: DRG proteome changes in dependence on age and sex of mice.

(A and C) Volcano plots show all proteins detected in the samples of indicated comparisons by age or sex as indicated. Those proteins exhibiting adjusted p-value ≤ 0.05 (i.e., are considered as significantly altered) and a |log2 FC| >0.585 (|log2 FC| = 0.585 marked as dashed lines in the plots) are considered to be differentially expressed proteins (DEPs). DEPs are highlighted in cyan in male comparisons and in age comparisons with a higher expression in male, and in magenta in female comparisons or in age comparisons with a higher expression in female. Protein IDs with a very high significance and fold change were labelled with their names. (B and D) Venn Diagrams of differentially expressed proteins of the comparisons in (A)(cyan, male and magenta, female) in (B) and of the comparisons in (C) (orange, 4w and green, 14w) in (D). Examples of DEPs in male and female comparisons of both age groups are given. Data were generated using quantitative mass spectrometry on lDRG tissue for n = 4 mice/group. P-values were calculated using two-sample moderated t-tests, p-values were adjusted accordingly (Benjamini and Hochberg, for multiple testing (Storey, 2002), see Methods for detail). Contributions: Experiments were performed by Julia Sondermann and Feng Xian, analysis was performed by me together with Julia Sondermann and Feng Xian. Figures were generated by me.

To gain further insights into molecular functions which might be influenced by the DEPs we found, we completed a reactome pathway analysis including all DEPs for each comparison by means of the web interface of STRING (string-db.org, (Szklarczyk et al., 2021) (Supplemental Table 3). This allows the input of a list of proteins (in our case of the DEPs detected) and maps the protein input to functional classification frameworks. The output displays functions and systems that are more prominent as expected in the list of proteins entered (Szklarczyk et al., 2021). We chose the reactome pathway knowledgebase (Jassal et al., 2020). In the male proteome between 4w and 14w multiple reactome pathways revealed an alteration, including *immune system, metabolism, innate immune system, hemostasis* and *extracellular matrix organization*. Due to the higher number of DEPs identified in the corresponding female comparison, many more altered pathways have been found, including *metabolism, extracellular matrix organization, collagen formation, hemostasis,* and *collagen biosynthesis and modifying enzymes* some of which overlap with the pathways influenced in males. The top 10 reactome pathways in both sexes ordered by the observed gene counts, reveal a lower number of genes counted per pathway in males (Figure 26A) than in females (Figure 27A). Three exemplary pathways found to be enriched in the age-related DEPs of both sexes are *immunoregulatory interactions between a lymphoid and a non-lymphoid cell, hemostasis and neutrophil degranulation* (Figure 26B, Figure 27B). This shows that the processes differ between juvenile and adult mice in both sexes, even though in females, the number of DEPs involved to the processes was increased compared to males.

We then grouped the pathways detected in each of the comparisons related to the immune system, metabolism and extracellular matrix. No pathways linked to (neuro)development were discovered. In males 8 pathways were linked to the immune system, in females this number increased slightly to 9. While in the male comparison, only 4 pathways were related to metabolism, this number doubles in the female results. The pathways that were linked to extracellular matrix increased from 7 in male to 12 in female. This indicates that in both male and female mice, processes involved in immune system, metabolism and extracellular matrix highly depend on age during maturation. Multiple pathways overlap between sexes, for example the pathways depicted in Figure 26B and Figure 27B and broad terms such as *immune system* and *metabolism*, suggesting that these processes are maturation-dependent in both sexes, while others are unique to one sex. Two processes for which the age-dependency was only detected in males were *G alpha (i) signalling events* and *retinoid metabolism and transport.* On the other hand, the age-dependency for *metabolism of lipids, metabolism of nucleotides* and *cell junction organization* was limited to female mice. Considering the low DEP numbers in the sex-related comparisons, the observed gene count was too low to report any relevant altered pathways for either age group (Supplemental Table 3).

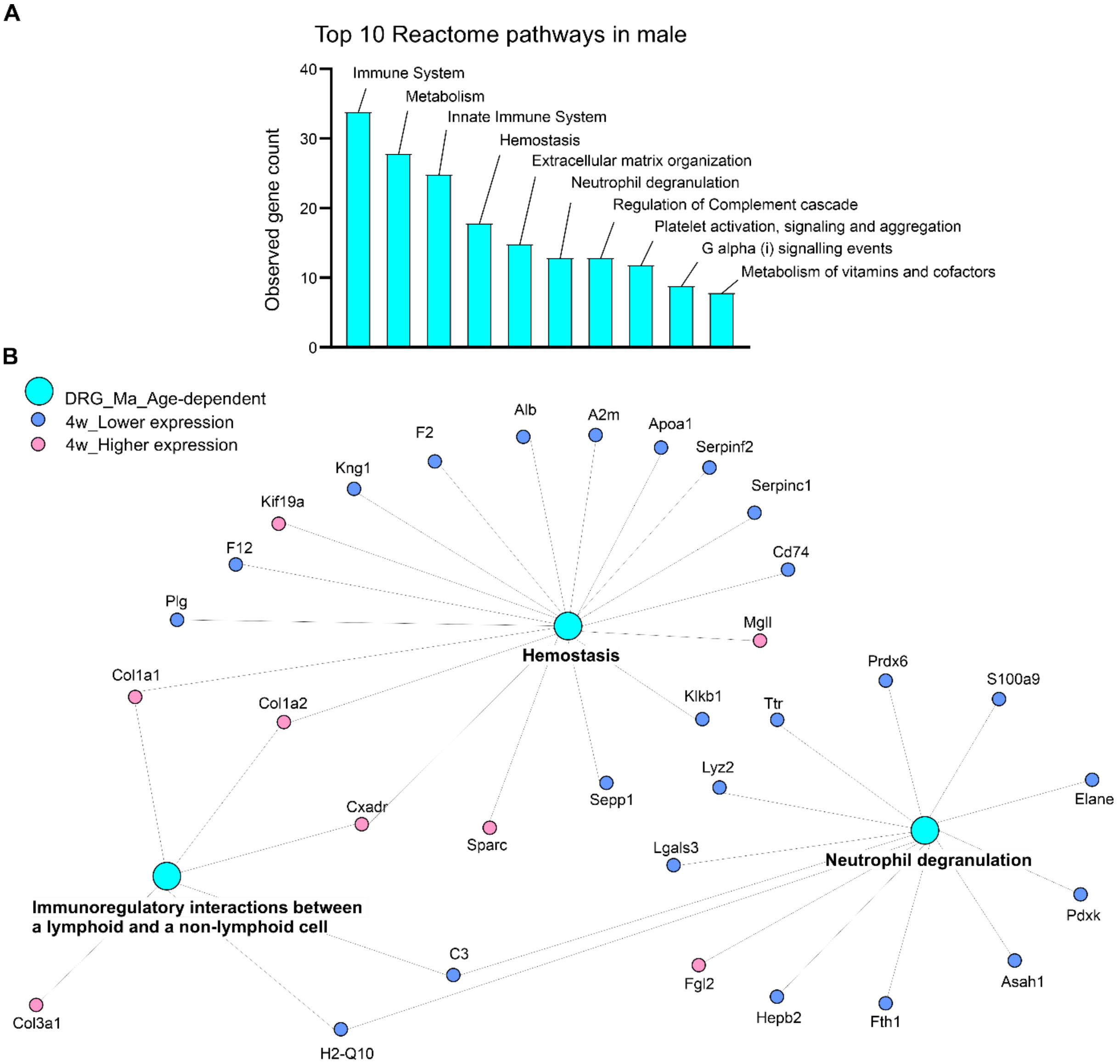

Figure 26: Age-dependent reactome pathways in male DRG

Differentially expressed proteins in the age-dependent comparison in male DRG were subjected to Reactome pathway analysis using the web interface of STRING[8]. Pathways revealed to be enriched within the input DEPs are displayed. (A) The top 10 reactome pathways are shown ordered by observed gene count. (B) Three regulated reactome pathways were selected and displayed, including the direction of regulation within our data and overlaps between the pathways. (A and B): Data were generated using quantitative mass spectrometry on lDRG tissue for n = 4 mice/group. Contributions: Experiments were performed by Julia Sondermann and Feng Xian, analysis was performed by me assisted by Julia Sondermann and Feng Xian. Figures were generated by me.

Our lab reported a differential expression of 94 proteins between skin samples from 4w and 14w old male mice (Xian, Sondermann, Varela, & Schmidt, 2022). Among them were proteins involved in *extrinsic apoptotic signaling pathways* and *notch signaling pathways* (exclusively in males) as well as skin developmental processes (both sexes), in addition, multiple proteins

[8] string-db.org Szklarczyk et al. (2021)

involved in neuroimmune signaling were found to be higher expressed in young mice (Xian, Sondermann, Varela, & Schmidt, 2022). This shows, as expected, that in the skin, the expression of proteins involved in skin development depends on age during maturation. Also, in young mice, neuroimmune interactions appear to play an even more prominent role compared to the adults. Interestingly, neither TRPV1, nor TRPV3 or TRPV4 were found to be differentially expressed in paw skin samples, as we hypothesized based on the behavioral results regarding different channels involved in thermosensitivity and heat nociception. In DRG data, male mice revealed differential expression depending on age in pathways such as *immune system, metabolism, innate immune system, hemostasis* and *extracellular matrix organization*. Those processes can possibly influence the *in vivo* and *in vitro* observations we made regarding thermal sensitivity and pain processing.

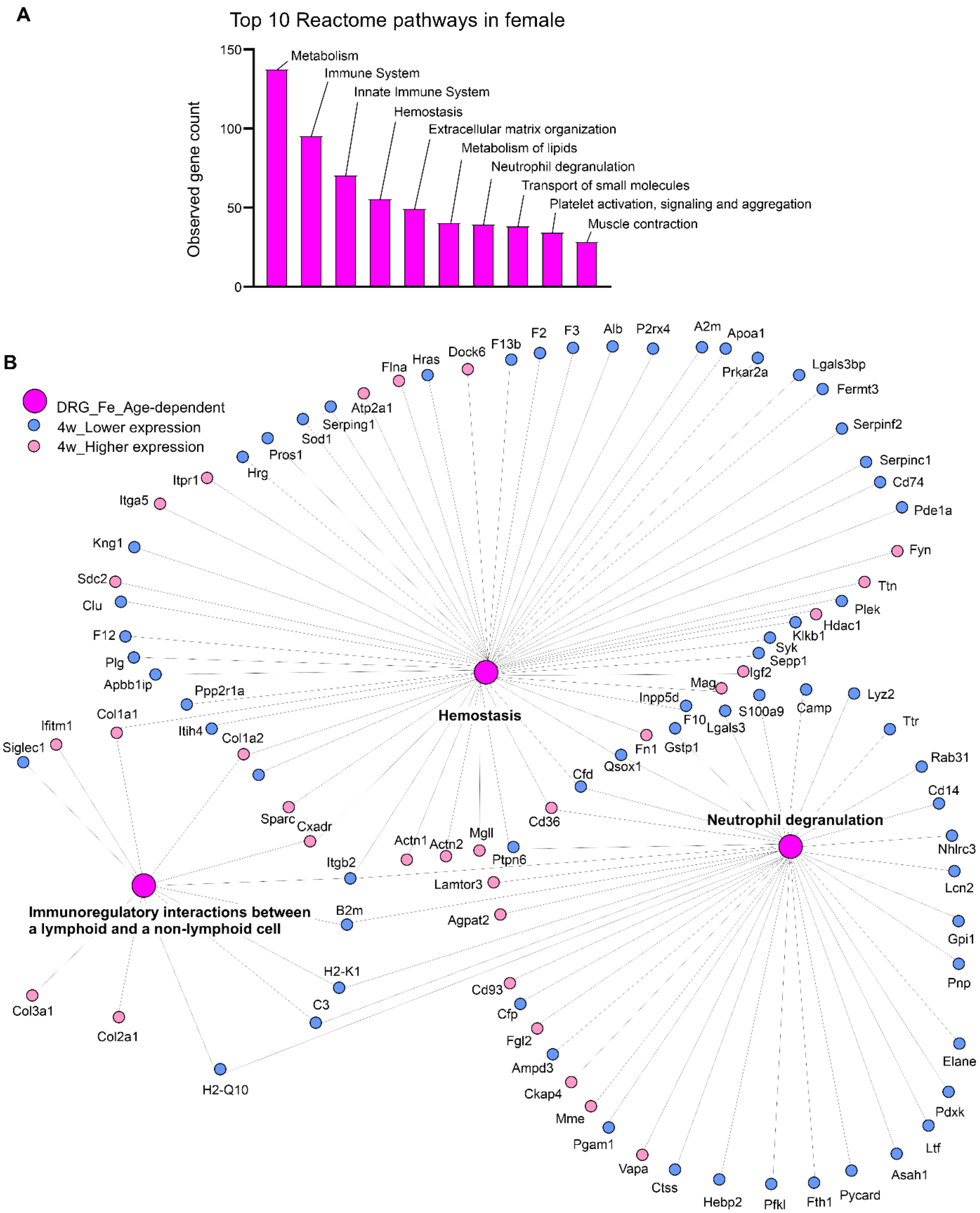

Figure 27: Age-dependent reactome pathways in female DRG

Differentially expressed proteins in the age-dependent comparison in female DRG were subjected to Reactome pathway analysis using the web interface of STRING[9]. Pathways revealed to be enriched within the input DEPs are displayed. (A) The top 10 reactome pathways are shown ordered by observed gene count. (B) Three regulated reactome pathways were selected and displayed, including the direction of regulation within our data and overlaps between the pathways. (A and B): Data were generated using quantitative mass spectrometry on lDRG tissue for n = 4 mice/group. Contributions: Experiments were performed by Julia Sondermann and Feng Xian, analysis was performed by me assisted by Julia Sondermann and Feng Xian. Figures were generated by me.

[9] string-db.org Szklarczyk et al. (2021)

To further understand the differences between ages and sexes and specially their functional implication in pain and other pain-related processes, e.g., neuroimmune functions, DEPs were compared to candidate-lists generated from multiple data bases and resources. The results of all comparisons are depicted in bar graphs showing the fold change for all DEPs overlapping with any of the resources checked (Figure 28). DRG are known to play a significant role in somatosensation (Santana-Varela et al., 2021; Usoskin et al., 2015; Zheng et al., 2019) and pain (Dubin & Patapoutian, 2010; Patapoutian et al., 2009; Vaso et al., 2014). A list of all DEPs, biologically relevant and statistically significant, from the DRG data in all relevant comparisons was compared to well-known pain-related candidates. These candidates were drawn from three different pain databases[10]. Furthermore, the same list of all DEPs was compared more specifically to a list of pain-related ion channels. Possibly explained by the higher total number of DEPs detected in female DRG, they also showed a higher number of pain-related DEPs (depicted in magenta) than male DRG (depicted in cyan) (Figure 28A). In females, most pain-related DEPs showed a higher expression at 14w compared to 4w. Possibly, this could indicate a higher sensitivity to pain in adult than in juvenile mice. It would be interesting to investigate whether this could be observed in *in vivo* studies. To do this, it would be of interest to apply different pain models in male and female mice of juvenile and adult age. More specifically, experiments on acute pain in response to Caps injection in females depending on age can give further insights on the question, whether the increase in nocifensive response with age is also sex-dependent and differs between males and females.

Additionally, neuroimmune interactions were of further interest in the DRG compared between all four conditions (4w female, 4w male, 14w female, 14w male), given their potential influence on neuronal functions in the context of pain. To learn more, the list of all DEPs was compared to a list of neuroimmune ligands and receptors in DRG (Wangzhou et al., 2021). Similar to the comparison to pain-related candidates, again, the number of neuroimmune-related DEPs was higher in females than in males and over both sexes but specifically in females, more neuroimmune-related candidates showed an enrichment at 4w (Figure 28B). This goes in line with the observations in the skin, that also revealed a higher expression of neuroimmune candidates at the juvenile age (Xian, Sondermann, Gomez Varela, & Schmidt, 2022).

[10] https://www.painresearchforum.org/, https://mogilab.ca, https://humanpaingeneticsdb.ca/hpgdb/

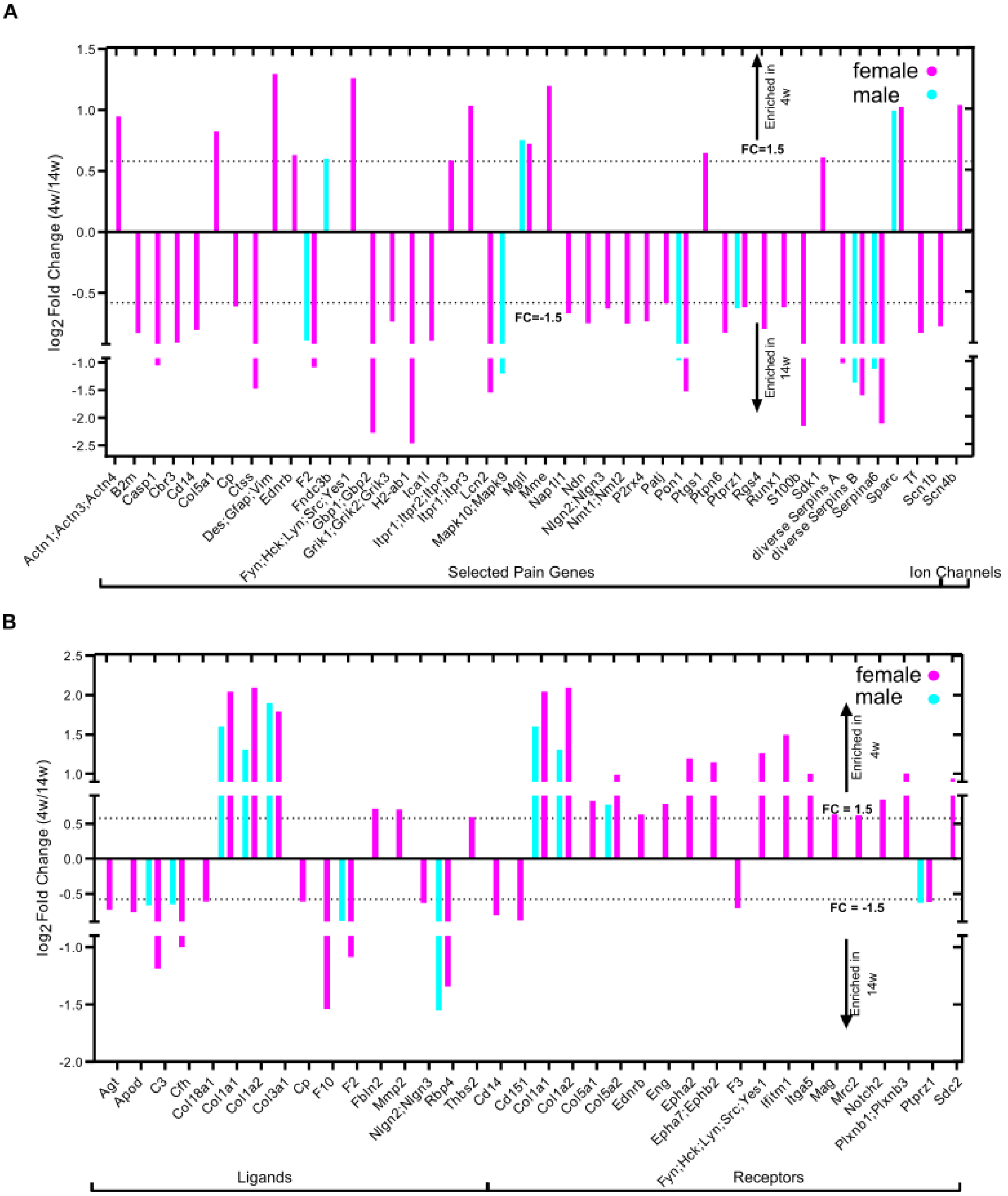

Figure 28: Age-dependent expression of pain- and neuroimmune-related candidates.

(A) Bar graphs depict $\log_2$ FC of DEP found in indicated comparisons (by age) that could be matched to one of the pain-related databases[11] and a list of known pain-related ion channels within these databases. Diverse Serpins A include the following: Serpina3c, Serpina3f, Serpina3k, Serpina3m, Serpina3n. Diverse Serpins B include the following: Serpina3c, Serpina3k, Serpina3m, Serpina3n. (B) Bar graphs depict $\log_2$ FC of DEP found in indicated comparisons (by age) that could be matched to a database of neuroimmune ligands and receptors in DRG (Wangzhou et al., 2021). (A and B): Data were generated using quantitative mass spectrometry on lDRG tissue for n = 4 mice/group. All DEPs indicated show an adjusted p-value of ≤ 0.05. Contributions: Experiments were performed by Julia Sondermann and Feng Xian, analysis was performed by me assisted by Julia Sondermann and Feng Xian. Figures were generated by me.

[11] https://www.painresearchforum.org/, https://mogilab.ca, https://humanpaingeneticsdb.ca/hpgdb/

In all aforementioned comparisons to data bases and other resources, it was of specific interest that, whenever a DEP was confirmed in both the male and the female age-dependent comparison, its regulation was always in the same direction. For example, Serpin family A member 6 (Serpina6), a protein relevant in the context of pain (Holliday et al., 2010), showed a higher expression at 14w compared to 4w for both male and female, while Secreted protein acidic and cystein rich (Sparc), which is connected to chronic low back pain in humans (Tajerian et al., 2011) showed a higher expression at 4w for both sexes. This direction of maturational regulation of Sparc is similar to the one observed in SCN (Xian, Sondermann, Gomez Varela, & Schmidt, 2022). A similar direction of FC value in the male and female age-dependent comparisons suggests that in the context of the development of pain- and neuroimmune-related candidates, the maturation occurs in a similar way in both males and females.

To understand differences between the sexes at certain maturational time points, the same comparisons were performed for the sex-dependent observations. Given the low number of DEPs, only Serpina6 was found to be a protein of interest that was differentially regulated by sex at 14w. It showed a higher expression in female tissue (data not shown). This indicates that at the level of the naïve DRG proteome, the difference in expression of pain- and neuroimmune-candidates between male and female is minimal both in juvenile and adult mice. This is somewhat unexpected since many behavioral and mechanistical differences in pain signaling were observed in multiple studies, as described above. A hypothesis to explain this is either, an involvement of other proteins, so far undescribed in the context of pain or a differential proteome in other parts of the pain neuraxis. The second hypothesis is supported by the proteome data from SCN. In SCN the number of pain-related candidates among DEPs is noticeably higher than in DRG (Xian, Sondermann, Gomez Varela, & Schmidt, 2022).

Overall, the results from the comparisons of DEPs to pain- and neuroimmune-related candidates support the hypothesis that age has a stronger influence on the proteome of skin SCN and DRG in mice than sex, when considering these two biological variables. This suggests that more processes should be studied in juvenile mice to potentially translate to a better understanding of pediatric pain (see Introduction).

3.2.7 Maturation and Sex do Not Influence Cytokine/Chemokine Levels in DRG of Naïve Mice

Multiple candidates involved in neuroimmune interactions were found to be differentially expressed in the age-dependent comparisons in both sexes (Figure 28B). Cytokines and chemokines are very small proteins relevant in neuroimmune crosstalk. They are well known contributors fulfilling a messenger function (Cook et al., 2018). Due to their size, they are often difficult to detect in mass spectrometry studies. Nevertheless, we were convinced that information on relative expression levels of cytokines and chemokines could help understanding which processes differed between ages and sexes and how. A potential change in cytokine expression could suggest a distinct influence of this part of the crosstalk during maturation or in dependence of sex. The level of cytokines and chemokines in naïve DRG lysates was assessed using a commercially available kit. The results of the experiments, showing the ratio of protein abundance between two conditions, revealed none of the cytokines/chemokines investigate to be significantly differentially expressed in the relevant comparisons (4w male vs 12w male, 4w female vs 12w female, 4w male vs 4w female, 12w male vs 12w female) (Figure 29). Others have described similar observations when comparing sexes in transcriptomic DRG studies, both under naïve conditions, and within the spinal nerve ligation (Lopes, Malek, et al., 2017) or the partial sciatic nerve injury for chronic pain, not revealing differences between male and female regarding neuroimmune and pro-inflammatory processes (Liang et al., 2020). It will be of interest to study cytokine levels in the SNI model using mice of different sexes and ages to reveal potential model-specific influences.

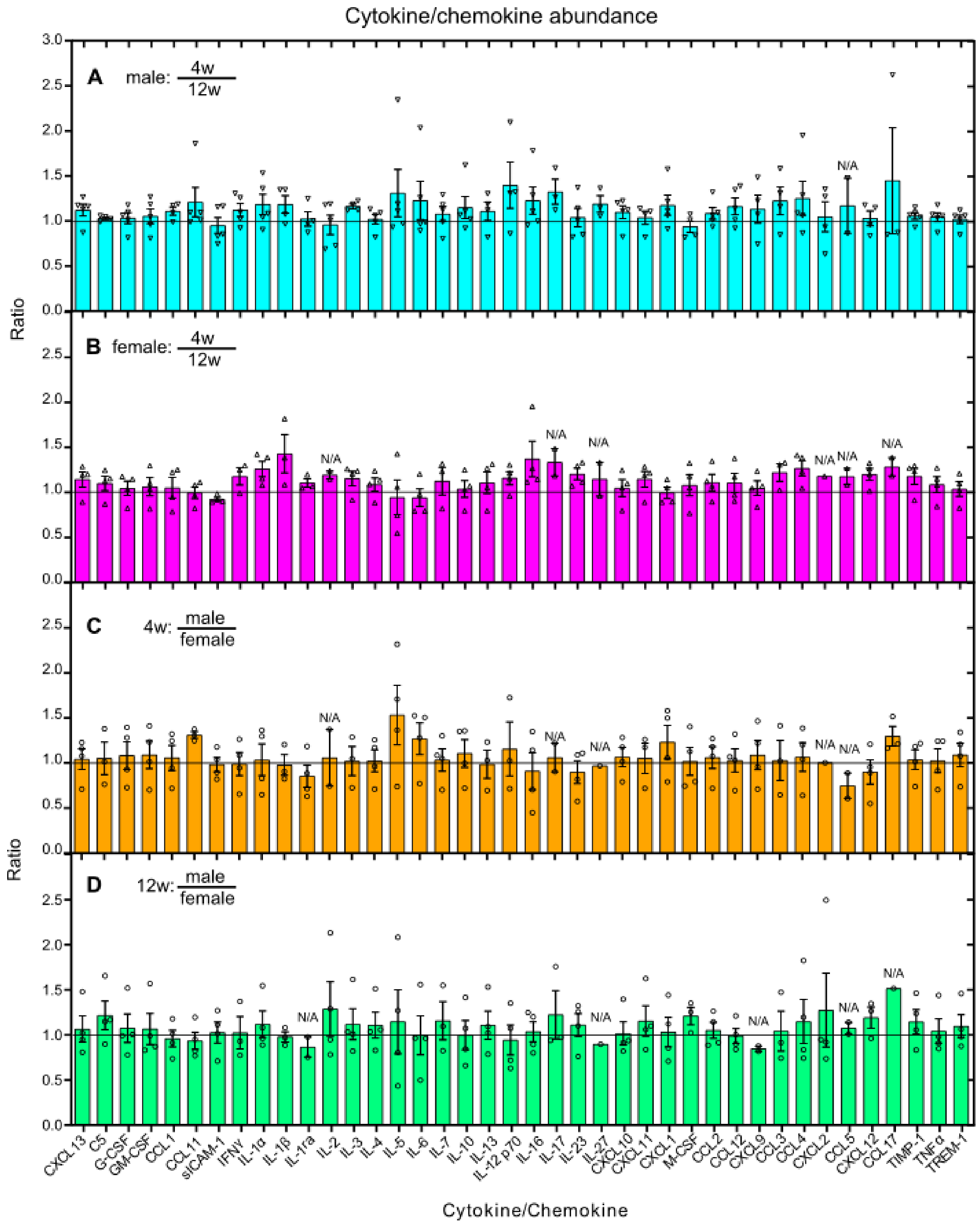

Figure 29: Age- and sex-dependent relative cytokine/chemokine levels in naïve DRG.

Cytokine/chemokine levels in DRG lysates of four groups were detected and compared. (A) Bar graphs depict the ratio of cytokine level comparing male 4w vs 12w DRG. (B) Bar graphs depict the ratio of cytokine level comparing female 4w vs 12w DRG. (C) Bar graphs depict the ratio of cytokine level comparing 4w male vs female DRG. (D) Bar graphs depict the ratio of cytokine level comparing 12w male vs female DRG. (A-D) Data are depicted as mean ± SEM in a scatter bar plot. Multiple testing using ratio-paired t-tests. ǂ for comparison between genotypes. ǂ $p \leq 0.05$. If ≤ 2 values/genotype were obtained per cytokine/chemokine, the significance could not be assessed (N/A). N = 5 (male, 4w) and N = 5 (male, 12w), N = 4 (female, 4w) and N = 4 (female, 12w) mice. n = 1 membrane/mice. Contributions: Data were generated by me with help from David Steiner and analyzed by me. Figures were generated by me.

3.2.8 Comparison of the DRG Mass Spectrometry Data Sets to Relevant Proteomic and Transcriptomic Data Sets Published Previously

To further understand, why we performed the DRG mass spectrometry experiments, it is important to compare the newly generated data sets to other proteomic or transcriptomic DRG data sets published to date. This will explain, how our study adds to a better understanding of the constitution of the DRG in mice. Different subsets of our DRG data, i.e., all IDs detected in the appropriate groups (4w female, 4w male, 14w female, 14w male) or in their overlaps, were compared with multiple publications (methods for details) (Pogatzki-Zahn et al., 2021; Rouwette et al., 2016; Usoskin et al., 2015; Zeisel et al., 2018). This served to find out, if we detect the same IDs in our experiments (Figure 30, Supplemental Table 4). We were able to increase the output compared to previous proteomic sets while still detecting most of the previously reported proteins (Pogatzki-Zahn et al., 2021; Rouwette et al., 2016). A higher output is desirable since it gives more details on the proteome. For the data set of Pogatzki-Zahn et al. (Pogatzki-Zahn et al., 2021) a model for acute incisional pain in 10w old male mice has been applied. They reported 44 regulated proteins, among those Myosin-1 (Myh1), Fibronectin (Fn1), Myoglobin (Mb), Asporin (Aspn), and Serotransferrin (Tf), all of which we also detected in our data set (Figure 30A). This indicates that we would also be able to find differences in expression level of those protein, described in the context of pain, if they were changed within our data sets. In 2016, a specific enrichment protocol was applied to investigate the membrane-enriched proteome in DRG in models for both inflammatory and neuropathic pain (Rouwette et al., 2016). This study revealed multiple DEPs compared to the appropriate controls, among which 12 were regulated in both pain models (Figure 2). One of the DEPs in both pain models was Tmem160. This study of membrane-enriched DRG proteome proved relevance by suggesting Tmem160 as a protein of interest. Here, in the present study, we reported the expression of multiple membrane-bound proteins even without an enrichment step, being indicative of technical advances in the field. The channels detected included transient receptor potential (TRP) channels (TRPA1, TRPV1) as well as transmembrane proteins (Tmem11, Tmem115, Tmem160, Tmem205). We even found expression information for some ion channels that were not detected by Rouwette et al. (Rouwette et al., 2016) for example TRPM2, TRPM4 and TRPM8 (Figure 30B). Transcriptomic data sets usually provide a higher number of IDs detected compared to proteomics. This is due to the difference in biomolecule and methodology used (Manzoni et al., 2018). It is important to note, though, that despite the higher output of transcriptomics, proteomics is more comprehensive, since most processes in the body are directly dependent on proteins and not on their mRNA levels. Those do not always correlate, specifically when fast changes occur as a cellular response (Twyman, 2012). While our general detection quota was lower, we did detect some IDs not published in the transcriptomics data bases (Usoskin et al., 2015; Zeisel et al., 2018). When comparing the

IDs we reported, with the Top 50 of different DRG neuronal subtypes provided by Usoskin et al. we detected IDs throughout the subpopulations, confirming, that we most likely sample from all different DRG cell types (Supplemental Table 4) (Usoskin et al., 2015). Comparing our IDs to these other data set allowed us to conclude, that due to an improvement in methodology and technical advances, our data set provides quantitative insights about more IDs than reported previously across different neuronal subpopulations in murine DRG.

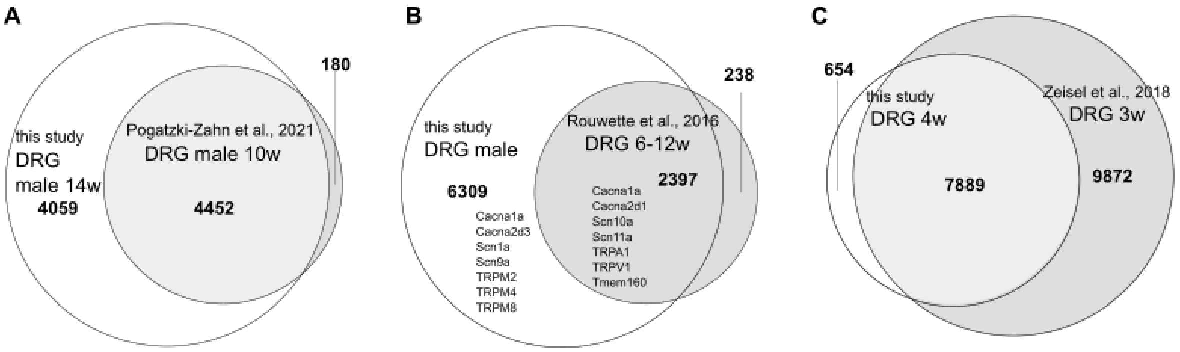

Figure 30: Comparison of IDs detected in our quantitative proteomic data sets with relevant data sets published.

(A) Comparison of all IDs detected in our 14w male group with the data set published by Pogatzki-Zahn et al. (Pogatzki-Zahn et al., 2021). (B) Comparison of all IDs detected in at least one of our male experimental groups with the membrane-enriched data set published by Rouwette et al. (Rouwette et al., 2016) including examples. (C) Comparison of all IDs detected in at least one of the 4w experimental groups with the data set published by Zeisel et al. (mousebrain.org (Zeisel et al., 2018)). (A-C) Comparisons were performed as described in the methods section. Data were generated using quantitative mass spectrometry on lDRG tissue for n = 4 mice/group. Contributions: Experiments were performed by Julia Sondermann and Feng Xian, analysis was performed by me assisted by Julia Sondermann and Feng Xian. Figures were generated by me.

As a next step, we specifically checked for our DEPs (differentially expressed proteins in the relevant comparison, statistically significant and biologically relevant) with the Top50 mentioned above, to reveal hints toward a change of composition or relevance of the neuronal subtypes with age. While for the neuronal subpopulation TH, most of our overlapping DEPs where higher expressed in the younger mice, for most other subtypes, a higher expression in adults was revealed (Supplemental Table 4). The website mousebrain.org and the underlying transcriptomic data set generated by Zeisel et al. (Zeisel et al., 2018) is a commonly used reference regarding gene expression in mice. Their data set for DRG stood out by using male and female mice at an age of 3w (Zeisel et al., 2018) which is very close to our young age time point. Our study detected around 45% of the IDs from that data set and some additional IDs (Figure 30C). Due to the young age used in the Zeisel et al. data set, we were then interested to check whether the presence or absence of specific proteins in their data base could be due to the age of the subject. In that matter, we investigated whether the absence of a protein in their data base would correlate with a significantly higher expression in 14w vs 4w in our data set (DEPs, Figure 31A) or with IDs that we only detected in the 14w and not in the 4w age group (Figure 31B) (Supplemental Table 4).

Indeed, the hypothesis, that an absence in the data set from Zeisel et al. could correlate with being a DEP with higher expression in the adult group in our data set, proved true for some proteins, including Serum paraoxonase and arylesterase 1 (Pon1) and Serpina6. Both were higher expressed at 14w in male and female mice and showed no expression in the data base from Zeisel et al. In addition, both of those proteins are known to be involved in pain processes (Holliday et al., 2010; Roomruangwong et al., 2021; Selek et al., 2011) (Figure 28A). 280 proteins were found in male 14w but not 4w of which 36 were absent in Zeisel et al., e.g., Matrix metallopeptidase 9 (MMP9), Serpin family A member 7 (Serpina7) and Carboxylesterase 1 (Ces1) some of which were identical to the same comparison in females. In the female comparison, 680 IDs were reported at 14w but not at 4w, 68 of them were absent from Zeisel et al., e.g., Bridging integrator-2 (Bin2), BUD23, rRNA methyltransferase and ribosome maturation factor (Bud23), Erbb2 interacting protein (Erbin), MMP9 and Cluster of differentiation 48 (CD48) and Dispatched 3 gene (Disp3) (Figure 31B).

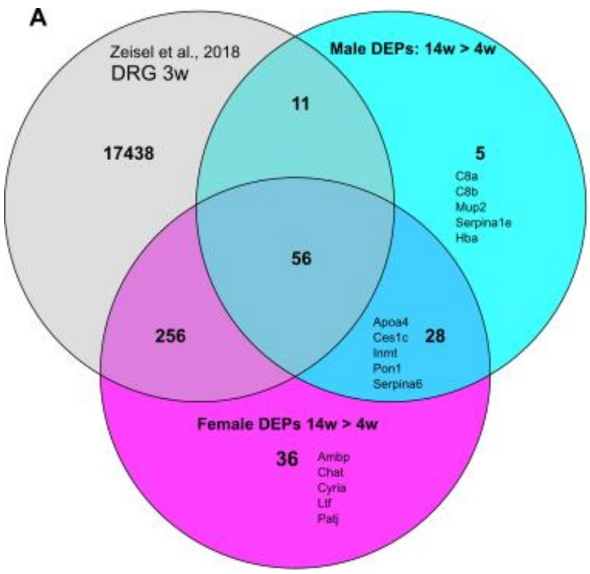

Figure 31: Comparisons of DEPs or IDs detected only in adult samples with the data set published by Zeisel et al. (Zeisel et al., 2018).

(A) Comparison of the DEPs showing a higher expression at 14w in male or female mice, relative to the respective 4w age group, with the data set published by Zeisel et al. (Zeisel et al., 2018) including examples. (E) Comparison of the IDs uniquely detected at 14w in male or female, but not in the corresponding 4w age group, with the data set published by Zeisel et al. (Zeisel et al., 2018) including examples. (A-B) Comparisons were performed as described in the methods section. Data were generated using quantitative mass spectrometry on lDRG tissue for n = 4 mice/group. Contributions: Experiments were performed by Julia Sondermann and Feng Xian, analysis was performed by me assisted by Julia Sondermann and Feng Xian. Figures were generated by me.

For both our male and our female data set, we report that roughly around 10% of the IDs uniquely expressed in adults were missing from the data generated by Zeisel et al. (Figure 31B). Many of the differences can be accounted to by the different way of sampling (Zeisel et al. used single cell collection specifically of neurons while we collected whole DRG without differentiation for cell type). An example for this would be MMP9, known to be mainly expressed in immune cells or fibroblasts (Yabluchanskiy et al., 2013), which we detected in our data set in contrast to Zeisel et al.. Bin2 has been reported in leukocytes or leukemic cells (Sánchez-Barrena et al., 2013) while CD48 was detected in lymphocytes (McArdel et al., 2016). Many other proteins that we reported uniquely in our data set, which were not detected by Zeisel et al., are known contributors to the immune system. Nevertheless, some proteins for which we add information on expression to Zeisel et al. have been reported to show neuronal expression, e.g., Erbin (Arikkath et al., 2008), Major Facilitator Superfamily Domain Containing 14B (MFSD14B) (Lekholm et al., 2017) and Choline acetyltransferase (Chat) (Trifonov et al., 2009). Indole-N-methyl transferase (INMT) (Mavlyutov et al., 2012) as well as Septin 7 (Y. Xie et al., 2007) also showed neuronal expression. Disp3 expression was mainly limited to the central nervous system (Zíková et al., 2014) whereas Desmoplakin (Dsp) was found specifically in motor neurons (Gess et al., 2015) (Supplemental Table 4). All in all, it can be concluded, that we complement the data set from Zeisel et al. and parts of this could be due to the age of the subjects in both studies.

4 Summary and Outlook

Pain research faces pivotal challenges to further improve treatment options for patients. In this context, it is important to deepen the basic understanding of the differences between physiological acute pain and pathological chronic pain. As described above, membrane proteins play a relevant role in pain signaling. There are multiple ways to find prospective proteins of interest that can serve as a target for future pain treatment. One way to do this is to use proteomics as a hypothesis-generating resource. In this regard, murine inflammatory and neuropathic pain models were applied and afterwards the membrane-enriched proteome of the mouse DRG was compared to controls. The focus was to find membrane proteins that were regulated in both models and were - to this point – undescribed in the context of chronic pain.

4.1 Characterization of Tmem160

The transmembrane (Tmem) protein family is highly promising since its proteins are defined by a lack of functional and structural information. A protein found to be downregulated in the murine models for inflammatory and neuropathic pain was Tmem160. This study aimed to find out more about its localization, function and effect on acute and chronic pain in mice to eventually reveal its potential as a target for human pain treatment in the future.

To this end, two different knockout mouse lines for *Tmem160* were generated – a global and a conditional *Tmem160* KO - and multiple *in vivo* and *in vitro* experiments were performed. In the global *Tmem160* KO mouse line, *Tmem160* is knocked out in all cells of the body, while in the conditional *Tmem160* KO, *Tmem160* is only knocked out in approximately 80% of the sensory neurons. Our broad experimental battery allowed us to discover the following phenotype in male global *Tmem160* KO mice: delayed initiation of tactile hypersensitivity and self-grooming in the early phase or neuropathic pain as modeled by SNI. Non-evoked pain as well as locomotion was found unchanged. Additionally, all other pain models (inflammatory, acute, and incisional pain) tested did not reveal differences between the *Tmem160* KO and WT. Also, the conditional *Tmem160* cKO as well as the female global *Tmem160* KO exhibited WT-like behaviors in all experiments.

Mechanistically, we propose the following working model, supported by our experimental results: it seems as if Tmem160 influences cytokine/chemokine releases in the early phase (up to 7 days) of neuropathic pain as represented by the SNI model. At later time points, Tmem160 does not seem to further influence pain behavior, since both *Tmem160* KO and WT developed tactile hypersensitivity by day 14 post SNI. The influence on cytokine release either occurs directly in the immune cells or via influence on neuroimmune crosstalk. It is less likely that the influence on cytokine levels occurs from neuronal Tmem160, since the *Tmem160* cKO in sensory neurons did not elicit the same changes. These cytokines possibly cause peripheral sensitization and pain-related behaviors. Lower levels of TNFα and other cytokines were found in *Tmem160* KO and Ca^{2+}-imaging experiments revealed a reduction in percentage of responders to AITC in *Tmem160* KO mice. This could be “rescued” to WT level by external substitution of the lack of TNFα. These results support the hypothesis that Tmem160 influences neuronal excitability via TNFα together with TRPA1 and an activation of microglia in the spinal cord. The processes where Tmem160 showed relevance in the chronic pain context suggested a specificity to male mice. It is likely, that the increase in microglia activation – as influenced by Tmem160 – in the spinal cord post SNI influences tactile hypersensitivity. It was shown before that a reduction of spinal cord microglia delays but not completely evades the initiation of tactile hypersensitivity which goes in hand with our observations in *Tmem160* KO (Peng et al., 2016).

Briefly summarizing the results: our experiments revealed that the action of Tmem160 is somewhat specific to tactile hypersensitivity in male mice in the early phase of neuropathic pain, even though further studies are needed to find out more about specific action mechanisms. Particularly the lack of an influence of Tmem160 on the physiologically necessary acute pain is promising. This makes Tmem160 a hopeful target for future pain treatment, specifically in men, but there are still multiple open questions after this study which must be addressed first.

One of the most important goals in subsequent research is to get further insights into the cell types or subpopulations in which Tmem160 performs its main actions. Based on the findings so far, it is likely that Tmem160 acts in immune cells, potentially in macrophages and/or microglia. Also, subclasses of central spinal (Niehaus et al., 2021) and peripheral (X. Yu et al., 2020) macrophages are known to be involved in the generation of neuropathic pain. For the central macrophages, anti-inflammatory MRC1+ macrophages (“Macro1” and “Macro2”) have been identified (Niehaus et al., 2021), which supposedly reduce inflammation and pain caused by nerve injury. This can likely occur in DRG. When checking for Tmem160 expression changes post SNI in all different cell types, Tmem160 was found to be downregulated in a subpopulation of excitatory neurons (“Excit15”) as well as in the “Macro2” macrophages described above. As mentioned previously, Tansley and colleagues confirmed the expression of Tmem160 in a subpopulation of spinal microglia that is upregulated in the early phase of neuropathic pain in WT mice (Tansley et al., 2022). Unfortunately, specific targeting of the subpopulation is complicated given their sparsity of e.g. only 0.035% for “cluster 9” microglia under naïve conditions (Tansley et al., 2022). Nevertheless, to further investigate the role of Tmem160 in microglia or macrophages it would be necessary to deplete *Tmem160* by genetically modifying all microglia/macrophages or, more specifically, the subpopulations described by Tansley and colleagues (Tansley et al., 2022) and Niehaus and colleagues (Niehaus et al., 2021). With these KO conditions, it would be helpful to repeat the behavioral and *in vitro* experiments to gain further insights. To investigate the levels of cytokines and chemokines in other body parts upon global *Tmem160* KO, e.g., in serum, would shed light on the questions whether Tmem160 influences the neuroimmune crosstalk rather locally in DRG or also affects other areas of the body. All those experiments would enable a confirmation of the hypothesis that Tmem160 fulfills its function in microglia or macrophages and to support the role of Tmem160 in neuroimmune interactions.

In addition, it would be of interest to investigate other cell types of DRG and spinal cord in mice with regards to action mechanisms of Tmem160, e.g., satellite glia, fibroblast, oligodendrocytes, Schwann cells or astrocytes. It is possible for all these cells to play a role in how Tmem160 could contribute to the initiation of pain and tactile hypersensitivity. Furthermore, additional insight into molecular actions of Tmem160 could be gained by studying more receptors and intracellular signaling pathways, e.g., phosphorylations.

While we only described the first 28 days within the SNI model, according to more recent studies, this might not be sufficient to catch all potential behavioral changes (Millecamps et al., 2022). It cannot be completely ruled out, that Tmem160 has an additional effect that only has an impact in very late phases after the SNI surgery. To investigate this in more detail, ideally, it would be necessary to repeat the behavioral studies over a time frame longer than 28 days. This comes with several drawbacks including further – possibly unnecessary – strain on the animals and high costs of animal housing. Regarding the ethical side of the 3R rule in animal experiments – replacement, reduction and refinement – it is very important to appreciate the mice as living beings. Therefore, it should be refrained from performing animal experiments if the output is not expected to have a further relevance. Additionally, the high amount of data generated in such an experiment – with the high animal numbers required to expect statistical relevance – would increase the amount of personnel necessary to analyze the data and gain insights into all relevant time points. A repetition over a longer time frame would be desirable under optimal conditions regarding ethics of animal welfare, staff-availability, and finances. Nevertheless, since the in vivo and in vitro differences we found upon *Tmem160* deletion were limited to the early phase and diminished over time, it is unlikely that we missed an effect of Tmem160 in the late phase of neuropathic pain.

Moreover, we might have missed minor defects in mitochondrial function by the global analysis methods used, even though the methods are well established (Aich et al., 2018; Dennerlein et al., 2015). Therefore, it is of particular interest that Yamashita and colleagues decided to investigate the mitochondrial function of Tmem160 further based on our findings recently (Yamashita et al., 2022). While our studies were performed in mice and HEK cells, they used siRNA (Small interfering RNA) to cause a knockdown of Tmem160 in HepG2 cells and then studied various intracellular responses upon Tmem160 depletion. In addition to the confirmation of Tmem160's submitochondrial localization as discussed earlier, they found an increased expression both on mRNA and protein level of 60 kDa mitochondrial heat shock protein (HSPD1) (Yamashita et al., 2022), a chaperone that is known to play a role in the mitochondrial unfolded protein response (UPR^{mt}) (Münch, 2018). This is a response to an accumulation of misfolded and/or unfolded proteins in mitochondria and eventually causes them to refold or be digested (Münch, 2018). UPR^{mt} is induced by a combination of transcription factors, namely ATF4, ATF5, and DDIT3 (Melber & Haynes, 2018), all of which showed an upregulated protein expression upon Tmem160 depletion (Yamashita et al., 2022). This further supports the hypothesis that a UPR^{mt} is elicited. Additionally, two mitochondrial protein import receptors (TOMM22 and TOMM20) were reported to be upregulated (Yamashita et al., 2022). They hypothesized that this response was caused by mitochondrial protein damage (Yamashita et al., 2022). Mitochondrial damage also causes an increase in ROS, so the next step was to study this in the Tmem160 knockdown cells. Indeed, they found an increase in ROS generation (Yamashita et al., 2022). This increase potentially leads to oxidative stress and as a final consequence to cell death by apoptosis (R. Li et al., 2016). To figure out, whether the increase in ROS upon Tmem160 depletion is met by an increase in ROS degrading enzymes, their expression was tested on the mRNA level. They analyzed catalase (CAT), glutathione S-transferase alpha 1 and 2 (GSTA1 and GSTA2), peroxiredoxin 3 (PRDX3), superoxide dismutase 1 and 2 (SOD1 and SOD2) and thioredoxin2 (TXN2). Neither of them showed a differential expression upon Tmem160 knockdown, except for GSTA1 and GSTA2 which showed an increased expression level (Yamashita et al., 2022). Yamashita et al. also checked whether a scavenging of ROS at day 1 post knockdown using N-acetylcysteine (NAC) for 48 hours showed any influence on UPR^{mt} induction and TOMM22 upregulation. This was not the case (Yamashita et al., 2022). It has to be kept in mind, that while mitochondria are the main intracellular source of ROS, other organelles and intracellular processes can also cause ROS production, e.g., peroxisomes, endoplasmic reticulum, transition metal ions and different catabolisms (Snezhkina et al., 2019). It has been reported that ROS are specifically increased in tumor cells (Snezhkina et al., 2019), so it is noteworthy that HeLa, HepG2 and HEK293T are immortal human cell lines, with HeLa (Lucey et al., 2009) and HepG2 (Arzumanian et al., 2021) being directly based on cancerous tissue. Therefore, it can be assumed, that they show a higher internal ROS level compared to healthy human cells. Since the same cell lines served as internal controls (Yamashita et al., 2022), this should not have a high influence on the experimental results but nevertheless this is a potential difference to the mice and their cells we studied *in vivo* and *in vitro*. Yamashita et al. suggest, that UPR^{mt}, the increase in TOMM22 and TOMM20 expression, together with the increase in GSTA1 and

GSTA2 might suffice to counteract the potential mitochondrial damages caused by Tmem160 knockdown in their cell lines. This seems plausible since the apoptosis in Tmem160 depleted cells was only slightly elevated compared to controls (Yamashita et al., 2022). In addition, they studied different processes than we looked at in our research. We checked specifically for Complex IV activity and oxygen consumption rate in brain tissue in mice meaning that both the experimental model as well as the experimental processes differed between the studies. This could also explain, why we did not see any indications for a mitochondrial dysfunction in our experiments, along with the explanation given by Yamashita and colleagues as described above (Yamashita et al., 2022). Based on the findings discussed here, it would be beneficial to apply the methods used by Yamashita and colleagues on murine DRG cultures or to find a way to adapt them to an application in vivo.

4.2 Characterization of Age- and Sex-Differences in the DRG Proteome and Their Effect on Somatosensation

Multiple experiments were performed to investigate the role of maturation on somatosensation and the DRG proteome by studying differences between juvenile and adult mice of both sexes. The DRG was chosen as a tissue of interest due to its relevance in somatosensation and nociception. We contribute to previous publications on the DRG proteome by using both sexes and different age points, and therefore, add a new resource to the field.

Quantitative proteomic studies in DRG revealed multiple immune- and pain-related candidate proteins to be differentially expressed between juvenile and adult mice. Female mice revealed more age-dependent DEPs than males. Many of the pain-related candidates were higher expressed in adult mice compared to juvenile mice. The majority of candidates regulated in males appeared to be higher expressed in adult mice compared to juvenile mice, which could explain the observed higher pain sensitivity and stronger nocifensive response at that age as observed in our acute pain experiments in male mice post unilateral injection of Caps. In contrast more neuroimmune-related candidates showed an enrichment at juvenile age compared to adult in both sexes. Overall, many more differentially expressed proteins were revealed when comparing within sex groups between different ages than comparing within the age groups between sex. Comparing male and female DRG very few DEPs were found while beeing nevertheless higher at adult than at juvenile age. This increase could be based on a conceivably higher difference between males and females post- compared to presexual maturity. Overall, the number of DEPs and their involvement in different processes led us to conclude that during maturation, age has a stronger influence on the DRG proteome than sex. Nevertheless, it must be kept in mind that even though we barely see differences when directly comparing the sexes at the same age, the age comparison was very different between the sexes. While in male samples 154 proteins were differentially expressed between juvenile and adult age, the same comparison in females revealed 733 DEPs, indicating that the changes throughout maturation are bigger in female than in male mice. Due to pronounced age- and sex-differences in the DRG proteome, we highly suggest proper age- and sex-matching of experimental groups and controls, as well as specific description of age and sex of animals used in the publication in the methods section. This has the potential to improve reproducibility and reliability in multiple different biomedical disciplines.

Male mice revealed differences regarding naïve and acute pain behavior *in vivo*, as well as *in vitro* in Ca^{2+}-imaging experiments and immunostainings. Under acute pain conditions, by unilateral injection of Caps, we described an increased nocifensive response throughout maturation in male mice. In this context, further experiments could provide more insights into the underlying mechanisms explaining the differences we observed between juvenile and adult mice. It would be of interest to repeat the acute pain experiments by unilateral caps injection with an expanded experimental setup. To improve our recording method of nocifensive behavior, it will be advantageous to provide video recordings that can be analyzed afterwards, specifically regarding the time course of the response, as discussed above, and also to differentiate between the nocifensive behaviors (lifting, licking, and flicking). It is conceivable, that the different nocifensive behaviors might not be equivalent. Tracking the different behaviors separately would provide a higher resolution to the acute pain response observations. Additionally, it would be useful to analyze potential changes in the central nervous system regarding the nocifensive response post capsaicin, potentially involving the S1 (Vierck et al., 2013) and ACC (Bushnell et al., 2013; Fuchs et al., 2014; Sewards & Sewards, 2002; Vogt, 2005) region of the brain, known to be involved in pain perception, to understand possible age-dependencies in the central nervous system. Moreover, it would be valuable to repeat the thermal sensitivity recordings to better understand the reasons for the higher data variability I observed in Vienna compared to Göttingen. To find evidence for higher TRPV1 levels in the cell membranes in juvenile mice versus adults, live labelling experiments for TRPV1 could be performed in DRG cultures of both ages. This study revealed influences of age on heat response and TRPV1 stimulation in the context of acute pain. Furthermore, it would be interesting to study the acute pain situation with a different stimulus, for example the TRRA1 agonist AITC. This would reveal whether the age-dependency we observed was connected to TRPV1 directly or more generally to other proteins involved in acute pain. Research on other pain models is already planned and performed by my coworkers using the SNI model for neuropathic pain in juvenile and adult mice of both sexes. This will reveal whether the differences we observed in this study also occur in other pain models. They will additionally perform proteomic analyses of different tissues for all four experimental conditions (juvenile female, juvenile male, adult female, adult male) at different time points within the neuropathic pain model. This will add to our proteomic data under pathological conditions. Tissue collected in this experimental context would provide a valuable resource to study cytokine/chemokine levels under pathological conditions and compare them between ages and sexes. Additional insights on a more systemic role of cytokines could be gathered by measuring serum cytokines under naïve, but even more interesting, under pathological conditions.

To this point, our behavioral data were only collected in male mice. Only one sex was chosen for gathering first results to reduce animal experiments. It was decided to use male mice for a better comparability to previously published data (Michel et al., 2020; Michel, 2020). Additionally, the lack of menstrual cycle in males reduced inter-individual variability. To further complete our data set, it would be helpful to perform all experiments (acute pain post caps, thermal hypersensitivity, Ca^{2+}-imaging, immunostainings) additionally in female mice, specifically given the fact that our proteomic data set revealed more age-dependent changes in naïve female DRG than for the male comparison. Additionally, one could further focus on sexual hormones, both by documenting the menstrual cycle within experiments including female mice, but also by influencing hormonal levels and consequently detecting potential influences in the same sex. One could for example measure or influence testosterone levels to determine, whether the behavioral differences we observed between juvenile and adult male mice could depend on their testosterone levels. Nevertheless, it has to be considered that according to the 3R (replacement, reduction and refinement) principles, animal experiments should be kept to a minimum whenever possible.

4.3 Final Remarks

This dissertation aimed at a better understanding of somatosensation, pain and pain chronification to eventually improve the limited treatment options for chronic pain. Therefore, the role of specific proteins for the development of chronic pain and their importance for acute pain was investigated. Furthermore, the study tried to diversify the investigation on chronic pain and somatosensation by including parameters like sex and age aiming at a strategy to make pain treatment better targeted to individuals. To achieve this goal, multiple methods were applied, including behavioral analysis in different pain models *in vivo*, investigations of neuronal excitability *in vitro* and the composition of the DRG regarding their proteome and more specifically their levels of cytokines and chemokines. DRG are of specific relevance in the context of pain and somatosensation since they contain the somata of the primary sensory neurons responsible for stimulus detection.

The confirmation of the relevance of Tmem160 in neuropathic pain in this study further supports proteomics as a promising hypothesis-generating resource. The DRG proteomic data set generated within the second part of this study can provide similarly promising hypothesis to be then further studied in detail, this time specifically focusing on the age- and sex-differences. The study revealed prominent differences between juvenile and adult mice, even more pronounced in female than in male. These differences include proteins relevant in the pain and neuroimmune context. In the current proteomic data sets, Tmem160 was not within the age- or sex-dependent DEPs. This is highly plausible, given that this data set was collected under naïve conditions, while Tmem160's action mechanisms seem to depend on neuropathic pain.

Studies on the role of Tmem160 were so far only performed in adult mice. It would be of interest to further investigate its role in juvenile mice. Since the experiments are a burden for the mice, this only makes sense to investigate if promising results are expected. An ongoing study of my coworkers investigates the influence of age and sex on neuropathic pain within the SNI model. If the study reveals differences in tactile hypersensitivity based on age, it would be promising to repeat the experiments of the Tmem160 section in juvenile male mice. A proteomic study of the DRG under neuropathic pain conditions including juvenile and adult mice of both sexes is currently ongoing.

This dissertation as a whole emphasizes the importance of understanding pain chronification while taking into account sex- and age-dependencies in somatosensation and pain. In the long run, this will help to understand the underlying mechanisms in detail and hence improve treatment options. Our studies revealed differences in behavior and constitution of the DRG proteome depending on age and sex, indicating that for a treatment to be promising, it has to fit to the individual, regarding their sex, type of pain and social surroundings. Additionally, a target for treatment should not be involved in physiological functions, it must be be somewhat specific to the pathological state. As an example, regarding this specificity, our study shows Tmem160 as a potential target, even though it still needs further investigation before being considered. Overall, better treatment of chronic pain will reduce the personal, societal, and economic burden of pain, and most importantly lead to less suffering for chronic pain patients.

5 Bibliography

Aich, A., Wang, C., Chowdhury, A., Ronsör, C., Pacheu-Grau, D., Richter-Dennerlein, R., Dennerlein, S., & Rehling, P. (2018). Cox16 promotes COX2 metallation and assembly during respiratory complex IV biogenesis. *ELife*, *7.* https://doi.org/10.7554/eLife.32572

Andersson, D. A., Gentry, C., Moss, S., & Bevan, S. (2008). Transient Receptor Potential A1 Is a Sensory Receptor for Multiple Products of Oxidative Stress. *Journal of Neuroscience*, *28*(10), 2485–2494. https://doi.org/10.1523/JNEUROSCI.5369-07.2008

Arikkath, J., Israely, I., Tao, Y., Mei, L., Liu, X [Xin], & Reichardt, L. F. (2008). Erbin controls dendritic morphogenesis by regulating localization of delta-catenin. *Journal of Neuroscience*, *28*(28), 7047–7056. https://doi.org/10.1523/JNEUROSCI.0451-08.2008

Arzumanian, V. A., Kiseleva, O. I., & Poverennaya, E. V. (2021). The Curious Case of the HepG2 Cell Line: 40 Years of Expertise. *International Journal of Molecular Sciences*, *22*(23). https://doi.org/10.3390/ijms222313135

Avenali, L., Narayanan, P., Rouwette, T., Cervellini, I., Sereda, M., Gomez-Varela, D., & Schmidt, M. (2014). Annexin A2 regulates TRPA1-dependent nociception. *Journal of Neuroscience*, *34*(44), 14506–14516. https://doi.org/10.1523/JNEUROSCI.1801-14.2014

Bai, L [Liying], Wang, X [Xinru], Li, Z., Kong, C., Zhao, Y., Qian, J.-L., Kan, Q., Zhang, W., & Xu, J.-T. (2016). Upregulation of Chemokine CXCL12 in the Dorsal Root Ganglia and Spinal Cord Contributes to the Development and Maintenance of Neuropathic Pain Following Spared Nerve Injury in Rats. *Neuroscience Bulletin*, *32*(1), 27–40. https://doi.org/10.1007/s12264-015-0007-4

Banchereau, J., Pascual, V., & O'Garra, A. (2012). From IL-2 to IL-37: The expanding spectrum of anti-inflammatory cytokines. *Nature Immunology*, *13*(10), 925–931. https://doi.org/10.1038/ni.2406

Basbaum, A. I., Bautista, D. M., Scherrer, G., & Julius, D. (2009). Cellular and molecular mechanisms of pain. *Cell*, *139*(2), 267–284. https://doi.org/10.1016/j.cell.2009.09.028

Bautista, D. M., Jordt, S.-E., Nikai, T., Tsuruda, P. R., Read, A. J., Poblete, J., Yamoah, E. N., Basbaum, A. I., & Julius, D. (2006). Trpa1 mediates the inflammatory actions of environmental irritants and proalgesic agents. *Cell*, *124*(6), 1269–1282. https://doi.org/10.1016/j.cell.2006.02.023

Belmonte, C., & Viana, F. (2008). Molecular and cellular limits to somatosensory specificity. *Molecular Pain*, *4*, 14. https://doi.org/10.1186/1744-8069-4-14

Bennett, D. L. H., & Woods, C. G. (2014). Painful and painless channelopathies. *The Lancet Neurology*, *13*(6), 587–599. https://doi.org/10.1016/S1474-4422(14)70024-9

Bennett, G. J., Doyle, T., & Salvemini, D. (2014). Mitotoxicity in distal symmetrical sensory peripheral neuropathies. *Nature Reviews Neurology*, *10*(6), 326–336. https://doi.org/10.1038/nrneurol.2014.77

Beyer, C., Roberts, L. A., & Komisaruk, B. R. (1985). Hyperalgesia induced by altered glycinergic activity at the spinal cord. *Life Sciences*, *37*(9), 875–882. https://doi.org/10.1016/0024-3205(85)90523-5

Bootman, M. D., Rietdorf, K., Collins, T., Walker, S., & Sanderson, M. (2013). Ca2+-sensitive fluorescent dyes and intracellular Ca2+ imaging. *Cold Spring Harbor Protocols*, *2013*(2), 83–99. https://doi.org/10.1101/pdb.top066050

Borsook, D., Hargreaves, R., Bountra, C., & Porreca, F. (2014). Lost but making progress--Where will new analgesic drugs come from? *Science Translational Medicine*, *6*(249), 249sr3. https://doi.org/10.1126/scitranslmed.3008320

Bourinet, E., Altier, C., Hildebrand, M. E., Trang, T., Salter, M. W., & Zamponi, G. W. (2014). Calcium-permeable ion channels in pain signaling. *Physiological Reviews*, *94*(1), 81–140. https://doi.org/10.1152/physrev.00023.2013

Breivik, H., Collett, B., Ventafridda, V., Cohen, R., & Gallacher, D. (2006). Survey of chronic pain in Europe: Prevalence, impact on daily life, and treatment. *European Journal of Pain (London, England)*, *10*(4), 287–333. https://doi.org/10.1016/j.ejpain.2005.06.009

Bushnell, M. C., Ceko, M., & Low, L. A. (2013). Cognitive and emotional control of pain and its disruption in chronic pain. *Nature Reviews Neuroscience*, *14*(7), 502–511. https://doi.org/10.1038/nrn3516

Callahan (2008). Modulation of mechanical and thermal nociceptive sensitivity in the laboratory mouse by behavioral state. *J. Pain*, *9*, 174.

Cannino, G., El-Khoury, R., Pirinen, M., Hutz, B., Rustin, P., Jacobs, H. T., & Dufour, E. (2012). Glucose modulates respiratory complex I activity in response to acute mitochondrial dysfunction. *The Journal of Biological Chemistry*, *287*(46), 38729–38740. https://doi.org/10.1074/jbc.M112.386060

Catterall, W. A. (2011). Voltage-gated calcium channels. *Cold Spring Harbor Perspectives in Biology*, *3*(8), a003947. https://doi.org/10.1101/cshperspect.a003947

Chen, G., Zhang, Y.-Q., Qadri, Y. J., Serhan, C. N., & Ji, R.-R. (2018). Microglia in Pain: Detrimental and Protective Roles in Pathogenesis and Resolution of Pain. *Neuron*, *100*(6), 1292–1311. https://doi.org/10.1016/j.neuron.2018.11.009

Chen, Y., & Huang, L.-Y. M. (2017). A simple and fast method to image calcium activity of neurons from intact dorsal root ganglia using fluorescent chemical Ca2+ indicators. *Molecular Pain*, *13*, 1744806917748051. https://doi.org/10.1177/1744806917748051

Cicchetti, D. V., & Sparrow, S. A. (1981). Developing criteria for establishing interrater reliability of specific items: Applications to assessment of adaptive behavior. *American Journal of Mental Deficiency*, *86*(2), 127–137.

Claros, M. G., & Vincens, P. (1996). Computational method to predict mitochondrially imported proteins and their targeting sequences. *European Journal of Biochemistry*, *241*(3), 779–786. https://doi.org/10.1111/j.1432-1033.1996.00779.x

Cobo, M. M., Green, G., Andritsou, F., Baxter, L., Evans Fry, R., Grabbe, A., Gursul, D., Hoskin, A., Mellado, G. S., van der Vaart, M., Adams, E., Bhatt, A., Denk, F., Hartley, C., & Slater, R. (2022). Early life inflammation is associated with spinal cord excitability and nociceptive sensitivity in human infants. *Nature Communications*, *13*(1), 3943. https://doi.org/10.1038/s41467-022-31505-y

Cobos, E. J., Nickerson, C. A., Gao, F., Chandran, V., Bravo-Caparrós, I., González-Cano, R., Riva, P., Andrews, N. A., Latremoliere, A., Seehus, C. R., Perazzoli, G., Nieto, F. R., Joller, N., Painter, M. W., Ma, C. H. E., Omura, T., Chesler, E. J., Geschwind, D. H., Coppola, G., . . . Costigan, M. (2018). Mechanistic Differences in Neuropathic Pain Modalities Revealed by Correlating Behavior with Global Expression Profiling. *Cell Reports*, *22*(5), 1301–1312. https://doi.org/10.1016/j.celrep.2018.01.006

Cook, A. D., Christensen, A. D., Tewari, D., McMahon, S. B., & Hamilton, J. A. (2018). Immune Cytokines and Their Receptors in Inflammatory Pain. *Trends in Immunology*, *39*(3), 240–255. https://doi.org/10.1016/j.it.2017.12.003

Costigan, M., Scholz, J., & Woolf, C. J. (2009). Neuropathic pain: A maladaptive response of the nervous system to damage. *Annual Review of Neuroscience*, *32*(1), 1–32. https://doi.org/10.1146/annurev.neuro.051508.135531

Cox, J., Hein, M. Y., Luber, C. A., Paron, I., Nagaraj, N., & Mann, M. (2014). Accurate proteome-wide label-free quantification by delayed normalization and maximal peptide ratio extraction, termed MaxLFQ. *Molecular & Cellular Proteomics : MCP*, *13*(9), 2513–2526. https://doi.org/10.1074/mcp.M113.031591

Cunha, A. M., Pereira-Mendes, J., Almeida, A., Guimarães, M. R., & Leite-Almeida, H. (2020). Chronic pain impact on rodents' behavioral repertoire. *Neuroscience and Biobehavioral Reviews*, *119*, 101–127. https://doi.org/10.1016/j.neubiorev.2020.09.022

Dahlhamer, J., Lucas, J., Zelaya, C., Nahin, R., Mackey, S., DeBar, L., Kerns, R., Korff, M. von, Porter, L., & Helmick, C. (2018). Prevalence of Chronic Pain and High-Impact Chronic Pain Among Adults - United States, 2016. *MMWR. Morbidity and Mortality Weekly Report*, *67*(36), 1001–1006. https://doi.org/10.15585/mmwr.mm6736a2

Dance, A. (2019). Why the sexes don't feel pain the same way. *Nature*, *567*(7749), 448–450. https://doi.org/10.1038/d41586-019-00895-3

Davis, K. D., Aghaeepour, N., Ahn, A. H., Angst, M. S., Borsook, D., Brenton, A., Burczynski, M. E., Crean, C., Edwards, R., Gaudilliere, B., Hergenroeder, G. W., Iadarola, M. J., Iyengar, S., Jiang, Y., Kong, J.-T., Mackey, S., Saab, C. Y., Sang, C. N., Scholz, J., . . . Pelleymounter, M. A. (2020). Discovery and validation of biomarkers to aid the development of safe and effective pain therapeutics: Challenges and opportunities. *Nature Reviews Neurology*, *16*(7), 381–400. https://doi.org/10.1038/s41582-020-0362-2

Decosterd, I., & Woolf, C. J. (2000). Spared nerve injury: an animal model of persistent peripheral neuropathic pain. *Pain*, *87*(2), 149–158. https://doi.org/10.1016/S0304-3959(00)00276-1

Demichev, V., Messner, C. B., Vernardis, S. I., Lilley, K. S., & Ralser, M. (2020). Dia-NN: Neural networks and interference correction enable deep proteome coverage in high throughput. *Nature Methods*, *17*(1), 41–44. https://doi.org/10.1038/s41592-019-0638-x

Dennerlein, S., Oeljeklaus, S., Jans, D., Hellwig, C., Bareth, B., Jakobs, S., Deckers, M., Warscheid, B., & Rehling, P. (2015). Mitrac7 Acts as a COX1-Specific Chaperone and Reveals a Checkpoint during Cytochrome c Oxidase Assembly. *Cell Reports*, *12*(10), 1644–1655. https://doi.org/10.1016/j.celrep.2015.08.009

Dhaka, A., Viswanath, V., & Patapoutian, A. (2006). Trp ion channels and temperature sensation. *Annual Review of Neuroscience*, *29*, 135–161. https://doi.org/10.1146/annurev.neuro.29.051605.112958

DiMauro, S., & Schon, E. A. (2003). Mitochondrial respiratory-chain diseases. *The New England Journal of Medicine*, *348*(26), 2656–2668. https://doi.org/10.1056/NEJMra022567

Dispersyn, G., Nuydens, R., Connors, R., Borgers, M., & Geerts, H. (1999). Bcl-2 protects against FCCP-induced apoptosis and mitochondrial membrane potential depolarization in PC12 cells. *Biochimica Et Biophysica Acta*, *1428*(2-3), 357–371. https://doi.org/10.1016/s0304-4165(99)00073-2

Doench, J. G., Fusi, N., Sullender, M., Hegde, M., Vaimberg, E. W., Donovan, K. F., Smith, I., Tothova, Z., Wilen, C., Orchard, R., Virgin, H. W., Listgarten, J., & Root, D. E. (2016). Optimized sgRNA design to maximize activity and minimize off-target effects of CRISPR-Cas9. *Nature Biotechnology*, *34*(2), 184–191. https://doi.org/10.1038/nbt.3437

Doth, A. H., Hansson, P. T., Jensen, M. P., & Taylor, R. S. (2010). The burden of neuropathic pain: A systematic review and meta-analysis of health utilities. *Pain*, *149*(2), 338–344. https://doi.org/10.1016/j.pain.2010.02.034

Du Percie Sert, N., & Rice, A. S. C. (2014). Improving the translation of analgesic drugs to the clinic: Animal models of neuropathic pain. *British Journal of Pharmacology*, *171*(12), 2951–2963. https://doi.org/10.1111/bph.12645

Dubin, A. E., & Patapoutian, A. (2010). Nociceptors: The sensors of the pain pathway. *The Journal of Clinical Investigation*, *120*(11), 3760–3772. https://doi.org/10.1172/JCI42843

DuBreuil, D. M., Lopez Soto, E. J., Daste, S., Meir, R., Li, D., Wainger, B., Fleischmann, A., & Lipscombe, D. (2021). Heat But Not Mechanical Hypersensitivity Depends on Voltage-Gated CaV2.2 Calcium Channel Activity in Peripheral Axon Terminals Innervating Skin. *Journal of Neuroscience*, *41*(36), 7546–7560. https://doi.org/10.1523/JNEUROSCI.0195-21.2021

Dudek, J., Cheng, I.-F., Chowdhury, A., Wozny, K., Balleininger, M., Reinhold, R., Grunau, S., Callegari, S., Toischer, K., Wanders, R. J., Hasenfuß, G., Brügger, B., Guan, K., & Rehling, P. (2016). Cardiac-specific succinate dehydrogenase deficiency in Barth syndrome. *EMBO Molecular Medicine*, *8*(2), 139–154. https://doi.org/10.15252/emmm.201505644

Duggett, N. A., Griffiths, L. A., McKenna, O. E., Santis, V. de, Yongsanguanchai, N., Mokori, E. B., & Flatters, S. J. L. (2016). Oxidative stress in the development, maintenance and resolution of paclitaxel-induced painful neuropathy. *Neuroscience*, *333*, 13–26. https://doi.org/10.1016/j.neuroscience.2016.06.050

Dunham, N. W., & Miya, T. S. (1957). A note on a simple apparatus for detecting neurological deficit in rats and mice. *Journal of the American Pharmaceutical Association. American Pharmaceutical Association*, *46*(3), 208–209. https://doi.org/10.1002/jps.3030460322

Eccleston, C., Morlion, B., & Wells, C. (2018) (Vol. 1). Oxford University Press. https://doi.org/10.1093/med/9780198785750.003.0001

El Karim, I., McCrudden, M. T. C., Linden, G. J., Abdullah, H., Curtis, T. M., McGahon, M., About, I., Irwin, C., & Lundy, F. T. (2015). Tnf-α-induced p38MAPK activation regulates TRPA1 and TRPV4 activity in odontoblast-like cells. *The American Journal of Pathology*, *185*(11), 2994–3002. https://doi.org/10.1016/j.ajpath.2015.07.020

Fischer, H. K. (2019). *Functional Characterization of a Novel Mitochondrial Protein in the Context of Chronic Pain* [Master's Thesis]. Georg-August-University, Göttingen, Germany.

Fitzgerald, M. (2005). The development of nociceptive circuits. *Nature Reviews. Neuroscience*, *6*(7), 507–520. https://doi.org/10.1038/nrn1701

Flatters, S. J. L. (2015). *The contribution of mitochondria to sensory processing and pain* (Progress in Molecular Biology and Translational Science). Elsevier. *Progress in Molecular Biology and Translational Science*, *131*, pp. 119–146.

Flurkey, K., Currer, J. M., & Harrison, D. E. (2007). Mouse models in aging research. In J. G. Fox, S. Barthold, M. Davisson, C. Newcomer, F. Quimby, & A. Smith (Eds.), *American College of Laboratory Animal Medicine series. The mouse in biomedical research* (2nd ed.). Academic Press; Elsevier.

Friedrichsdorf, S. J., Giordano, J., Desai Dakoji, K., Warmuth, A., Daughtry, C., & Schulz, C. A. (2016). Chronic Pain in Children and Adolescents: Diagnosis and Treatment of Primary Pain Disorders in Head, Abdomen, Muscles and Joints. *Children (Basel, Switzerland)*, *3*(4). https://doi.org/10.3390/children3040042

Fu, Y., Rusznák, Z., Herculano-Houzel, S., Watson, C., & Paxinos, G. (2013). Cellular composition characterizing postnatal development and maturation of the mouse brain and spinal cord. *Brain Structure & Function*, *218*(5), 1337–1354. https://doi.org/10.1007/s00429-012-0462-x

Fuchs, P. N., Peng, Y. B., Boyette-Davis, J. A., & Uhelski, M. L. (2014). The anterior cingulate cortex and pain processing. *Frontiers in Integrative Neuroscience*, *8*, 35. https://doi.org/10.3389/fnint.2014.00035

Georgiou, P., Zanos, P., Mou, T.-C. M., An, X., Gerhard, D. M., Dryanovski, D. I., Potter, L. E., Highland, J. N., Jenne, C. E., Stewart, B. W., Pultorak, K. J., Yuan, P., Powels, C. F., Lovett, J., Pereira, E. F. R., Clark, S. M., Tonelli, L. H., Moaddel, R., Zarate, C. A., . . . Gould, T. D. (2022). Experimenters' sex modulates mouse behaviors and neural responses to ketamine via corticotropin releasing factor. *Nature Neuroscience*, *25*(9), 1191–1200. https://doi.org/10.1038/s41593-022-01146-x

Gereau (2014). A pain research agenda for the 21st century. *J. Pain*, *15*, 1203.

Gess, B., Röhr, D., Lange, E., Halfter, H., & Young, P. (2015). Desmoplakin is involved in organization of an adhesion complex in peripheral nerve regeneration after injury. *Experimental Neurology*, *264*, 55–66. https://doi.org/10.1016/j.expneurol.2014.12.005

Gilchrist, H. D., Allard, B. L., & Simone, D. A. (1996). Enhanced withdrawal responses to heat and mechanical stimuli following intraplantar injection of capsaicin in rats. *Pain*, *67*(1), 179–188. https://doi.org/10.1016/0304-3959(96)03104-1

Glare, P., Aubrey, K. R., & Myles, P. S. (2019). Transition from acute to chronic pain after surgery. *The Lancet*, *393*(10180), 1537–1546. https://doi.org/10.1016/S0140-6736(19)30352-6

Grace, P. M., Hutchinson, M. R., Maier, S. F., & Watkins, L. R. (2014). Pathological pain and the neuroimmune interface. *Nature Reviews Immunology*, *14*(4), 217–231. https://doi.org/10.1038/nri3621

Grace, P. M., Tawfik, V. L., Svensson, C. I., Burton, M. D., Loggia, M. L., & Hutchinson, M. R. (2021). The Neuroimmunology of Chronic Pain: From Rodents to Humans. *The Journal of Neuroscience : The Official Journal of the Society for Neuroscience*, *41*(5), 855–865. https://doi.org/10.1523/JNEUROSCI.1650-20.2020

Graven-Nielsen, T., & Arendt-Nielsen, L. (2002). Peripheral and central sensitization in musculoskeletal pain disorders: An experimental approach. *Current Rheumatology Reports*, *4*(4), 313–321. https://doi.org/10.1007/s11926-002-0040-y

Guan, Z., Hellman, J., & Schumacher, M. (2016). Contemporary views on inflammatory pain mechanisms: Trping over innate and microglial pathways. *F1000Research*, *5*, 2425. https://doi.org/10.12688/f1000research.8710.1

Guo, B., Sui, B., Wang, X.-Y., Wei, Y.-Y., Huang, J., Chen, J., Wu, S.-X., Li, Y.-Q., Wang, Y [Ya-yun], & Yang, Y [Yan-ling] (2013). Significant changes in mitochondrial distribution in different pain models of mice. *Mitochondrion*, *13*(4), 292–297. https://doi.org/10.1016/j.mito.2013.03.007

Hanack, C., Moroni, M., Lima, W. C., Wende, H., Kirchner, M., Adelfinger, L., Schrenk-Siemens, K., Tappe-Theodor, A., Wetzel, C., Kuich, P. H., Gassmann, M., Roggenkamp, D., Bettler, B., Lewin, G. R., Selbach, M., & Siemens, J. (2015). Gaba blocks pathological but not acute TRPV1 pain signals. *Cell*, *160*(4), 759–770. https://doi.org/10.1016/j.cell.2015.01.022

Harding, E. K., & Zamponi, G. W. (2022). Central and peripheral contributions of T-type calcium channels in pain. *Molecular Brain*, *15*(1), 39. https://doi.org/10.1186/s13041-022-00923-w

Heck, J., Palmeira Do Amaral, A. C., Weißbach, S., El Khallouqi, A., Bikbaev, A., & Heine, M. (2021). More than a pore: How voltage-gated calcium channels act on different levels of neuronal communication regulation. *Channels (Austin, Tex.)*, *15*(1), 322–338. https://doi.org/10.1080/19336950.2021.1900024

Holliday, K. L., Nicholl, B. I., Macfarlane, G. J., Thomson, W., Davies, K. A., & McBeth, J. (2010). Genetic variation in the hypothalamic-pituitary-adrenal stress axis influences susceptibility to musculoskeletal pain: Results from the EPIFUND study. *Annals of the Rheumatic Diseases*, *69*(3), 556–560. https://doi.org/10.1136/ard.2009.116137

Holzenberger, M., Lenzner, C., Leneuve, P., Zaoui, R., Hamard, G., Vaulont, S., & Bouc, Y. L. (2000). Cre-mediated germline mosaicism: A method allowing rapid generation of several alleles of a target gene. *Nucleic Acids Research*, *28*(21), E92. https://doi.org/10.1093/nar/28.21.e92

Husi, H., & Albalat, A. (2014). Proteomics. In *Handbook of Pharmacogenomics and Stratified Medicine* (pp. 147–179). Elsevier. https://doi.org/10.1016/B978-0-12-386882-4.00009-8
Hütte, M. (2019). *Exploring the Function of a Novel Chronic Pain Player.* https://doi.org/10.53846/goediss-7536
Hylands-White, N., Duarte, R. V., & Raphael, J. H. (2017). An overview of treatment approaches for chronic pain management. *Rheumatology International*, *37*(1), 29–42. https://doi.org/10.1007/s00296-016-3481-8
Jackson, S. J., Andrews, N., Ball, D., Bellantuono, I., Gray, J., Hachoumi, L., Holmes, A., Latcham, J., Petrie, A., Potter, P., Rice, A., Ritchie, A., Stewart, M., Strepka, C., Yeoman, M., & Chapman, K. (2017). Does age matter? The impact of rodent age on study outcomes. *Laboratory Animals*, *51*(2), 160–169. https://doi.org/10.1177/0023677216653984
Jassal, B., Matthews, L., Viteri, G., Gong, C., Lorente, P., Fabregat, A., Sidiropoulos, K., Cook, J., Gillespie, M., Haw, R., Loney, F., May, B., Milacic, M., Rothfels, K., Sevilla, C., Shamovsky, V., Shorser, S., Varusai, T., Weiser, J., . . . D'Eustachio, P. (2020). The reactome pathway knowledgebase. *Nucleic Acids Research*, *48*(D1), D498-D503. https://doi.org/10.1093/nar/gkz1031
Jeffry, J. A., Yu, S.-Q., Sikand, P., Parihar, A., Evans, M. S., & Premkumar, L. S. (2009). Selective targeting of TRPV1 expressing sensory nerve terminals in the spinal cord for long lasting analgesia. *PloS One*, *4*(9), e7021. https://doi.org/10.1371/journal.pone.0007021
Ji, R.-R., Chamessian, A., & Zhang, Y.-Q. (2016). Pain regulation by non-neuronal cells and inflammation. *Science*, *354*(6312), 572–577. https://doi.org/10.1126/science.aaf8924
Ji, R.-R., Xu, Z.-Z., & Gao, Y.-J. (2014). Emerging targets in neuroinflammation-driven chronic pain. *Nature Reviews. Drug Discovery*, *13*(7), 533–548. https://doi.org/10.1038/nrd4334
Jirkof, P., Cesarovic, N., Rettich, A., Fleischmann, T., & Arras, M. (2012). Individual housing of female mice: Influence on postsurgical behaviour and recovery. *Laboratory Animals*, *46*(4), 325–334. https://doi.org/10.1258/la.2012.012027
Kaneko, Y., & Szallasi, A. (2014). Transient receptor potential (TRP) channels: A clinical perspective. *British Journal of Pharmacology*, *171*(10), 2474–2507. https://doi.org/10.1111/bph.12414
Kiguchi, N [Norikazu], Kobayashi, Y [Yuka], Saika, F [Fumihiro], Sakaguchi, H., Maeda, T., & Kishioka, S [Shiroh] (2015). Peripheral interleukin-4 ameliorates inflammatory macrophage-dependent neuropathic pain. *Pain*, *156*(4), 684–693. https://doi.org/10.1097/j.pain.0000000000000097
Kincade, P. W. (1981). Formation of B lymphocytes in fetal and adult life. *Advances in Immunology*, *31*, 177–245. https://doi.org/10.1016/s0065-2776(08)60921-9
Koch, A., Zacharowski, K., Boehm, O., Stevens, M., Lipfert, P., Giesen, H.-J. von, Wolf, A., & Freynhagen, R. (2007). Nitric oxide and pro-inflammatory cytokines correlate with pain intensity in chronic pain patients. *Inflammation Research : Official Journal of the European Histamine Research Society … [Et Al.]*, *56*(1), 32–37. https://doi.org/10.1007/s00011-007-6088-4
Korwisi, B., Barke, A., Rief, W., Treede, R.-D., & Kleinstäuber, M. (2022). Chronic pain in the 11th Revision of the International Classification of Diseases : Users' questions answered. *Pain*, *163*(9), 1675–1687. https://doi.org/10.1097/j.pain.0000000000002551
Krames, E. S. (2014). The role of the dorsal root ganglion in the development of neuropathic pain. *Pain Medicine*, *15*(10), 1669–1685. https://doi.org/10.1111/pme.12413
Lakso, M., Pichel, J. G., Gorman, J. R., Sauer, B., Okamoto, Y., Lee, E., Alt, F. W., & Westphal, H. (1996). Efficient in vivo manipulation of mouse genomic sequences at

the zygote stage. *Proceedings of the National Academy of Sciences of the United States of America*, *93*(12), 5860–5865. https://doi.org/10.1073/pnas.93.12.5860

Latremoliere, A., & Woolf, C. J. (2009). Central sensitization: A generator of pain hypersensitivity by central neural plasticity. *The Journal of Pain*, *10*(9), 895–926. https://doi.org/10.1016/j.jpain.2009.06.012

Laumet, G., Ma, J., Robison, A. J., Kumari, S., Heijnen, C. J., & Kavelaars, A. (2019). T Cells as an Emerging Target for Chronic Pain Therapy. *Frontiers in Molecular Neuroscience*, *12*, 216. https://doi.org/10.3389/fnmol.2019.00216

Lee, H., Iida, T., Mizuno, A., Suzuki, M., & Caterina, M. J. (2005). Altered thermal selection behavior in mice lacking transient receptor potential vanilloid 4. *Journal of Neuroscience*, *25*(5), 1304–1310. https://doi.org/10.1523/JNEUROSCI.4745.04.2005

Lees, J. G., Duffy, S. S., & Moalem-Taylor, G. (2013). Immunotherapy targeting cytokines in neuropathic pain. *Frontiers in Pharmacology*, *4*, 142. https://doi.org/10.3389/fphar.2013.00142

Lekholm, E., Perland, E., Eriksson, M. M., Hellsten, S. V., Lindberg, F. A., Rostami, J., & Fredriksson, R. (2017). Putative Membrane-Bound Transporters MFSD14A and MFSD14B Are Neuronal and Affected by Nutrient Availability. *Frontiers in Molecular Neuroscience*, *10*, 11. https://doi.org/10.3389/fnmol.2017.00011

Li, J., Ma, J., Lacagnina, M. J., Lorca, S., Odem, M. A., Walters, E. T., Kavelaars, A., & Grace, P. M. (2020). Oral Dimethyl Fumarate Reduces Peripheral Neuropathic Pain in Rodents via NFE2L2 Antioxidant Signaling. *Anesthesiology*, *132*(2), 343–356. https://doi.org/10.1097/ALN.0000000000003077

Li, R., Jia, Z., & Trush, M. A. (2016). Defining ROS in Biology and Medicine. *Reactive Oxygen Species (Apex, N.C.)*, *1*(1), 9–21. https://doi.org/10.20455/ros.2016.803

Liang, Z., Hore, Z., Harley, P., Uchenna Stanley, F., Michrowska, A., Dahiya, M., La Russa, F., Jager, S. E., Villa-Hernandez, S., & Denk, F. (2020). A transcriptional toolbox for exploring peripheral neuroimmune interactions. *Pain*, *161*(9), 2089–2106. https://doi.org/10.1097/j.pain.0000000000001914

Lindborg, J. A., Niemi, J. P., Howarth, M. A., Liu, K. W., Moore, C. Z., Mahajan, D., & Zigmond, R. E. (2018). Molecular and cellular identification of the immune response in peripheral ganglia following nerve injury. *Journal of Neuroinflammation*, *15*(1), 192. https://doi.org/10.1186/s12974-018-1222-5

Liu, X [Xiaojuan], Tonello, R., Ling, Y., Gao, Y.-J., & Berta, T. (2019). Paclitaxel-activated astrocytes produce mechanical allodynia in mice by releasing tumor necrosis factor-α and stromal-derived cell factor 1. *Journal of Neuroinflammation*, *16*(1), 209. https://doi.org/10.1186/s12974-019-1619-9

Lopes, D. M., Denk, F., & McMahon, S. B. (2017). The Molecular Fingerprint of Dorsal Root and Trigeminal Ganglion Neurons. *Frontiers in Molecular Neuroscience*, *10*, 304. https://doi.org/10.3389/fnmol.2017.00304

Lopes, D. M., Malek, N., Edye, M., Jager, S. B., McMurray, S., McMahon, S. B., & Denk, F. (2017). Sex differences in peripheral not central immune responses to pain-inducing injury. *Scientific Reports*, *7*(1), 16460. https://doi.org/10.1038/s41598-017-16664-z

Lucey, B. P., Nelson-Rees, W. A., & Hutchins, G. M. (2009). Henrietta Lacks, HeLa cells, and cell culture contamination. *Archives of Pathology & Laboratory Medicine*, *133*(9), 1463–1467. https://doi.org/10.5858/133.9.1463

Luchting, B., Hinske, L. C. G., Rachinger-Adam, B., Celi, L. A., Kreth, S., & Azad, S. C. (2017). Soluble intercellular adhesion molecule-1: A potential biomarker for pain intensity in chronic pain patients. *Biomarkers in Medicine*, *11*(3), 265–276. https://doi.org/10.2217/bmm-2016-0246

Lumpkin, E. A., & Caterina, M. J. (2007). Mechanisms of sensory transduction in the skin. *Nature*, *445*(7130), 858–865. https://doi.org/10.1038/nature05662

Luo, L [Lei], Wang, Y [Yunfei], Li, B., Xu, L., Kamau, P. M., Zheng, J., Yang, F., Yang, S., & Lai, R. (2019). Molecular basis for heat desensitization of TRPV1 ion channels. *Nature Communications*, *10*(1), 2134. https://doi.org/10.1038/s41467-019-09965-6

Luo, X., Chen, O., Wang, Z., Bang, S., Ji, J., Lee, S. H., Huh, Y., Furutani, K., He, Q., Tao, X., Ko, M.-C., Bortsov, A., Donnelly, C. R., Chen, Y., Nackley, A., Berta, T., & Ji, R.-R. (2021). Il-23/IL-17A/TRPV1 axis produces mechanical pain via macrophage-sensory neuron crosstalk in female mice. *Neuron*, *109*(17), 2691-2706.e5. https://doi.org/10.1016/j.neuron.2021.06.015

Manzoni, C., Kia, D. A., Vandrovcova, J., Hardy, J., Wood, N. W., Lewis, P. A., & Ferrari, R. (2018). Genome, transcriptome and proteome: The rise of omics data and their integration in biomedical sciences. *Briefings in Bioinformatics*, *19*(2), 286–302. https://doi.org/10.1093/bib/bbw114

Mapplebeck, J. C. S., Beggs, S., & Salter, M. W. (2016). Sex differences in pain: A tale of two immune cells. *Pain*, *157 Suppl 1*(Supplement 1), S2-S6. https://doi.org/10.1097/j.pain.0000000000000389

Mapplebeck, J. C. S., Dalgarno, R., Tu, Y., Moriarty, O., Beggs, S., Kwok, C. H. T., Halievski, K., Assi, S., Mogil, J. S., Trang, T., & Salter, M. W. (2018). Microglial P2X4R-evoked pain hypersensitivity is sexually dimorphic in rats. *Pain*, *159*(9), 1752–1763. https://doi.org/10.1097/j.pain.0000000000001265

Marx, S., Dal Maso, T., Chen, J.-W., Bury, M., Wouters, J., Michiels, C., & Le Calvé, B. (2020). Transmembrane (TMEM) protein family members: Poorly characterized even if essential for the metastatic process. *Seminars in Cancer Biology*, *60*, 96–106. https://doi.org/10.1016/j.semcancer.2019.08.018

Mathie, A. (2010). Ion channels as novel therapeutic targets in the treatment of pain. *The Journal of Pharmacy and Pharmacology*, *62*(9), 1089–1095. https://doi.org/10.1111/j.2042-7158.2010.01131.x

Mavlyutov, T. A., Epstein, M. L., Liu, P [P.], Verbny, Y. I., Ziskind-Conhaim, L., & Ruoho, A. E. (2012). Development of the sigma-1 receptor in C-terminals of motoneurons and colocalization with the N,N'-dimethyltryptamine forming enzyme, indole-N-methyl transferase. *Neuroscience*, *206*, 60–68. https://doi.org/10.1016/j.neuroscience.2011.12.040

McArdel, S. L., Terhorst, C., & Sharpe, A. H. (2016). Roles of CD48 in regulating immunity and tolerance. *Clinical Immunology (Orlando, Fla.)*, *164*, 10–20. https://doi.org/10.1016/j.clim.2016.01.008

McCarson, K. E., & Fehrenbacher, J. C. (2021). Models of Inflammation: Carrageenan- or Complete Freund's Adjuvant (CFA)-Induced Edema and Hypersensitivity in the Rat. *Current Protocols*, *1*(7), e202. https://doi.org/10.1002/cpz1.202

Melber, A., & Haynes, C. M. (2018). Uprmt regulation and output: A stress response mediated by mitochondrial-nuclear communication. *Cell Research*, *28*(3), 281–295. https://doi.org/10.1038/cr.2018.16

Meng, J., Wang, J [Jiafu], Steinhoff, M., & Dolly, J. O. (2016). Tnfα induces co-trafficking of TRPV1/TRPA1 in VAMP1-containing vesicles to the plasmalemma via Munc18-1/syntaxin1/SNAP-25 mediated fusion. *Scientific Reports*, *6*(1), 21226. https://doi.org/10.1038/srep21226

Michel, N. (2020). *Touch comes of Age - Maturational Plasticity in Somatosensory Mechanosensation.* https://doi.org/10.53846/goediss-8140

Michel, N., Narayanan, P., Shomroni, O., & Schmidt, M. (2020). Maturational Changes in Mouse Cutaneous Touch and Piezo2-Mediated Mechanotransduction. *Cell Reports*, *32*(3), 107912. https://doi.org/10.1016/j.celrep.2020.107912

Millecamps, M., Sotocinal, S. G., Austin, J.-S., Stone, L. S., & Mogil, J. S. (2022). Sex-specific effects of neuropathic pain on long-term pain behavior and mortality in mice. *Pain.* Advance online publication. https://doi.org/10.1097/j.pain.0000000000002742

Mogil (2020). The measurement of pain in the laboratory rodent, 27.
Mogil, J. S. (2009). Animal models of pain: Progress and challenges. *Nature Reviews Neuroscience*, *10*(4), 283–294. https://doi.org/10.1038/nrn2606
Mogil, J. S. (2012). Sex differences in pain and pain inhibition: Multiple explanations of a controversial phenomenon. *Nature Reviews Neuroscience*, *13*(12), 859–866. https://doi.org/10.1038/nrn3360
Moraes, E. R. de, Kushmerick, C., & Naves, L. A. (2017). Morphological and functional diversity of first-order somatosensory neurons. *Biophysical Reviews*, *9*(5), 847–856. https://doi.org/10.1007/s12551-017-0321-3
Münch, C. (2018). The different axes of the mammalian mitochondrial unfolded protein response. *BMC Biology*, *16*(1), 81. https://doi.org/10.1186/s12915-018-0548-x
Murphy, E., Ardehali, H., Balaban, R. S., DiLisa, F., Dorn, G. W., Kitsis, R. N., Otsu, K., Ping, P., Rizzuto, R., Sack, M. N., Wallace, D., & Youle, R. J. (2016). Mitochondrial Function, Biology, and Role in Disease: A Scientific Statement From the American Heart Association. *Circulation Research*, *118*(12), 1960–1991. https://doi.org/10.1161/RES.0000000000000104
Murphy, K., & Weaver, C. (2018). *Janeway Immunologie* ((L. Seidler, Trans.)) (9. Aufl. 2018). Springer Berlin Heidelberg. http://nbn-resolving.org/urn:nbn:de:bsz:31-epflicht-1584460
Nicholls, D. G., & Budd, S. L. (2000). Mitochondria and neuronal survival. *Physiological Reviews*, *80*(1), 315–360. https://doi.org/10.1152/physrev.2000.80.1.315
Niehaus, J. K., Taylor-Blake, B., Loo, L., Simon, J. M., & Zylka, M. J. (2021). Spinal macrophages resolve nociceptive hypersensitivity after peripheral injury. *Neuron*, *109*(8), 1274-1282.e6. https://doi.org/10.1016/j.neuron.2021.02.018
O'Donnell, F. T., & Rosen, K. R. (2014). Pediatric Pain Management: A Review. *Missouri Medicine*, *111*(3), 231–237.
Oliveros, J. C. (2007-2015). *Venny. An interactive tool for comparing lists with Venn's diagrams.* https://bioinfogp.cnb.csic.es/tools/venny/index.html
Ono, K., Xu, S., Hitomi, S., & Inenaga, K. (2012). Comparison of the electrophysiological and immunohistochemical properties of acutely dissociated and 1-day cultured rat trigeminal ganglion neurons. *Neuroscience Letters*, *523*(2), 162–166. https://doi.org/10.1016/j.neulet.2012.06.069
Paldy, E., Simonetti, M., Worzfeld, T., Bali, K. K [Kiran Kumar], Vicuña, L., Offermanns, S., & Kuner, R. (2017). Semaphorin 4C Plexin-B2 signaling in peripheral sensory neurons is pronociceptive in a model of inflammatory pain. *Nature Communications*, *8*(1), 176. https://doi.org/10.1038/s41467-017-00341-w
Pancekauskaitė, G., & Jankauskaitė, L. (2018). Paediatric Pain Medicine: Pain Differences, Recognition and Coping Acute Procedural Pain in Paediatric Emergency Room. *Medicina (Kaunas, Lithuania)*, *54*(6). https://doi.org/10.3390/medicina54060094
Parisien, M., Lima, L. V., Dagostino, C., El-Hachem, N., Drury, G. L., Grant, A. V., Huising, J., Verma, V., Meloto, C. B., Silva, J. R., Dutra, G. G. S., Markova, T., Dang, H., Tessier, P. A., Slade, G. D., Nackley, A. G., Ghasemlou, N., Mogil, J. S., Allegri, M., & Diatchenko, L. (2022). Acute inflammatory response via neutrophil activation protects against the development of chronic pain. *Science Translational Medicine*, *14*(644), eabj9954. https://doi.org/10.1126/scitranslmed.abj9954
Patapoutian, A., Tate, S., & Woolf, C. J. (2009). Transient receptor potential channels: Targeting pain at the source. *Nature Reviews Drug Discovery*, *8*(1), 55–68. https://doi.org/10.1038/nrd2757
Peng, J., Gu, N., Zhou, L., B Eyo, U., Murugan, M., Gan, W.-B., & Wu, L.-J. (2016). Microglia and monocytes synergistically promote the transition from acute to chronic pain after nerve injury. *Nature Communications*, *7*(1), 12029. https://doi.org/10.1038/ncomms12029

Pitake, S., Middleton, L. J., Abdus-Saboor, I., & Mishra, S. K. (2019). Inflammation Induced Sensory Nerve Growth and Pain Hypersensitivity Requires the N-Type Calcium Channel Cav2.2. *Frontiers in Neuroscience*, *13*, 1009. https://doi.org/10.3389/fnins.2019.01009

Pitzer, C., Kuner, R., & Tappe-Theodor, A. (2016). Voluntary and evoked behavioral correlates in inflammatory pain conditions under different social housing conditions. *PAIN Reports*, *1*(1), e564. https://doi.org/10.1097/PR9.0000000000000564

Pogatzki, E. M., & Raja, S. N. (2003). A mouse model of incisional pain. *Anesthesiology*, *99*(4), 1023–1027. https://doi.org/10.1097/00000542-200310000-00041

Pogatzki-Zahn, E. M., Gomez-Varela, D., Erdmann, G., Kaschube, K., Segelcke, D., & Schmidt, M. (2021). A proteome signature for acute incisional pain in dorsal root ganglia of mice. *Pain*, *162*(7), 2070–2086. https://doi.org/10.1097/j.pain.0000000000002207

Price, T. J., Basbaum, A. I., Bresnahan, J., Chambers, J. F., Koninck, Y. de, Edwards, R. R., Ji, R.-R., Katz, J., Kavelaars, A., Levine, J. D., Porter, L., Schechter, N., Sluka, K. A., Terman, G. W., Wager, T. D., Yaksh, T. L., & Dworkin, R. H. (2018). Transition to chronic pain: Opportunities for novel therapeutics. *Nature Reviews Neuroscience*, *19*(7), 383–384. https://doi.org/10.1038/s41583-018-0012-5

Price, T. J., & Gold, M. S. (2018). From Mechanism to Cure: Renewing the Goal to Eliminate the Disease of Pain. *Pain Medicine*, *19*(8), 1525–1549. https://doi.org/10.1093/pm/pnx108

Purves, D. (Ed.). (2008). *Neuroscience* (4. ed.). Sinauer Assoc.

Purves, D., Augustine, G. J., Fitzpatrick, D., Katz, L. C., LaMantia, A.-S., McNamara, J. O., & Williams, S. M. (Eds.). (2001). *Neuroscience. 2nd edition*. Sinauer Associates.

Raja, S. N., Carr, D. B., Cohen, M., Finnerup, N. B., Flor, H., Gibson, S., Keefe, F. J., Mogil, J. S., Ringkamp, M., Sluka, K. A., Song, X.-J., Stevens, B., Sullivan, M. D., Tutelman, P. R., Ushida, T., & Vader, K. (2020). The revised International Association for the Study of Pain definition of pain: Concepts, challenges, and compromises. *Pain*, *161*(9), 1976–1982. https://doi.org/10.1097/j.pain.0000000000001939

Ren, K., & Dubner, R. (2010). Interactions between the immune and nervous systems in pain. *Nature Medicine*, *16*(11), 1267–1276. https://doi.org/10.1038/nm.2234

Richardson, C. A., & Flecknell, P. A. (2005). Anaesthesia and post-operative analgesia following experimental surgery in laboratory rodents: Are we making progress? *Alternatives to Laboratory Animals : ATLA*, *33*(2), 119–127. https://doi.org/10.1177/026119290503300207

Roomruangwong, C., Sirivichayakul, S., Matsumoto, A. K., Michelin, A. P., Oliveira Semeão, L. de, Lima Pedrão, J. V. de, Barbosa, D. S., Moreira, E. G., & Maes, M. (2021). Menstruation distress is strongly associated with hormone-immune-metabolic biomarkers. *Journal of Psychosomatic Research*, *142*, 110355. https://doi.org/10.1016/j.jpsychores.2020.110355

Rosen, S., Ham, B., & Mogil, J. S. (2017). Sex differences in neuroimmunity and pain. *Journal of Neuroscience Research*, *95*(1-2), 500–508. https://doi.org/10.1002/jnr.23831

Rouwette, T., Sondermann, J., Avenali, L., Gomez-Varela, D., & Schmidt, M. (2016). Standardized Profiling of The Membrane-Enriched Proteome of Mouse Dorsal Root Ganglia (DRG) Provides Novel Insights Into Chronic Pain. *Molecular & Cellular Proteomics : MCP*, *15*(6), 2152–2168. https://doi.org/10.1074/mcp.M116.058966

Saastamoinen, P., Laaksonen, M., Kääriä, S.-M., Lallukka, T., Leino-Arjas, P., Rahkonen, O., & Lahelma, E. (2012). Pain and disability retirement: A prospective cohort study. *Pain*, *153*(3), 526–531. https://doi.org/10.1016/j.pain.2011.11.005

Saika, F [F.], Kiguchi, N [N.], Kobayashi, Y [Y.], Fukazawa, Y., & Kishioka, S [S.] (2012). Cc-chemokine ligand 4/macrophage inflammatory protein-1β participates in the induction of neuropathic pain after peripheral nerve injury. *European Journal of Pain (London, England)*, *16*(9), 1271–1280. https://doi.org/10.1002/j.1532-2149.2012.00146.x

Sánchez-Barrena, M. J., Vallis, Y., Clatworthy, M. R., Doherty, G. J., Veprintsev, D. B., Evans, P. R., & McMahon, H. T. (2013). Correction: Bin2 Is a Membrane Sculpting N-BAR Protein That Influences Leucocyte Podosomes, Motility and Phagocytosis. *PloS One*, *8*(8). https://doi.org/10.1371/annotation/3bdc487b-5e25-4cd7-a354-b2952eec943d

Santana-Varela, S., Bogdanov, Y. D., Gossage, S. J., Okorokov, A. L., Li, S., Clauser, L. de, Alves-Simoes, M., Sexton, J. E., Iseppon, F., Luiz, A. P., Zhao, J., Wood, J. N., & Cox, J. J. (2021). Tools for analysis and conditional deletion of subsets of sensory neurons. *Wellcome Open Research*, *6.* https://doi.org/10.12688/wellcomeopenres.17090.1

Sanz-Salvador, L., Andrés-Borderia, A., Ferrer-Montiel, A., & Planells-Cases, R. (2012). Agonist- and Ca2+-dependent desensitization of TRPV1 channel targets the receptor to lysosomes for degradation. *The Journal of Biological Chemistry*, *287*(23), 19462–19471. https://doi.org/10.1074/jbc.M111.289751

Schindelin, J., Arganda-Carreras, I., Frise, E., Kaynig, V., Longair, M., Pietzsch, T., Preibisch, S., Rueden, C., Saalfeld, S., Schmid, B., Tinevez, J.-Y., White, D. J., Hartenstein, V., Eliceiri, K., Tomancak, P., & Cardona, A. (2012). Fiji: An open-source platform for biological-image analysis. *Nature Methods*, *9*(7), 676–682. https://doi.org/10.1038/nmeth.2019

Schmit, K., & Michiels, C. (2018). Tmem Proteins in Cancer: A Review. *Frontiers in Pharmacology*, *9*, 1345. https://doi.org/10.3389/fphar.2018.01345

Schor, I. E., Rascovan, N., Pelisch, F., Alló, M., & Kornblihtt, A. R. (2009). Neuronal cell depolarization induces intragenic chromatin modifications affecting NCAM alternative splicing. *Proceedings of the National Academy of Sciences*, *106*(11), 4325–4330. https://doi.org/10.1073/pnas.0810666106

Segelcke, D., Fischer, H. K., Hütte, M., Dennerlein, S., Benseler, F., Brose, N., Pogatzki-Zahn, E. M., & Schmidt, M. (2021). Tmem160 contributes to the establishment of discrete nerve injury-induced pain behaviors in male mice. *Cell Reports*, *37*(12), 110152. https://doi.org/10.1016/j.celrep.2021.110152

Segelcke, D., Pradier, B., Reichl, S., Schäfer, L. C., & Pogatzki-Zahn, E. M. (2021). Investigating the Role of Ly6G+ Neutrophils in Incisional and Inflammatory Pain by Multidimensional Pain-Related Behavioral Assessments: Bridging the Translational Gap. *Frontiers in Pain Research*, *2*, 735838. https://doi.org/10.3389/fpain.2021.735838

Selek, Ş., ALP, R., Alp, S. I., & TAŞKIN, A. (2011). Relationship between PON1 phenotype and headache duration in migraine patients. *Turkish Journal of Medical Sciences.* Advance online publication. https://doi.org/10.3906/sag-1002-636

Sewards, T. V., & Sewards, M. A. (2002). The medial pain system: Neural representations of the motivational aspect of pain. *Brain Research Bulletin*, *59*(3), 163–180. https://doi.org/10.1016/S0361-9230(02)00864-X

Shilpi, J. A., & Uddin, S. J. (2020). Analgesic and antipyretic natural products. In *Annual Reports in Medicinal Chemistry. Medicinal Natural Products: A Disease-Focused Approach* (Vol. 55, pp. 435–458). Elsevier. https://doi.org/10.1016/bs.armc.2020.03.003

Snezhkina, A. V., Kudryavtseva, A. V., Kardymon, O. L., Savvateeva, M. V., Melnikova, N. V., Krasnov, G. S., & Dmitriev, A. A. (2019). Ros Generation and Antioxidant Defense Systems in Normal and Malignant Cells. *Oxidative Medicine and Cellular Longevity*, *2019*, 6175804. https://doi.org/10.1155/2019/6175804

Solinski, H. J., & Hoon, M. A. (2019). Cells and circuits for thermosensation in mammals. *Neuroscience Letters*, *690*, 167–170. https://doi.org/10.1016/j.neulet.2018.10.026

Somatosensory system - Latest research and news | Nature. (2022, November 22). https://www.nature.com/subjects/somatosensory-system

Sommer, C., Leinders, M., & Üçeyler, N. (2018). Inflammation in the pathophysiology of neuropathic pain. *Pain*, *159*(3), 595–602. https://doi.org/10.1097/j.pain.0000000000001122

Sondermann, J. R [Julia R.], Barry, A. M., Jahn, O., Michel, N., Abdelaziz, R., Kügler, S., Gomez-Varela, D., & Schmidt, M. (2019). Vti1b promotes TRPV1 sensitization during inflammatory pain. *Pain*, *160*(2), 508–527. https://doi.org/10.1097/j.pain.0000000000001418

Sorge, R. E., LaCroix-Fralish, M. L., Tuttle, A. H., Sotocinal, S. G., Austin, J.-S., Ritchie, J., Chanda, M. L., Graham, A. C., Topham, L., Beggs, S., Salter, M. W., & Mogil, J. S. (2011). Spinal cord Toll-like receptor 4 mediates inflammatory and neuropathic hypersensitivity in male but not female mice. *Journal of Neuroscience*, *31*(43), 15450–15454. https://doi.org/10.1523/JNEUROSCI.3859-11.2011

Sorge, R. E., Mapplebeck, J. C. S., Rosen, S., Beggs, S., Taves, S., Alexander, J. K., Martin, L. J., Austin, J.-S., Sotocinal, S. G., Di Chen, Yang, M., Shi, X. Q., Huang, H., Pillon, N. J., Bilan, P. J., Tu, Y., Klip, A., Ji, R.-R., Zhang, J., . . . Mogil, J. S. (2015). Different immune cells mediate mechanical pain hypersensitivity in male and female mice. *Nature Neuroscience*, *18*(8), 1081–1083. https://doi.org/10.1038/nn.4053

Sorge, R. E., Martin, L. J., Isbester, K. A., Sotocinal, S. G., Rosen, S., Tuttle, A. H., Wieskopf, J. S., Acland, E. L., Dokova, A., Kadoura, B., Leger, P., Mapplebeck, J. C. S., McPhail, M., Delaney, A., Wigerblad, G., Schumann, A. P., Quinn, T., Frasnelli, J., Svensson, C. I., . . . Mogil, J. S. (2014). Olfactory exposure to males, including men, causes stress and related analgesia in rodents. *Nature Methods*, *11*(6), 629–632. https://doi.org/10.1038/nmeth.2935

Stein, C., Millan, M. J., & Herz, A. (1988). Unilateral inflammation of the hindpaw in rats as a model of prolonged noxious stimulation: Alterations in behavior and nociceptive thresholds. *Pharmacology Biochemistry and Behavior*, *31*(2), 445–451. https://doi.org/10.1016/0091-3057(88)90372-3

Storey, J. D. (2002). A direct approach to false discovery rates. *Journal of the Royal Statistical Society: Series B (Statistical Methodology)*, *64*(3), 479–498. https://doi.org/10.1111/1467-9868.00346

Sui, B., Xu, T., Liu, J., Wei, W., Zheng, C., Guo, B., Wang, Y [Ya-yun], & Yang, Y [Yan-ling] (2013). Understanding the role of mitochondria in the pathogenesis of chronic pain. *Postgraduate Medical Journal*, *89*(1058), 709–714. https://doi.org/10.1136/postgradmedj-2012-131068

Szklarczyk, D., Gable, A. L., Nastou, K. C., Lyon, D., Kirsch, R., Pyysalo, S., Doncheva, N. T., Legeay, M., Fang, T., Bork, P., Jensen, L. J., & Mering, C. von (2021). The STRING database in 2021: Customizable protein-protein networks, and functional characterization of user-uploaded gene/measurement sets. *Nucleic Acids Research*, *49*(D1), D605-D612. https://doi.org/10.1093/nar/gkaa1074

Tajerian, M., Alvarado, S., Millecamps, M., Dashwood, T., Anderson, K. M., Haglund, L., Ouellet, J., Szyf, M., & Stone, L. S. (2011). Dna methylation of SPARC and chronic low back pain. *Molecular Pain*, *7*, 65. https://doi.org/10.1186/1744-8069-7-65

Tansley, S., Uttam, S., Ureña Guzmán, A., Yaqubi, M., Pacis, A., Parisien, M., Deamond, H., Wong, C., Rabau, O., Brown, N., Haglund, L., Ouellet, J., Santaguida, C., Ribeiro-da-Silva, A., Tahmasebi, S., Prager-Khoutorsky, M., Ragoussis, J., Zhang, J., Salter, M. W., . . . Khoutorsky, A. (2022). Single-cell RNA sequencing reveals time- and sex-specific responses of mouse spinal cord microglia to peripheral nerve injury and links ApoE to chronic pain. *Nature Communications*, *13*(1), 843. https://doi.org/10.1038/s41467-022-28473-8

Thakur, M., Crow, M., Richards, N., Davey, G. I. J., Levine, E., Kelleher, J. H., Agley, C. C., Denk, F., Harridge, S. D. R., & McMahon, S. B. (2014). Defining the nociceptor transcriptome. *Frontiers in Molecular Neuroscience*, *7*, 87. https://doi.org/10.3389/fnmol.2014.00087

Tominaga, M., & Caterina, M. J. (2004). Thermosensation and pain. *Journal of Neurobiology*, *61*(1), 3–12. https://doi.org/10.1002/neu.20079

Touska, F [Filip], Marsakova, L., Teisinger, J., & Vlachova, V. (2011). A "cute" desensitization of TRPV1. *Current Pharmaceutical Biotechnology*, *12*(1), 122–129. https://doi.org/10.2174/138920111793937826

Treede, R.-D. (2018). The International Association for the Study of Pain definition of pain: As valid in 2018 as in 1979, but in need of regularly updated footnotes. *PAIN Reports*, *3*(2), e643. https://doi.org/10.1097/PR9.0000000000000643.

Treede, R.-D., Rief, W., Barke, A., Aziz, Q., Bennett, M. I., Benoliel, R., Cohen, M., Evers, S., Finnerup, N. B., First, M. B., Giamberardino, M. A., Kaasa, S., Korwisi, B., Kosek, E., Lavand'homme, P., Nicholas, M., Perrot, S., Scholz, J., Schug, S., . . . Wang, S.-J. (2019). Chronic pain as a symptom or a disease: The IASP Classification of Chronic Pain for the International Classification of Diseases (ICD-11). *Pain*, *160*(1), 19–27. https://doi.org/10.1097/j.pain.0000000000001384

Trifonov, S., Houtani, T., Hamada, S., Kase, M., Maruyama, M., & Sugimoto, T. (2009). In situ hybridization study of the distribution of choline acetyltransferase mRNA and its splice variants in the mouse brain and spinal cord. *Neuroscience*, *159*(1), 344–357. https://doi.org/10.1016/j.neuroscience.2008.12.054

Tsagareli, M. G. (2020). Chapter 3 Thermo-TRP Channels in Pain Sensation: An Overview. In *Modern Advances in Pharmaceutical Research.* https://www.researchgate.net/publication/339017655_Chapter_3_Thermo-TRP_Channels_in_Pain_Sensation_An_Overview

Turner, P. V., Pang, D. S., & Lofgren, J. L. (2019). A Review of Pain Assessment Methods in Laboratory Rodents. *Comparative Medicine*, *69*(6), 451–467. https://doi.org/10.30802/AALAS-CM-19-000042

Twyman, R. M. (2012). Proteomics. In *Encyclopedia of Applied Ethics* (pp. 642–649). Elsevier. https://doi.org/10.1016/B978-0-12-373932-2.00047-8

Tycko, J., Wainberg, M., Marinov, G. K., Ursu, O., Hess, G. T., Ego, B. K., Aradhana, Li, A., Truong, A., Trevino, A. E., Spees, K., Yao, D., Kaplow, I. M., Greenside, P. G., Morgens, D. W., Phanstiel, D. H., Snyder, M. P., Bintu, L., Greenleaf, W. J., . . . Bassik, M. C. (2019). Mitigation of off-target toxicity in CRISPR-Cas9 screens for essential non-coding elements. *Nature Communications*, *10*(1), 4063. https://doi.org/10.1038/s41467-019-11955-7

Usoskin, D., Furlan, A., Islam, S., Abdo, H., Lönnerberg, P., Lou, D., Hjerling-Leffler, J., Haeggström, J., Kharchenko, O., Kharchenko, P. V., Linnarsson, S., & Ernfors, P. (2015). Unbiased classification of sensory neuron types by large-scale single-cell RNA sequencing. *Nature Neuroscience*, *18*(1), 145–153. https://doi.org/10.1038/nn.3881

van den Ameele, J., Fuge, J., Pitceathly, R. D. S., Berry, S., McIntyre, Z., Hanna, M. G., Lee, M., & Chinnery, P. F. (2020). Chronic pain is common in mitochondrial disease. *Neuromuscular Disorders : NMD*, *30*(5), 413–419. https://doi.org/10.1016/j.nmd.2020.02.017

Vandewauw, I., Clercq, K. de, Mulier, M., Held, K., Pinto, S., van Ranst, N., Segal, A., Voet, T., Vennekens, R., Zimmermann, K., Vriens, J., & Voets, T. (2018). A TRP channel trio mediates acute noxious heat sensing. *Nature*, *555*(7698), 662–666. https://doi.org/10.1038/nature26137

Vardeh, D., & Naranjo, J. F. (2017). Peripheral and Central Sensitization. In R. J. Yong, M. Nguyen, E. Nelson, & R. D. Urman (Eds.), *Pain Medicine* (pp. 15–17). Springer International Publishing. https://doi.org/10.1007/978-3-319-43133-8_4

Vasconcelos, M., Hollis, K., Nowbahari, E., & Kacelnik, A. (2012). Pro-sociality without empathy. *Biology Letters*, *8*(6), 910–912. https://doi.org/10.1098/rsbl.2012.0554

Vaso, A., Adahan, H.-M., Gjika, A., Zahaj, S., Zhurda, T., Vyshka, G., & Devor, M. (2014). Peripheral nervous system origin of phantom limb pain. *Pain*, *155*(7), 1384–1391. https://doi.org/10.1016/j.pain.2014.04.018

Vicuña, L., Strochlic, D. E., Latremoliere, A., Bali, K. K [Kiran Kumar], Simonetti, M., Husainie, D., Prokosch, S., Riva, P., Griffin, R. S., Njoo, C., Gehrig, S., Mall, M. A., Arnold, B., Devor, M., Woolf, C. J., Liberles, S. D., Costigan, M., & Kuner, R. (2015). The serine protease inhibitor SerpinA3N attenuates neuropathic pain by inhibiting T cell-derived leukocyte elastase. *Nature Medicine*, *21*(5), 518–523. https://doi.org/10.1038/nm.3852

Vierck, C. J., Whitsel, B. L., Favorov, O. V., Brown, A. W., & Tommerdahl, M. (2013). Role of primary somatosensory cortex in the coding of pain. *Pain*, *154*(3), 334–344. https://doi.org/10.1016/j.pain.2012.10.021

Vogt, B. A. (2005). Pain and emotion interactions in subregions of the cingulate gyrus. *Nature Reviews. Neuroscience*, *6*(7), 533–544. https://doi.org/10.1038/nrn1704

Vowles, K. E., McEntee, M. L., Julnes, P. S., Frohe, T., Ney, J. P., & van der Goes, D. N. (2015). Rates of opioid misuse, abuse, and addiction in chronic pain: A systematic review and data synthesis. *Pain*, *156*(4), 569–576. https://doi.org/10.1097/01.j.pain.0000460357.01998.f1

Vriens, J., Nilius, B., & Voets, T. (2014). Peripheral thermosensation in mammals. *Nature Reviews Neuroscience*, *15*(9), 573–589. https://doi.org/10.1038/nrn3784

Vyklický, L., Nováková-Tousová, K., Benedikt, J., Samad, A., Touska, F [F.], & Vlachová, V. (2008). Calcium-dependent desensitization of vanilloid receptor TRPV1: A mechanism possibly involved in analgesia induced by topical application of capsaicin. *Physiological Research*, *57 Suppl 3*, S59-S68. https://doi.org/10.33549/physiolres.931478

Wang, H., Yang, H., Shivalila, C. S., Dawlaty, M. M., Cheng, A. W., Zhang, F., & Jaenisch, R. (2013). One-step generation of mice carrying mutations in multiple genes by CRISPR/Cas-mediated genome engineering. *Cell*, *153*(4), 910–918. https://doi.org/10.1016/j.cell.2013.04.025

Wangzhou, A., McIlvried, L. A., Paige, C., Barragan-Iglesias, P., Shiers, S., Ahmad, A., Guzman, C. A., Dussor, G., Ray, P. R., Gereau, R. W., & Price, T. J. (2020). Pharmacological target-focused transcriptomic analysis of native vs cultured human and mouse dorsal root ganglia. *Pain*, *161*(7), 1497–1517. https://doi.org/10.1097/j.pain.0000000000001866

Wangzhou, A., Paige, C., Neerukonda, S. V., Naik, D. K., Kume, M., David, E. T., Dussor, G., Ray, P. R., & Price, T. J. (2021). A ligand-receptor interactome platform for discovery of pain mechanisms and therapeutic targets. *Science Signaling*, *14*(674). https://doi.org/10.1126/scisignal.abe1648

Webster, C. I., Hatcher, J., Burrell, M., Thom, G., Thornton, P., Gurrell, I., & Chessell, I. (2017). Enhanced delivery of IL-1 receptor antagonist to the central nervous system as a novel anti-transferrin receptor-IL-1RA fusion reverses neuropathic mechanical hypersensitivity. *Pain*, *158*(4), 660–668. https://doi.org/10.1097/j.pain.0000000000000810

Wei, S.-Q., Tao, Z.-Y., Xue, Y., & Cao, D.-Y. (2020). Peripheral Sensitization. In H. Turker, L. Garcia Benavides, G. Ramos Gallardo, & M. Del Méndez Villar (Eds.), *Peripheral Nerve Disorders and Treatment.* IntechOpen. https://doi.org/10.5772/intechopen.90319

Wenig, C. M., Schmidt, C. O., Kohlmann, T., & Schweikert, B. (2009). Costs of back pain in Germany. *European Journal of Pain (London, England)*, *13*(3), 280–286. https://doi.org/10.1016/j.ejpain.2008.04.005

Wetzel, C., Pifferi, S., Picci, C., Gök, C., Hoffmann, D., Bali, K. K [Kiran K.], Lampe, A., Lapatsina, L., Fleischer, R., Smith, E. S. J., Bégay, V., Moroni, M., Estebanez, L., Kühnemund, J., Walcher, J., Specker, E., Neuenschwander, M., Kries, J. P. von, Haucke, V., . . . Lewin, G. R. (2017). Small-molecule inhibition of STOML3 oligomerization reverses pathological mechanical hypersensitivity. *Nature Neuroscience*, *20*(2), 209–218. https://doi.org/10.1038/nn.4454

Willemen, Hanneke L. D. M., Kavelaars, A., Prado, J., Maas, M., Versteeg, S., Nellissen, L. J. J., Tromp, J., Gonzalez Cano, R., Zhou, W., Jakobsson, M. E., Małecki, J., Posthuma, G., Habib, A. M., Heijnen, C. J., Falnes, P. Ø., & Eijkelkamp, N. (2018). Identification of FAM173B as a protein methyltransferase promoting chronic pain. *PLOS Biology*, *16*(2), e2003452. https://doi.org/10.1371/journal.pbio.2003452

Witkowska, A. M., & Borawska, M. H. (2004). Soluble intercellular adhesion molecule-1 (sICAM-1): An overview. *European Cytokine Network*, *15*(2), 91–98. https://doi.org/Review

Wu, Z.-Z., Chen, S.-R., & Pan, H.-L. (2006). Signaling mechanisms of down-regulation of voltage-activated Ca2+ channels by transient receptor potential vanilloid type 1 stimulation with olvanil in primary sensory neurons. *Neuroscience*, *141*(1), 407–419. https://doi.org/10.1016/j.neuroscience.2006.03.023

Xian, F., Sondermann, J. R [Julia Regina], Gomez Varela, D., & Schmidt, M. (2022). Deep proteome profiling reveals signatures of age and sex differences in paw skin and sciatic nerve of naïve mice. *ELife*, *11.* https://doi.org/10.7554/eLife.81431

Xian, F., Sondermann, J. R [Julia Regina], Varela, D. G., & Schmidt, M. (2022). Deep Proteome Profiling Reveals Signatures of Age and Sex Differences in Paw Skin and Sciatic Nerve of Naïve Mice. *BioRxiv*, 2022.07.04.498721. https://doi.org/10.1101/2022.07.04.498721

Xie, J., & Black, D. L. (2001). A CaMK IV responsive RNA element mediates depolarization-induced alternative splicing of ion channels. *Nature*, *410*(6831), 936–939. https://doi.org/10.1038/35073593

Xie, Y., Vessey, J. P., Konecna, A., Dahm, R., Macchi, P., & Kiebler, M. A. (2007). The GTP-binding protein Septin 7 is critical for dendrite branching and dendritic-spine morphology. *Current Biology : CB*, *17*(20), 1746–1751. https://doi.org/10.1016/j.cub.2007.08.042

Yabluchanskiy, A., Ma, Y., Iyer, R. P., Hall, M. E., & Lindsey, M. L. (2013). Matrix metalloproteinase-9: Many shades of function in cardiovascular disease. *Physiology*, *28*(6), 391–403. https://doi.org/10.1152/physiol.00029.2013

Yamashita, K., Haraguchi, M., & Yano, M. (2022). Knockdown of TMEM160 leads to an increase in reactive oxygen species generation and the induction of the mitochondrial unfolded protein response. *FEBS Open Bio.* Advance online publication. https://doi.org/10.1002/2211-5463.13496

Yang, H., Wang, H., & Jaenisch, R. (2014). Generating genetically modified mice using CRISPR/Cas-mediated genome engineering. *Nature Protocols*, *9*(8), 1956–1968. https://doi.org/10.1038/nprot.2014.134

Yang, Y [Yang], Luo, L [Lan], Cai, X., Fang, Y., Wang, J [Jiaqi], Chen, G., Yang, J., Zhou, Q., Sun, X., Cheng, X., Yan, H., Lu, W., Hu, C., & Cao, P. (2018). Nrf2 inhibits oxaliplatin-induced peripheral neuropathy via protection of mitochondrial function. *Free Radical Biology & Medicine*, *120*, 13–24. https://doi.org/10.1016/j.freeradbiomed.2018.03.007

Yousuf, M. S., Maguire, A. D., Simmen, T., & Kerr, B. J. (2020). Endoplasmic reticulum-mitochondria interplay in chronic pain: The calcium connection. *Molecular Pain*, *16*, 1744806920946889. https://doi.org/10.1177/1744806920946889

Yu, X., Liu, H., Hamel, K. A., Morvan, M. G., Yu, S., Leff, J., Guan, Z., Braz, J. M., & Basbaum, A. I. (2020). Dorsal root ganglion macrophages contribute to both the initiation and persistence of neuropathic pain. *Nature Communications*, *11*(1), 264. https://doi.org/10.1038/s41467-019-13839-2

Yu, Y., Huang, X., Di, Y., Qu, L., & Fan, N. (2017). Effect of CXCL12/CXCR4 signaling on neuropathic pain after chronic compression of dorsal root ganglion. *Scientific Reports*, *7*(1), 5707. https://doi.org/10.1038/s41598-017-05954-1

Zamponi, G. W., Lewis, R. J., Todorovic, S. M., Arneric, S. P., & Snutch, T. P. (2009). Role of voltage-gated calcium channels in ascending pain pathways. *Brain Research Reviews*, *60*(1), 84–89. https://doi.org/10.1016/j.brainresrev.2008.12.021

Zeisel, A., Hochgerner, H., Lönnerberg, P., Johnsson, A., Memic, F., van der Zwan, J., Häring, M., Braun, E., Borm, L. E., La Manno, G., Codeluppi, S., Furlan, A., Lee, K., Skene, N., Harris, K. D., Hjerling-Leffler, J., Arenas, E., Ernfors, P., Marklund, U., & Linnarsson, S. (2018). Molecular Architecture of the Mouse Nervous System. *Cell*, *174*(4), 999-1014.e22. https://doi.org/10.1016/j.cell.2018.06.021

Zelaya, C. E., Dahlhamer, J. M., Lucas, J. W., & Connor, E. M. (2020). Chronic Pain and High-impact Chronic Pain Among U.S. Adults, 2019. *NCHS Data Brief*(390), 1–8.

Zeviani, M., & Di Donato, S. (2004). Mitochondrial disorders. *Brain : A Journal of Neurology*, *127*(Pt 10), 2153–2172. https://doi.org/10.1093/brain/awh259

Zhang, J.-M., & An, J. (2007). Cytokines, inflammation, and pain. *International Anesthesiology Clinics*, *45*(2), 27–37. https://doi.org/10.1097/AIA.0b013e318034194e

Zhao, D., Han, D.-F., Wang, S.-S., Lv, B., Wang, X [Xu], & Ma, C. (2019). Roles of tumor necrosis factor-α and interleukin-6 in regulating bone cancer pain via TRPA1 signal pathway and beneficial effects of inhibition of neuro-inflammation and TRPA1. *Molecular Pain*, *15*, 1744806919857981. https://doi.org/10.1177/1744806919857981

Zheng, Y., Liu, P [Pin], Bai, L [Ling], Trimmer, J. S., Bean, B. P., & Ginty, D. D. (2019). Deep Sequencing of Somatosensory Neurons Reveals Molecular Determinants of Intrinsic Physiological Properties. *Neuron*, *103*(4), 598-616.e7. https://doi.org/10.1016/j.neuron.2019.05.039

Zíková, M., Konířová, J., Ditrychová, K., Corlett, A., Kolář, M., & Bartůněk, P. (2014). Disp3 promotes proliferation and delays differentiation of neural progenitor cells. *FEBS Letters*, *588*(21), 4071–4077. https://doi.org/10.1016/j.febslet.2014.09.036

Zimmermann, M. (1983). Ethical guidelines for investigations of experimental pain in conscious animals. *Pain*, *16*(2), 109–110. https://doi.org/10.1016/0304-3959(83)90201-4

Zurborg, S., Piszczek, A., Martínez, C., Hublitz, P., Al Banchaabouchi, M., Moreira, P., Perlas, E., & Heppenstall, P. A. (2011). Generation and characterization of an Advillin-Cre driver mouse line. *Molecular Pain*, *7*, 66. https://doi.org/10.1186/1744-8069-7-66

6 Supplemental Information

All supplemental information is available in digital format upon request:

- Publication:
  Segelcke, D.*, **Fischer, H. K.*,** Hütte, M., Dennerlein, S., Benseler, F., Brose, N., Pogatzki-Zahn, E. M., & Schmidt, M. (2021). Tmem160 contributes to the establishment of discrete nerve injury-induced pain behaviors in male mice. Cell Reports, 37(12), 110152. https://doi.org/10.1016/j.celrep.2021.110152. * equal contribution, including supplemental information
- Supplemental Table 1, containing information on protein IDs expressed across four different age- and sex- groups, as detected using relative proteomic studies, related to Figure 24
- Supplemental Table 2, containing information on relative protein expression levels in DRG across four different age- and sex-groups, as detected using relative proteomic studies, related to Figure 25
- Supplemental Table 3, containing information on differentially expressed proteins and their involvement in reactome pathways, related to Figure 26 and Figure 28
- Supplemental Table 4, containing information on comparisons of DRG proteome with relevant literature, related to Figure 30 and Figure 31